

Supporting Information

Ni(II)-Catalyzed Asymmetric Addition of Arylboronic Acids to Cyclic Imines

Mao Quan, Liang Tang, Jiaqi Shen, Guoqiang Yang,* and Wanbin Zhang*

^a School of Chemistry and Chemical Engineering, Shanghai Jiao Tong University, 800 Dongchuan Road, Shanghai 200240, P. R. China.
Fax: +86-21-5474-3265; Tel: +86-21-5474-3265; E-mail: gqyang@sjtu.edu.cn; wanbin@sjtu.edu.cn.

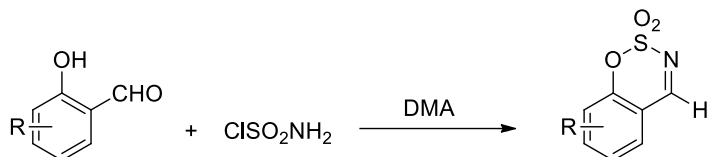
CONTENTS

1. General	2
2. Synthesis of Substrates	2
3. Full Results of the Optimization of Reaction Conditions	3
4. Asymmetric Catalysis	5
5. Computational Details and Two Plausible Reaction Mechanisms	12
6. NMR Spectra	15
7. HPLC Spectra of Products	56
8. Cartesian Coordinates	92
9. X-Ray Crystal Structure Data	93
10. References	101

1. General

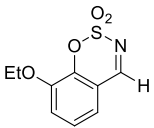
All air and moisture sensitive manipulations were carried out with standard Schlenk techniques nitrogen atmosphere. Column chromatography was performed using 100-200 mesh silica gels. All the reagents were purchased from Adamas-Beta Ltd., Energy Chemical Inc. or J&K Scientific Inc. and used without further purification unless otherwise specified. The NMR spectra were recorded on a Varian MERCURY plus-400 (400 MHz, ¹H; 101 MHz, ¹³C) spectrometer with chemical shifts reported in ppm relative to the residual deuterated solvents. Mass spectrometry analysis was carried out using an electrospray spectrometer Waters Micromass Q-TOF Premier Mass Spectrometer. Melting points were measured with SGW X-4 micro melting point apparatus. Optical rotations were measured on a Rudolph Research Analytical Autopol VI automatic polarimeter using a 50 mm path-length cell at 589 nm. Chiral analyses were performed on a Shimadzu LC-2010 HPLC system, using an Enantiocol Chiral OX-3 column (Guangzhou Research & Creativity Biotechnology Co., Ltd.) or Daicel Chiralcel IC-3, OZ-H and AD-H columns with *n*-hexane / *i*-propyl alcohol as an eluent.

2. Synthesis of Substrates

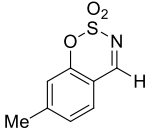


General procedure: A modified procedure of the literature was used.¹ To a solution of substituted salicylaldehyde (20 mmol) in 40.0 mL of DMA at 0 °C was slowly transferred solid H₂NSO₂Cl (60 mmol, 3.0 equiv). The mixture was allowed to warm to 100 °C and stirred overnight. The reaction was quenched with 100 mL water and transferred to a separatory funnel with 100 mL of EtOAc. The organic layer was separated, and the aqueous layer was extracted with 100 mL EtOAc. The combined organic layers were washed successively with 2 x 50 mL of H₂O and 1 x 50 mL of saturated aqueous NaCl, dried over MgSO₄, and concentrated under reduced pressure. Purification by chromatography on silica gel afforded the desired substrates.

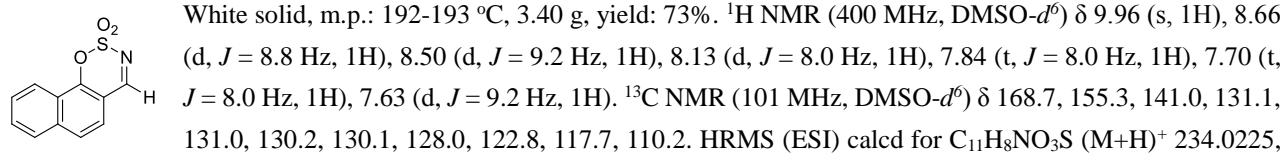
8-Ethoxybenzo[*e*][1,2,3]oxathiazine-2,2-dioxide (1d).

 White solid, m.p.: 69–70 °C, 4.31 g, yield: 95%. ¹H NMR (400 MHz, CDCl₃) δ 8.65 (s, 1H), 7.42 – 7.20 (m, 3H), 4.17 (q, *J* = 8.0 Hz, 2H), 1.48 (t, *J* = 8.0 Hz, 3H). ¹³C NMR (101 MHz, CDCl₃) δ 168.5, 147.9, 143.7, 126.4, 121.8, 121.3, 116.3, 65.8, 14.8. HRMS (ESI) calcd for C₉H₁₀NO₄S (M+H)⁺ 228.0331, found 228.0331.

7-Methylbenzo[*e*][1,2,3]oxathiazine-2,2-dioxide (1f).

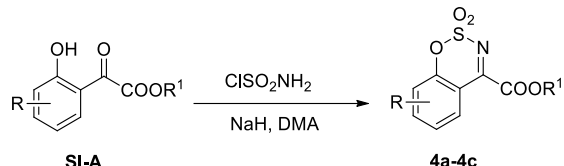
 White solid, m.p.: 67–68 °C, 3.43 g, yield: 87%. ¹H NMR (400 MHz, CDCl₃) δ 8.60 (s, 1H), 7.56 (d, *J* = 8.0 Hz, 1H), 7.22 (dd, *J* = 8.0, 0.4 Hz, 1H), 7.09 (s, 1H), 2.50 (s, 3H). ¹³C NMR (101 MHz, CDCl₃) δ 168.2, 154.4, 150.9, 131.2, 127.6, 118.8, 113.3, 22.6. HRMS (ESI) calcd for C₈H₈NO₃S (M+H)⁺ 198.0225, found 198.0229.

Naphtho[2,1-*e*][1,2,3]oxathiazine-2,2-dioxide (1i).



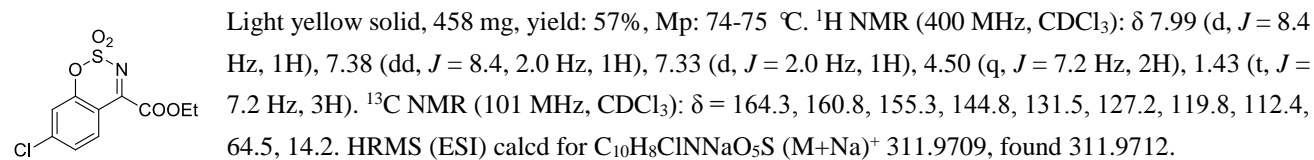
found 234.0232.

Other cyclic aldimine substrates (**1b**, **1c**, **1e**, **1g**, **1h**, **1j**) were synthesized according to the literatures.¹

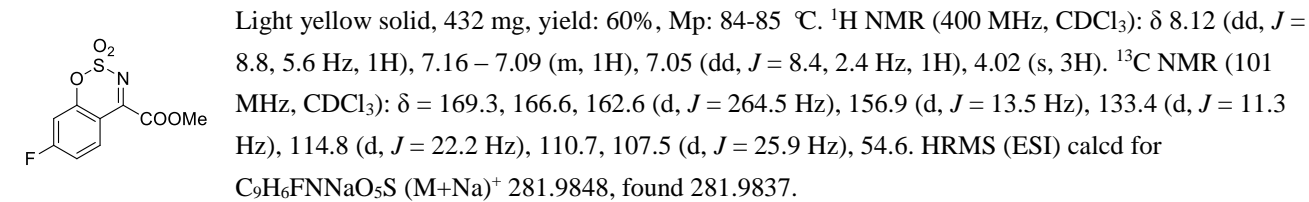


SI-A were synthesized based on the literature.² The synthesis procedure was followed by the literature.³ To a solution of **A** (2.78 mmol) in 5.0 mL of DMA was quickly transferred solid $\text{H}_2\text{NSO}_2\text{Cl}$ (1.12 g, 9.71 mmol, 3.5 equiv) and stirred for 1 h. NaH (60% in mineral oil, 388 mg, 9.71 mmol, 3.5 equiv) was added for 3 portions in 2 h and stirred for another 2 h at room temperature. After stirring at 50 °C for 12 h, the reaction was quenched by the addition of 5 mL of H_2O and transferred to a separatory funnel with 20 mL of Et_2O . The organic layer was separated, and the aqueous layer was extracted with 2 x 15 mL of Et_2O . The combined organic layers were dried over Na_2SO_4 and concentrated under reduced pressure. Purification by chromatography on silica gel (EtOAc/petroleum ether=1:4) afforded the product as a light yellow solid.

Ethyl-7-chlorobenzo[e][1,2,3]oxathiazine-4-carboxylate-2,2-dioxide (**4b**)

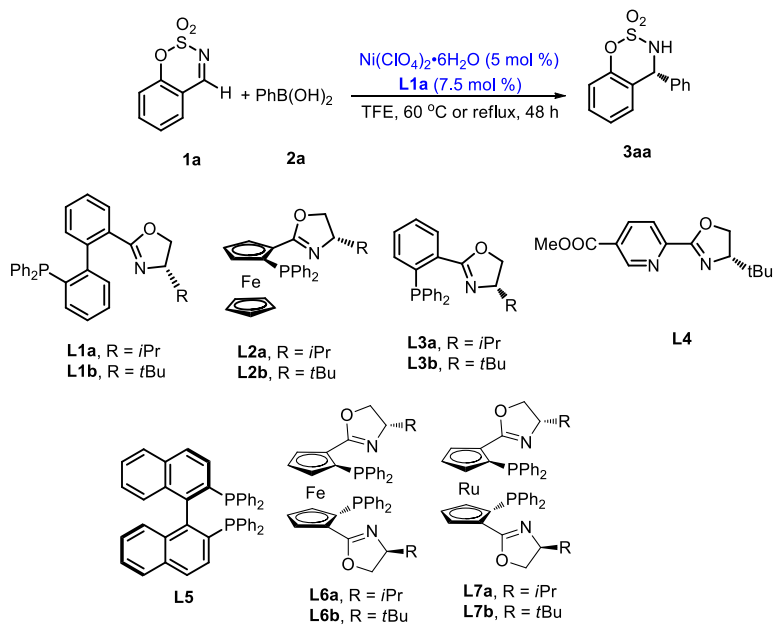


Methyl-7-fluorobenzo[e][1,2,3]oxathiazine-4-carboxylate-2,2-dioxide (**4c**)



The data of **4a** were reported by the literature.³

3. Full Results of the Optimization of Reaction Conditions^a



Entry	Variations from the standard conditions	Yield (%) ^b	ee (%) ^c
1	reflux	96	95
2	reflux, no L1a	NR	---
3	reflux, L1b instead of L1a	83	98
4	reflux, L2a instead of L1a	37	99
5	reflux, L2b instead of L1a	17	96
6	reflux, L3a instead of L1a	69	97
7	reflux, L3b instead of L1a	66	97
8	reflux, L4 instead of L1a	trace	---
9	reflux, L5 instead of L1a	trace	---
10	reflux, L6a instead of L1a	trace	---
11	reflux, L6b instead of L1a	trace	---
12	reflux, L7a instead of L1a	trace	---
13	reflux, L7b instead of L1a	trace	---
14	60 °C	94	96
15	50 °C	81	97
16	40 °C	58	97
17	60 °C, NiCl ₂ 6H ₂ O instead of Ni(ClO ₄) ₂ 6H ₂ O	90	94
18	60 °C, Ni(OAc) ₂ 4H ₂ O instead of Ni(ClO ₄) ₂ 6H ₂ O	74	96
19	60 °C, NiBr ₂ instead of Ni(ClO ₄) ₂ 6H ₂ O	72	96
20	60 °C, no Ni(ClO ₄) ₂ 6H ₂ O	NR	---
21	60 °C, MeOH instead of TFE	trace	---
22	60 °C, EtOH instead of TFE	trace	---
23	60 °C, DCE instead of TFE	trace	---
24	60 °C, toluene instead of TFE	trace	---
25	60 °C, CHCl ₃ instead of TFE	trace	---
26	60 °C, MeCN instead of TFE	trace	---

27	60 °C, EtOAc instead of TFE	trace	---
28	60 °C, dioxane instead of TFE	trace	---
29	60 °C, 40 mg 4 Å MS was added	92	96
30	60 °C, N ₂ instead of air	88	96
31	80 °C, N ₂ instead of air and a sealed tube was used instead of a test tube	87	95
32	60 °C, Ni(COD) ₂ instead of Ni(ClO ₄) ₂ 6H ₂ O, N ₂	NR	---
33	60 °C, N ₂ , with COD (10 mol%)	90	94

^a Reactions were carried out on a 0.20 mmol scale (**1a**) using PhB(OH)₂ (0.30 mmol), 5 mol% nickel salt, 7.5 mol% ligand in unpurified solvent (2.0 mL) in a test tube for 48 h which was opened to air. ^b Yield of isolated product. ^c Determined by HPLC using a chiral Daicel column. TFE = trifluoroethanol, DCE = 1,2-dichloroethane, NR = no reaction, MS = molecular sieves.

4. Asymmetric Catalysis

General procedure: A test tube (20 mL) was charged with Ni(ClO₄)₂ 6H₂O (3.5 mg, 0.010 mmol, 0.050 equiv), **L1a** (6.7 mg, 0.015 mmol, 0.075 equiv) and unpurified TFE (1.0 mL). The solution was stirred at 60 °C for 0.5 h, then substrate (0.20 mmol, 1.0 equiv) and arylboronic acid (0.30 mmol, 1.5 equiv) were added into the tube. The wall of the tube was rinsed with an additional portion of TFE (1.0 mL). After stirring at 60 °C (for aldimines) or reflux (for ketimines) for 48 h in air, the reaction mixture was cooled to room temperature and the solvent was removed by rotary evaporation. The residue was purified by preparative TLC on silica gel (petroleum ether/EtOAc = 5/1) to give the product.

(R)-4-Phenyl-3,4-dihydrobenzo[e][1,2,3]oxathiazine-2,2-dioxide(3aa).⁴

White solid, 49.0 mg, yield: 94%. ¹H NMR (400 MHz, CDCl₃) δ 7.47 – 7.40 (m, 3H), 7.37 – 7.28 (m, 3H), 7.09 (t, J = 7.6 Hz, 1H), 7.04 (d, J = 8.4 Hz, 1H), 6.81 (d, J = 7.6 Hz, 1H), 5.89 (d, J = 8.8 Hz, 1H), 4.90 (d, J = 8.8 Hz, 1H). ¹³C NMR (101 MHz, CDCl₃) δ 151.7, 138.0, 129.9, 129.8, 129.7, 129.1, 128.8, 125.5, 122.3, 119.0, 62.2. HPLC [Daicel Chiraldak IC-3, hexane/i-PrOH = 90/10, 220 nm, 1.0 mL/min. t_{R1} = 12.7 min (major), t_{R2} = 13.7 min (minor)]; ee = 96%.

(R)-4-(2-Methoxyphenyl)-3,4-dihydrobenzo[e][1,2,3]oxathiazine-2,2-dioxide(3ab).⁴

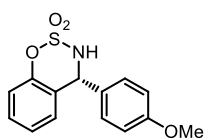
White solid, 58.0 mg, yield: 99%. ¹H NMR (400 MHz, CDCl₃) δ 7.46 – 7.40 (m, 1H), 7.35 (dd, J = 7.2, 1.6 Hz, 1H), 7.31 – 7.24 (m, 1H), 7.10 – 6.98 (m, 3H), 6.96 (d, J = 8.4 Hz, 1H), 6.68 (dt, J = 7.6 Hz, 1.2 Hz 1H), 5.90 (d, J = 10.4 Hz, 1H), 5.70 (d, J = 10.4 Hz, 1H), 3.68 (s, 3H). ¹³C NMR (101 MHz, CDCl₃) δ 157.5, 151.4, 131.5, 131.2, 129.4, 127.0, 125.1, 124.8, 123.0, 121.6, 118.6, 112.4, 60.6, 55.9. HPLC [Daicel Chiraldak IC-3, hexane/i-PrOH = 90/10, 220 nm, 0.5 mL/min. t_{R1} = 48.3 min (major), t_{R2} = 72.7 min (minor)]; ee = 89%.

(R)-4-(3-Methoxyphenyl)-3,4-dihydrobenzo[e][1,2,3]oxathiazine-2,2-dioxide(3ac).⁴

White solid, 57.0 mg, yield: 98%. ¹H NMR (400 MHz, CDCl₃) δ 7.38 – 7.27 (m, 2H), 7.13 – 7.00 (m, 2H), 7.00 – 6.88 (m, 2H), 6.88 – 6.81 (m, 2H), 5.85 (d, J = 8.0 Hz, 1H), 4.92 (d, J = 8.4 Hz, 1H), 3.80 (s, 3H). ¹³C NMR (101 MHz, CDCl₃) δ 160.5, 151.6, 139.4, 130.8, 130.0, 128.8, 125.5, 122.1, 121.2, 119.0, 115.2, 114.7, 62.1, 55.6. HPLC [Daicel Chiraldak IC-3, hexane/i-PrOH = 90/10, 220 nm, 1.0 mL/min. t_{R1} = 29.1 min (major), t_{R2} = 34.5 min (minor)]; ee = 95%.

(R)-4-(4-Methoxyphenyl)-3,4-dihydrobenzo[e][1,2,3]oxathiazine-2,2-dioxide(3ad).⁴

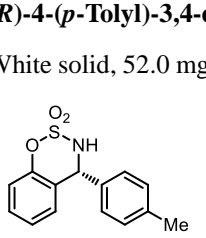
White solid, 56.0 mg, yield: 96%. ¹H NMR (400 MHz, CDCl₃) δ 7.31 (t, J = 8.0 Hz, 1H), 7.24 (d, J = 8.8 Hz, 1H), 7.08 (t, J = 7.6 Hz, 1H), 7.03 (d, J = 8.4 Hz, 1H), 6.93 (d, J = 8.8 Hz, 2H), 6.83 (d, J = 7.6 Hz, 1H), 5.84 (d, J = 8.8 Hz, 1H), 4.85



(d, J = 8.8 Hz, 1H), 3.82 (s, 3H). ¹³C NMR (101 MHz, CDCl₃) δ 160.5, 151.7, 130.4, 130.1, 129.9, 128.9, 125.4, 122.5, 119.0, 115.0, 61.7, 55.6. HPLC [Daicel Chiraldak IC-3, hexane/i-PrOH = 90/10, 220 nm, 1.0 mL/min. t_{R1} = 33.2 min (major), t_{R2} = 59.9 min (minor)]; ee = 96%.

(R)-4-(*m*-Tolyl)-3,4-dihydrobenzo[e][1,2,3]oxathiazine-2,2-dioxide(3ae).⁴

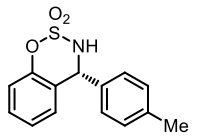
White solid, 48.0 mg, yield: 87%. ¹H NMR (400 MHz, CDCl₃) δ 7.37 – 7.20 (m, 3H), 7.18 – 7.01 (m, 4H), 6.82 (d, J = 7.6 Hz, 1H), 5.85 (s, 1H), 4.84 (br, 1H), 2.37 (s, 3H). ¹³C NMR (101 MHz, CDCl₃) δ 151.7, 139.6, 138.0, 130.5, 129.9, 129.6, 129.6, 128.8, 126.0, 125.5, 122.4, 119.0, 62.2, 21.6. HPLC [Daicel Chiraldak IC-3, hexane/i-PrOH = 90/10, 220 nm, 1.0 mL/min. t_{R1} = 14.4 min (major), t_{R2} = 16.8 min (minor)]; ee = 96%.



δ 151.7, 139.6, 138.0, 130.5, 129.9, 129.6, 129.6, 128.8, 126.0, 125.5, 122.4, 119.0, 62.2, 21.6. HPLC [Daicel Chiraldak IC-3, hexane/i-PrOH = 90/10, 220 nm, 1.0 mL/min. t_{R1} = 14.4 min (major), t_{R2} = 16.8 min (minor)]; ee = 96%.

(R)-4-(*p*-Tolyl)-3,4-dihydrobenzo[e][1,2,3]oxathiazine-2,2-dioxide(3af).⁴

White solid, 52.0 mg, yield: 95%. ¹H NMR (400 MHz CDCl₃) δ = 7.36 – 7.28 (m, 1H), 7.27 – 7.19 (m, 4H), 7.12 – 7.01 (m, 2H), 6.82 (d, J = 7.6 Hz, 1H), 5.86 (s, 1H), 2.39 (s, 3H). ¹³C NMR (101 MHz CDCl₃) δ = 151.7, 139.8, 135.1, 130.3, 129.9, 128.9, 128.8, 125.4, 122.4, 119.0, 62.0, 21.5. HPLC [Daicel Chiraldak IC-3, hexane/i-PrOH = 90/10, 220 nm, 1.0 mL/min. t_{R1} = 15.7 min (major), t_{R2} = 17.2 min (minor)]; ee = 95%.



δ 151.7, 139.8, 135.1, 130.3, 129.9, 128.9, 128.8, 125.4, 122.4, 119.0, 62.0, 21.5. HPLC [Daicel Chiraldak IC-3, hexane/i-PrOH = 90/10, 220 nm, 1.0 mL/min. t_{R1} = 15.7 min (major), t_{R2} = 17.2 min (minor)]; ee = 95%.

(R)-4-(4-(tert-Butyl)phenyl)-3,4-dihydrobenzo[e][1,2,3]oxathiazine-2,2-dioxide(3ag).

White solid, m.p.: 165–166 °C, 54.0 mg, yield: 89%. ¹H NMR (400 MHz, CDCl₃) δ 7.44 (d, J = 8.4 Hz, 2H), 7.32 (t, J = 7.6 Hz, 1H), 7.26 (d, J = 8.4 Hz, 2H), 7.13 – 7.00 (m, 2H), 6.85 (d, J = 8.0 Hz, 1H), 5.88 (d, J = 8.8 Hz, 1H), 4.74 (d, J = 8.8 Hz, 1H), 1.34 (s, 9H). ¹³C NMR (101 MHz, CDCl₃) δ 153.0, 151.7, 135.0, 129.8, 128.9, 128.7, 126.6, 125.4, 122.4, 119.0, 61.9, 35.0, 31.5. HPLC [Daicel Chiraldak IC-3, hexane/i-PrOH = 90/10, 220 nm, 1.0 mL/min. t_{R1} = 12.2 min (minor), t_{R2} = 14.2 min (major)]; ee = 94%, [α]²⁰_D = +2.6 (c = 1.0, CHCl₃); HRMS (ESI) calcd for C₁₇H₂₀NO₃S (M+H)⁺ 318.1164, found 318.1169.



δ 153.0, 151.7, 135.0, 129.8, 128.9, 128.7, 126.6, 125.4, 122.4, 119.0, 61.9, 35.0, 31.5. HPLC [Daicel Chiraldak IC-3, hexane/i-PrOH = 90/10, 220 nm, 1.0 mL/min. t_{R1} = 12.2 min (minor), t_{R2} = 14.2 min (major)]; ee = 94%, [α]²⁰_D = +2.6 (c = 1.0, CHCl₃); HRMS (ESI) calcd for C₁₇H₂₀NO₃S (M+H)⁺ 318.1164, found 318.1169.

(R)-4-([1,1'-Biphenyl]-4-yl)-3,4-dihydrobenzo[e][1,2,3]oxathiazine-2,2-dioxide(3ah).

White solid, m.p.: 181–182 °C, 60.0 mg, yield: 89%. ¹H NMR (400 MHz, CDCl₃) δ 7.70 – 7.56 (m, 4H), 7.52 – 7.44 (m, 2H), 7.44 – 7.30 (m, 4H), 7.18 – 7.03 (m, 2H), 6.89 (d, J = 7.6 Hz, 1H), 5.95 (d, J = 8.4 Hz, 1H), 4.86 (d, J = 8.8 Hz, 1H). ¹³C NMR (101 MHz, CDCl₃) δ 151.7, 142.8, 140.2, 136.9, 130.0, 129.5, 129.2, 128.9, 128.4, 128.1, 127.4, 125.5, 122.2, 119.1, 61.9. HPLC [Daicel Chiraldak IC-3, hexane/i-PrOH = 90/10, 220 nm, 1.0 mL/min. t_{R1} = 24.2 min (major), t_{R2} = 29.7 min (minor)]; ee = 95%, [α]²⁰_D = -14.4 (c = 0.5, CHCl₃); HRMS (ESI) calcd for C₁₉H₁₆NO₃S (M+H)⁺ 338.0851, found 338.0851.



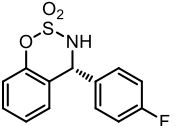
δ 151.7, 142.8, 140.2, 136.9, 130.0, 129.5, 129.2, 128.9, 128.4, 128.1, 127.4, 125.5, 122.2, 119.1, 61.9. HPLC [Daicel Chiraldak IC-3, hexane/i-PrOH = 90/10, 220 nm, 1.0 mL/min. t_{R1} = 24.2 min (major), t_{R2} = 29.7 min (minor)]; ee = 95%, [α]²⁰_D = -14.4 (c = 0.5, CHCl₃); HRMS (ESI) calcd for C₁₉H₁₆NO₃S (M+H)⁺ 338.0851, found 338.0851.

(S)-4-(2-Fluorophenyl)-3,4-dihydrobenzo[e][1,2,3]oxathiazine-2,2-dioxide(3ai).



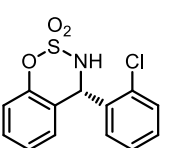
Colorless gummy oil, 55.0 mg, yield: 99%. ^1H NMR (400 MHz, CDCl_3) δ 7.50 – 7.40 (m, 1H), 7.38 – 7.29 (m, 2H), 7.23 (td, J = 7.6, 1.2 Hz, 1H), 7.20 – 7.13 (m, 1H), 7.09 (td, J = 7.6, 1.2 Hz, 1H), 7.05 (dd, J = 8.4, 1.2 Hz, 1H), 6.78 (d, J = 8.0 Hz, 1H), 6.12 (s, 1H), 5.11 (br, 1H). ^{13}C NMR (101 MHz, CDCl_3) δ 161.1 (d, J = 249.5 Hz), 151.5, 131.8 (d, J = 8.6 Hz), 131.0 (d, J = 2.5 Hz), 130.7, 127.7, 125.6, 125.5 (d, J = 26.3 Hz), 125.3, 121.6, 119.0, 116.8 (d, J = 21.0 Hz), 57.2 (d, J = 2.3 Hz). HPLC [Daicel Chiralpak IC-3, hexane/*i*-PrOH = 90/10, 220 nm, 1.0 mL/min. $t_{\text{R}1}$ = 59.6 min (minor), $t_{\text{R}2}$ = 61.7 min (major)]; ee = 97%, $[\alpha]^{20}_{\text{D}} = -7.0$ (c = 1.0, CHCl_3); HRMS (ESI) calcd for $\text{C}_{13}\text{H}_{11}\text{FNO}_3\text{S}$ ($\text{M}+\text{H}$) $^+$ 280.0444, found 280.0440.

(R)-4-(4-Fluorophenyl)-3,4-dihydrobenzo[e][1,2,3]oxathiazine-2,2-dioxide (3aj).



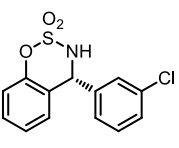
White solid, m.p.: 146–147 °C, 52.0 mg, yield: 93%. ^1H NMR (400 MHz, CDCl_3) δ 7.40 – 7.27 (m, 3H), 7.18 – 7.08 (m, 3H), 7.05 (d, J = 8.4 Hz, 1H), 6.81 (d, J = 7.6 Hz, 1H), 5.89 (s, 1H), 4.91 (br, 1H). ^{13}C NMR (101 MHz, CDCl_3) δ 163.4 (d, J = 242.4 Hz), 151.6, 134.0 (d, J = 2.8 Hz), 131.0 (d, J = 8.4 Hz), 130.1, 128.7, 125.6, 121.9, 119.2, 116.7 (d, J = 21.9 Hz), 61.4. HPLC [Daicel Chiralpak IC-3, hexane/*i*-PrOH = 90/10, 220 nm, 1.0 mL/min. $t_{\text{R}1}$ = 16.1 min (major), $t_{\text{R}2}$ = 23.0 min (minor)]; ee = 95%, $[\alpha]^{20}_{\text{D}} = +16.9$ (c = 0.5, CHCl_3); HRMS (ESI) calcd for $\text{C}_{13}\text{H}_{11}\text{FNO}_3\text{S}$ ($\text{M}+\text{H}$) $^+$ 280.0444, found 280.0444.

(S)-4-(2-Chlorophenyl)-3,4-dihydrobenzo[e][1,2,3]oxathiazine-2,2-dioxide (3ak).



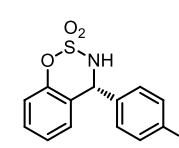
Colorless gummy oil, 51.0 mg, yield: 87%. ^1H NMR (400 MHz, CDCl_3) δ 7.48 (d, J = 7.6 Hz, 1H), 7.41 – 7.29 (m, 4H), 7.14 – 7.04 (m, 2H), 6.77 (d, J = 7.6 Hz, 1H), 6.30 (d, J = 9.2 Hz, 1H), 5.15 (d, J = 8.8 Hz, 1H). ^{13}C NMR (101 MHz, CDCl_3) δ 151.7, 135.2, 134.3, 131.5, 131.1, 131.0, 130.0, 128.0, 127.9, 125.6, 121.4, 119.2, 59.8. HPLC [Daicel Chiralpak IC-3, hexane/*i*-PrOH = 90/10, 220 nm, 1.0 mL/min. $t_{\text{R}1}$ = 11.5 min (minor), $t_{\text{R}2}$ = 12.3 min (major)]; ee = 82%, $[\alpha]^{25}_{\text{D}} = -8.1$ (c = 0.5, CHCl_3); HRMS (ESI) calcd for $\text{C}_{13}\text{H}_{11}\text{ClNO}_3\text{S}$ ($\text{M}+\text{H}$) $^+$ 296.0148, found 296.0154.

(R)-4-(3-Chlorophenyl)-3,4-dihydrobenzo[e][1,2,3]oxathiazine-2,2-dioxide (3al).⁴



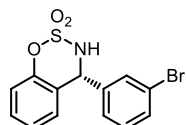
White solid, 53.0 mg, yield: 90%. ^1H NMR (400 MHz, CDCl_3) δ 7.55 – 7.29 (m, 4H), 7.28 – 7.21 (m, 1H), 7.17 – 7.00 (m, 2H), 6.82 (d, J = 7.6 Hz, 1H), 5.87 (d, J = 8.4 Hz, 1H), 4.92 (d, J = 8.4 Hz, 1H). ^{13}C NMR (101 MHz, CDCl_3) δ 151.6, 139.9, 135.5, 131.0, 130.2, 130.0, 129.2, 128.6, 127.3, 125.7, 121.4, 119.2, 61.6. HPLC [Daicel Chiralpak IC-3, hexane/*i*-PrOH = 90/10, 220 nm, 1.0 mL/min. $t_{\text{R}1}$ = 20.8 min (minor), $t_{\text{R}2}$ = 30.4 min (major)]; ee = 95%.

(R)-4-(4-Chlorophenyl)-3,4-dihydrobenzo[e][1,2,3]oxathiazine-2,2-dioxide (3am).⁴



White solid, 58.0 mg, yield: 98%. ^1H NMR (400 MHz, CDCl_3) δ 7.45 – 7.38 (m, 2H), 7.38 – 7.32 (m, 1H), 7.32 – 7.28 (m, 2H), 7.11 (td, J = 8.0, 1.2 Hz, 2H), 7.06 (d, J = 8.4 Hz, 2H), 6.80 (d, J = 7.6 Hz, 1H), 5.88 (d, J = 8.4 Hz, 1H), 4.87 (d, J = 8.4 Hz, 1H). ^{13}C NMR (101 MHz, CDCl_3) δ 151.7, 136.5, 135.8, 130.5, 130.2, 129.9, 128.6, 125.6, 121.7, 119.2, 61.5. HPLC [Daicel Chiralpak IC-3, hexane/*i*-PrOH = 90/10, 220 nm, 1.0 mL/min. $t_{\text{R}1}$ = 16.4 min (major), $t_{\text{R}2}$ = 28.0 min (minor)]; ee = 96%.

(R)-4-(3-Bromophenyl)-3,4-dihydrobenzo[e][1,2,3]oxathiazine-2,2-dioxide (3an).



Colorless gummy oil, 62.0 mg, yield: 91%. ^1H NMR (400 MHz, CDCl_3) δ 7.56 (dt, J = 7.6, 2.0 Hz, 1H), 7.50 (s, 1H), 7.39 – 7.23 (m, 3H), 7.16 – 7.02 (m, 2H), 6.82 (d, J = 8.0 Hz, 1H), 5.85 (d, J = 8.8 Hz, 1H), 4.93 (d, J = 8.4 Hz, 1H). ^{13}C NMR (101 MHz, CDCl_3) δ 151.6, 140.1, 133.0, 132.1,

131.2, 130.3, 128.6, 127.8, 125.7, 123.6, 121.4, 119.2, 61.5. HPLC [Daicel Chiralpak IC-3, hexane/*i*-PrOH = 90/10, 220 nm, 1.0 mL/min. t_{R1} = 24.5 min (minor), t_{R2} = 26.4 min (major)]; ee = 96%, $[\alpha]^{20}_D$ = +8.8 (c = 1.0, CHCl₃); HRMS (ESI) calcd for C₁₃H₁₁BrNO₃S (M+H)⁺ 339.9643, found 339.9659.

(*R*)-4-(4-Bromophenyl)-3,4-dihydrobenzo[e][1,2,3]oxathiazine-2,2-dioxide (3ao).

Colorless gummy oil, 67.0 mg, yield: 99%. ¹H NMR (400 MHz, CDCl₃) δ 7.56 (d, J = 8.4 Hz, 2H), 7.40 – 7.27 (m, 1H), 7.23 (d, J = 8.4 Hz, 2H), 7.16 – 7.00 (m, 2H), 6.80 (d, J = 7.6 Hz, 1H), 5.86 (d, J = 8.8 Hz, 1H), 4.90 (d, J = 8.4 Hz, 1H). ¹³C NMR (101 MHz, CDCl₃) δ 151.7, 137.0, 132.9, 130.8, 130.2, 128.6, 125.6, 124.0, 121.6, 119.2, 61.5. HPLC [Daicel Chiralpak IC-3, hexane/*i*-PrOH = 90/10, 220 nm, 1.0 mL/min. t_{R1} = 17.5 min (major), t_{R2} = 30.1 min (minor)]; ee = 96%, $[\alpha]^{20}_D$ = +2.3 (c = 1.0, CHCl₃); HRMS (ESI) calcd for C₁₃H₁₁BrNO₃S (M+H)⁺ 339.9643, found 339.9640.

(*R*)-4-(4-(Trifluoromethyl)phenyl)-3,4-dihydrobenzo[e][1,2,3]oxathiazine-2,2-dioxide (3ap).

Colorless gummy oil, 54.0 mg, yield: 82%. ¹H NMR (400 MHz, CDCl₃) δ 7.72 (d, J = 8.4 Hz, 2H), 7.51 (d, J = 8.0 Hz, 2H), 7.38 (t, J = 7.6 Hz, 1H), 7.20 – 7.06 (m, 2H), 6.81 (d, J = 8.0 Hz, 1H), 5.98 (d, J = 8.4 Hz, 1H), 4.97 (d, J = 8.4 Hz, 1H). ¹³C NMR (101 MHz, CDCl₃) δ 151.7, 141.8, 132.0 (q, J = 32.9 Hz), 130.3, 129.6, 128.5, 126.6, 126.6, 125.7, 121.3, 119.3, 61.5. HPLC [Daicel Chiralpak OZ-H, hexane/*i*-PrOH = 97/3, 220 nm, 0.5 mL/min. t_{R1} = 40.9 min (minor), t_{R2} = 49.1 min (major)]; ee = 95%, $[\alpha]^{20}_D$ = +17.6 (c = 0.5, CHCl₃); HRMS (ESI) calcd for C₁₄H₁₀F₃NO₃SNa (M+Na)⁺ 352.0231, found 352.0231.

(*S*)-4-(Thiophen-3-yl)-3,4-dihydrobenzo[e][1,2,3]oxathiazine-2,2-dioxide (3aq).

White solid, m.p.: 124–125 °C, 41.0 mg, yield: 77%. ¹H NMR (400 MHz, CDCl₃) δ 7.44 – 7.37 (m, 2H), 7.33 (t, J = 8.0 Hz, 1H), 7.12 (t, J = 7.6 Hz, 1H), 7.05 (d, J = 8.0 Hz, 1H), 7.01 (d, J = 4.8 Hz, 1H), 6.93 (d, J = 7.6 Hz, 1H), 6.04 (d, J = 8.4 Hz, 1H), 4.83 (d, J = 8.4 Hz, 1H). ¹³C NMR (101 MHz, CDCl₃) δ 151.3, 138.2, 130.1, 128.5, 128.1, 126.8, 126.1, 125.5, 121.9, 119.1, 77.6, 77.3, 76.9, 57.2. HPLC [Daicel Chiralpak IC-3, hexane/*i*-PrOH = 95/5, 220 nm, 1.0 mL/min. t_{R1} = 35.5 min (major), t_{R2} = 37.7 min (minor)]; ee = 94%, $[\alpha]^{20}_D$ = +32.4 (c = 0.5, CHCl₃); HRMS (ESI) calcd for C₁₁H₁₀NO₃S₂ (M+H)⁺ 268.0102, found 268.0104.

(*R*)-4-(Naphthalen-2-yl)-3,4-dihydrobenzo[e][1,2,3]oxathiazine-2,2-dioxide (3ar).⁴

White solid, 51.0 mg, yield: 82%. ¹H NMR (400 MHz, CDCl₃) δ 7.93 – 7.83 (m, 4H), 7.61 – 7.52 (m, 2H), 7.39 – 7.27 (m, 2H), 7.15 – 6.99 (m, 2H), 6.84 (d, J = 7.8 Hz, 1H), 6.06 (d, J = 8.5 Hz, 1H), 4.92 (d, J = 8.6 Hz, 1H). ¹³C NMR (101 MHz, CDCl₃) δ 151.7, 135.1, 133.8, 133.4, 130.0, 130.0, 129.0, 128.9, 128.4, 128.1, 127.4, 127.2, 125.5, 125.4, 122.2, 119.1, 62.4. HPLC [Daicel Chiralpak IC-3, hexane/*i*-PrOH = 90/10, 220 nm, 1.0 mL/min. t_{R1} = 21.6 min (major), t_{R2} = 41.9 min (minor)]; ee = 88%.

(*R*)-4-(Benzo[d][1,3]dioxol-5-yl)-3,4-dihydrobenzo[e][1,2,3]oxathiazine-2,2-dioxide (3as).

White solid, mp: 116–117 °C, 52.0 mg, yield: 85%, ¹H NMR (400 MHz, CDCl₃) δ 7.32 (t, J = 8.0 Hz, 1H), 7.14 – 7.01 (m, 2H), 6.92 – 6.80 (m, 3H), 6.73 (s, 1H), 6.00 (s, 2H), 5.81 (d, J = 8.2 Hz, 1H), 4.72 (d, J = 8.4 Hz, 1H). ¹³C NMR (101 MHz, CDCl₃) δ 151.6, 148.8, 148.8, 131.7, 130.0, 128.8, 125.5, 123.1, 122.3, 119.1, 109.0, 108.9, 101.9, 62.0. HPLC [Daicel Chiralpak IC-3, hexane/*i*-PrOH = 90/10, 220 nm, 1.0 mL/min. t_{R1} = 32.4 min (minor), t_{R2} = 34.8 min (major)]; ee = 87%, $[\alpha]^{20}_D$ = +3.6 (c = 1.0, CHCl₃); HRMS (ESI) calcd for C₁₄H₁₂NO₅S (M+H)⁺ 306.0436, found 306.0427.

(*R*)-4-(3,5-Dimethylphenyl)-3,4-dihydrobenzo[e][1,2,3]oxathiazine-2,2-dioxide (3at).

White solid, mp: 151–152 °C 53.0 mg, yield: 92%. ^1H NMR (400 MHz, CDCl_3) δ 7.36 – 7.28 (m, 1H), 7.13 – 7.02 (m, 3H), 6.93 (s, 2H), 6.84 (d, J = 7.7 Hz, 1H), 5.81 (d, J = 8.7 Hz, 1H), 4.71 (d, J = 8.7 Hz, 1H), 2.32 (s, 6H). ^{13}C NMR (101 MHz, CDCl_3) δ 151.7, 139.5, 138.0, 131.4, 129.8, 128.9, 126.7, 125.5, 122.5, 119.0, 62.3, 21.5. HPLC [Daicel Chiraldak IC-3, hexane/*i*-PrOH = 90/10, 220 nm, 1.0 mL/min. $t_{\text{R}1}$ = 16.4 min (minor), $t_{\text{R}2}$ = 17.8 min (major)]; ee = 93%, $[\alpha]^{20}_{\text{D}} = -1.8$ (c = 1.0, CHCl_3); HRMS (ESI) calcd for $\text{C}_{15}\text{H}_{16}\text{NO}_3\text{S}$ ($\text{M}+\text{H}$) $^+$ 290.0851, found 290.0858.

(S)-4-(2-Fluoro-4-methoxyphenyl)-3,4-dihydrobenzo[e][1,2,3]oxathiazine-2,2-dioxide (3au).

White solid, mp: 156–157 °C, 51.0 mg, yield: 83%. ^1H NMR (400 MHz, CDCl_3) δ 7.38 – 7.20 (m, 2H), 7.10 – 6.93 (m, 2H), 6.83 – 6.59 (m, 3H), 5.91 (d, J = 10.1 Hz, 1H), 5.58 (d, J = 10.1 Hz, 1H), 3.69 (s, 3H). ^{13}C NMR (101 MHz, CDCl_3) δ 164.6 (d, J = 250.1 Hz), 158.8 (d, J = 10.3 Hz), 151.4, 132.4 (d, J = 10.3 Hz), 129.6, 127.1, 125.3, 122.7, 120.9, 118.7, 108.0 (d, J = 21.7 Hz), 100.8 (d, J = 26.3 Hz), 59.6, 56.3. HPLC [Daicel Chiraldak IC-3, hexane/*i*-PrOH = 90/10, 220 nm, 1.0 mL/min. $t_{\text{R}1}$ = 17.1 min (major), $t_{\text{R}2}$ = 24.0 min (minor)]; ee = 89%, $[\alpha]^{20}_{\text{D}} = -21.1$ (c = 1.0, CHCl_3); HRMS (ESI) calcd for $\text{C}_{14}\text{H}_{13}\text{FNO}_4\text{S}$ ($\text{M}+\text{H}$) $^+$ 310.0549, found 310.0548.

(R)-8-Methoxy-4-phenyl-3,4-dihydrobenzo[e][1,2,3]oxathiazine-2,2-dioxide (3ba).⁴

White solid, 56.0 mg, yield: 96%. ^1H NMR (400 MHz, CDCl_3) δ 7.46 – 7.31 (m, 5H), 7.00 (t, J = 8.1 Hz, 1H), 6.89 (d, J = 8.2 Hz, 1H), 6.37 (d, J = 7.9 Hz, 1H), 5.89 (d, J = 8.5 Hz, 1H), 4.79 (d, J = 8.4 Hz, 1H), 3.88 (s, 3H). ^{13}C NMR (101 MHz, CDCl_3) δ 149.1, 141.6, 138.2, 129.7, 129.6, 129.0, 125.0, 123.3, 119.8, 112.1, 62.3, 56.5. HPLC [Daicel Chiraldak AD-H, hexane/*i*-PrOH = 90/10, 220 nm, 1.0 mL/min. $t_{\text{R}1}$ = 17.8 min (minor), $t_{\text{R}2}$ = 20.6 min (major)]; ee = 95%.

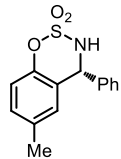
(R)-6-Methoxy-4-phenyl-3,4-dihydrobenzo[e][1,2,3]oxathiazine-2,2-dioxide (3ca).⁴

White solid, 56.0 mg, yield: 96%. ^1H NMR (400 MHz, CDCl_3) δ 7.47 – 7.31 (m, 5H), 6.99 (d, J = 9.0 Hz, 1H), 6.86 (dd, J = 9.0, 3.0 Hz, 1H), 6.30 (d, J = 2.9 Hz, 1H), 5.85 (d, J = 8.6 Hz, 1H), 4.86 (d, J = 8.6 Hz, 1H), 3.65 (s, 3H). ^{13}C NMR (101 MHz, CDCl_3) δ 156.7, 145.5, 138.0, 129.8, 129.7, 129.1, 123.1, 120.0, 115.4, 113.5, 62.3, 55.9. HPLC [Enantiocor Chiral OX-3, hexane/*i*-PrOH = 90/10, 220 nm, 1.0 mL/min. $t_{\text{R}1}$ = 31.4 min (minor), $t_{\text{R}2}$ = 38.9 min (major)]; ee = 95%.

(R)-8-Ethoxy-4-phenyl-3,4-dihydrobenzo[e][1,2,3]oxathiazine-2,2-dioxide (3da).

White solid, m.p.: 170–171 °C, 58.0 mg, yield: 95%. ^1H NMR (400 MHz, CDCl_3) δ 7.47 – 7.31 (m, 5H), 6.97 (t, J = 8.1 Hz, 1H), 6.85 (d, J = 8.1 Hz, 1H), 6.35 (d, J = 7.9 Hz, 1H), 5.89 (d, J = 8.6 Hz, 1H), 4.86 (d, J = 8.6 Hz, 1H), 4.05 (q, J = 7.2 Hz, 2H), 1.41 (t, J = 7.0 Hz, 3H). ^{13}C NMR (101 MHz, CDCl_3) δ 148.5, 141.7, 138.3, 129.7, 129.6, 129.0, 124.9, 123.3, 119.7, 113.2, 65.2, 62.4, 14.9. HPLC [Daicel Chiraldak IC-3, hexane/*i*-PrOH = 90/10, 220 nm, 1.0 mL/min. $t_{\text{R}1}$ = 12.8 min (minor), $t_{\text{R}2}$ = 31.0 min (major)]; ee = 97%, $[\alpha]^{20}_{\text{D}} = +1.8$ (c = 1.0, CHCl_3); HRMS (ESI) calcd for $\text{C}_{15}\text{H}_{16}\text{NO}_4\text{S}$ ($\text{M}+\text{H}$) $^+$ 306.0800, found 306.0807.

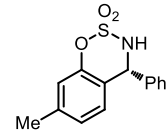
(R)-6-Methyl-4-phenyl-3,4-dihydrobenzo[e][1,2,3]oxathiazine-2,2-dioxide (3ea).⁴



White solid, 51.0 mg, yield: 93%. ¹H NMR (400 MHz, CDCl₃) δ 7.47 – 7.40 (m, 3H), 7.37 – 7.30 (m, 2H), 7.11 (dq, *J* = 8.4, 0.8 Hz, 1H), 6.94 (d, *J* = 8.4 Hz, 1H), 6.60 (d, *J* = 1.0 Hz, 1H), 5.85 (d, *J* = 8.6 Hz, 1H), 4.77 (d, *J* = 8.6 Hz, 1H). ¹³C NMR (101 MHz, CDCl₃) δ 149.7, 138.2, 135.3, 130.6, 129.7, 129.7, 129.0, 128.9, 121.8, 118.8, 62.2, 21.0. HPLC [Daicel Chiralpak IC-3, hexane/*i*-PrOH = 90/10, 220 nm, 1.0 mL/min. t_{R1} = 18.2 min (major), t_{R2} = 20.0 min (minor)]; ee = 92%.

(R)-7-Methyl-4-phenyl-3,4-dihydrobenzo[e][1,2,3]oxathiazine-2,2-dioxide(3fa).⁵

White solid, 49.5 mg, yield: 90%. ¹H NMR (400 MHz, CDCl₃) δ 7.47 – 7.38 (m, 3H), 7.37 – 7.30 (m, 2H), 6.89 (t, *J* = 8.0 Hz, 2H), 6.68 (d, *J* = 7.9 Hz, 1H), 5.85 (d, *J* = 8.6 Hz, 1H), 4.78 (d, *J* = 8.6 Hz, 1H), 2.34 (s, 3H). ¹³C NMR (101 MHz, CDCl₃) δ 151.5, 140.5, 138.3, 129.7, 129.6, 129.0, 128.5, 126.4, 119.2, 119.2, 62.0, 21.2. HPLC [Daicel Chiralpak IC-3, hexane/*i*-PrOH = 90/10, 220 nm, 1.0 mL/min. t_{R1} = 25.8 min (major), t_{R2} = 32.8 min (minor)]; ee = 96%.



(R)-7-Chloro-4-phenyl-3,4-dihydrobenzo[e][1,2,3]oxathiazine-2,2-dioxide(3ga).

Colorless gummy oil, 58.5 mg, yield: 99%. ¹H NMR (400 MHz, CDCl₃) δ 7.49 – 7.40 (m, 3H), 7.35 – 7.29 (m, 2H), 7.11 – 7.04 (m, 2H), 6.76 (d, *J* = 8.8 Hz, 1H), 5.85 (d, *J* = 8.7 Hz, 1H), 4.85 (d, *J* = 8.7 Hz, 1H). ¹³C NMR (101 MHz, CDCl₃) δ 152.0, 137.6, 135.3, 130.0, 129.8, 129.8, 129.0, 125.8, 120.9, 119.3, 61.9. HPLC [Daicel Chiralpak IC-3, hexane/*i*-PrOH = 90/10, 220 nm, 1.0 mL/min. t_{R1} = 11.1 min (major), t_{R2} = 12.6 min (minor)]; ee = 96%, [α]²⁰_D = +17.2 (c = 1.0, CHCl₃); HRMS (ESI) calcd for C₁₃H₁₀ClNO₃SnA (M+Na)⁺ 317.9968, found 317.9969.

(R)-6-Bromo-4-phenyl-3,4-dihydrobenzo[e][1,2,3]oxathiazine-2,2-dioxide(3ha).

White solid, m.p.: 155–156 °C, 59.0 mg, yield: 87%. ¹H NMR (400 MHz, CDCl₃) δ 7.56 – 7.40 (m, 4H), 7.37 – 7.29 (m, 2H), 6.95 (d, *J* = 8.8 Hz, 2H), 5.85 (d, *J* = 8.7 Hz, 1H), 4.87 (d, *J* = 8.7 Hz, 1H). ¹³C NMR (101 MHz, CDCl₃) δ 150.8, 137.2, 133.1, 131.4, 130.1, 129.9, 129.0, 124.3, 120.8, 118.2, 61.9. HPLC [Daicel Chiralpak IC-3, hexane/*i*-PrOH = 90/10, 220 nm, 1.0 mL/min. t_{R1} = 10.9 min (major), t_{R2} = 12.0 min (minor)]; ee = 95%, [α]²⁰_D = +84.2 (c = 1.0, CHCl₃); HRMS (ESI) calcd for C₁₃H₁₁BrNO₃S (M+H)⁺ 339.9643, found 339.9654.

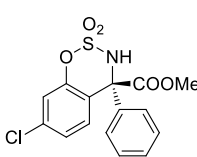
(R)-4-Phenyl-3,4-dihydronaphtho[2,1-*e*][1,2,3]oxathiazine-2,2-dioxide(3ia).

White solid, m.p.: 227–228 °C, 48.0 mg, yield: 77%. ¹H NMR (400 MHz, CD₃OD) δ 7.96 (d, *J* = 9.0 Hz, 1H), 7.91 – 7.85 (m, 1H), 7.44 – 7.15 (m, 9H), 6.35 (s, 1H). ¹³C NMR (101 MHz, DMSO-*d*6) δ 150.5, 139.3, 131.4, 130.9, 130.6, 128.8, 128.6, 128.3, 128.0, 127.0, 125.3, 124.2, 118.2, 114.5, 59.5. HPLC [Daicel Chiralpak IC-3, hexane/*i*-PrOH = 90/10, 220 nm, 1.0 mL/min. t_{R1} = 18.9 min (minor), t_{R2} = 22.0 min (major)]; ee = 98%, [α]²⁰_D = +26.7 (c = 1.0, CHCl₃); HRMS (ESI) calcd for C₁₇H₁₄NO₃S (M+H)⁺ 312.0694, found 312.0694.

(R)-1-Phenyl-1,2-dihydronaphtho[1,2-*e*][1,2,3]oxathiazine-3,3-dioxide (3ja).⁶

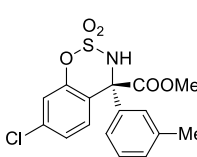
White solid, 51.7 mg, yield: 83%. ¹H NMR (400 MHz, CD₃OD) δ 7.97 (d, *J* = 9.0 Hz, 1H), 7.89 (d, *J* = 8.7 Hz, 1H), 7.48 – 7.12 (m, 9H), 6.35 (s, 1H). ¹³C NMR (101 MHz, DMSO-*d*6) δ 150.5, 139.3, 131.4, 130.9, 130.6, 128.8, 128.6, 128.3, 128.0, 127.0, 125.3, 124.2, 118.2, 114.5, 59.4. HPLC [Daicel Chiralpak IC-3, hexane/*i*-PrOH = 90/10, 220 nm, 1.0 mL/min. t_{R1} = 27.2 min (minor), t_{R2} = 30.7 min (major)]; ee = 97%.

(R)-Methyl-7-chloro-4-phenyl-3,4-dihydrobenzo[e][1,2,3]oxathiazine-4-carboxylate-2,2-dioxide (3ka).



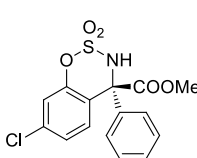
White solid, m.p.: 158–159 °C, 51.5 mg, yield: 73%. ^1H NMR (400 MHz, CDCl_3) δ 7.43 – 7.31 (m, 4H), 7.23 – 7.17 (m, 3H), 7.15 (d, J = 2.0 Hz, 1H), 6.44 (s, 1H), 3.90 (s, 3H). ^{13}C NMR (101 MHz, CDCl_3) δ 170.5, 151.4, 139.0, 136.5, 131.9, 129.5, 129.0, 127.6, 125.7, 120.0, 117.7, 71.2, 54.9. HPLC [Daicel Chiraldak AD-H, hexane/*i*-PrOH = 90/10, 210 nm, 1.0 mL/min. t_{R1} = 14.0 min (major), t_{R2} = 35.7 min (minor)]; ee = 99.5%, $[\alpha]^{20}_{\text{D}} = +5.5$ (c = 0.6, CHCl_3); HRMS (ESI) calcd for $\text{C}_{15}\text{H}_{13}\text{ClNO}_5\text{S}$ ($\text{M}+\text{H}$) $^+$ 354.0203, found 354.0205.

(R)-Methyl-7-chloro-4-(*m*-tolyl)-3,4-dihydrobenzo[e][1,2,3]oxathiazine-4-carboxylate-2,2-dioxide (3ke).



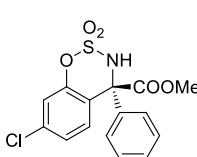
Yellow oil, 58.7 mg, yield: 80%. ^1H NMR (400 MHz CDCl_3) δ = 7.38 (d, J = 8.6, Hz, 1H), 7.25 – 7.12 (m, 4H), 7.00 (dd, J = 5.5, 4.8 Hz, 2H), 6.42 (s, 1H), 3.89 (s, 3H), 2.32 (s, 3H). ^{13}C NMR (100 MHz CDCl_3) δ 170.6, 151.3, 139.0, 136.4, 132.2, 130.4, 128.9, 128.1, 125.7, 124.7, 119.9, 118.1, 71.3, 54.8, 21.8. HPLC [Daicel Chiraldak AD-H, hexane/*i*-PrOH = 90/10, 210 nm, 1.0 mL/min. t_{R1} = 11.9 min (major), t_{R2} = 19.4 min (minor)]; ee = 99.8%, $[\alpha]^{20}_{\text{D}} = +7.6$ (c = 0.5, CHCl_3); HRMS (ESI) calcd for $\text{C}_{16}\text{H}_{15}\text{ClNO}_5\text{S}$ ($\text{M}+\text{H}$) $^+$ 368.0359, found 368.0361.

(R)-Methyl-7-chloro-4-(*p*-tolyl)-3,4-dihydrobenzo[e][1,2,3]oxathiazine-4-carboxylate-2,2-dioxide (3kf).



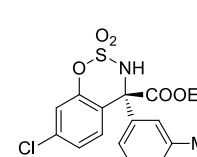
Yellow solid, m.p.: 152–153 °C, 55.8 mg, yield: 76%. ^1H NMR (400 MHz, CDCl_3) δ 7.41 (d, J = 8.4 Hz, 1H), 7.23 – 7.04 (m, 6H), 6.45 (s, 1H), 3.90 (s, 3H), 2.36 (s, 3H). ^{13}C NMR (101 MHz, CDCl_3) δ 170.6, 151.4, 139.6, 136.4, 136.2, 132.0, 129.7, 127.5, 125.7, 119.9, 118.0, 71.1, 54.9, 21.4. HPLC [Daicel Chiraldak AD-H, hexane/*i*-PrOH = 90/10, 210 nm, 1.0 mL/min. t_{R1} = 16.0 min (major), t_{R2} = 51.7 min (minor)]; ee = 99%, $[\alpha]^{20}_{\text{D}} = +7.0$ (c = 0.5, CHCl_3); HRMS (ESI) calcd for $\text{C}_{16}\text{H}_{15}\text{ClNO}_5\text{S}$ ($\text{M}+\text{H}$) $^+$ 368.0359, found 368.0363.

(R)-Methyl-4-(4-(*tert*-butyl)phenyl)-7-chloro-3,4-dihydrobenzo[e][1,2,3]oxathiazine-4-carboxylate-2,2-dioxide (3kg).



White solid, m.p.: 177–178 °C, 62.2 mg, yield: 76%. ^1H NMR (400 MHz, CDCl_3) δ 7.46 – 7.33 (m, 3H), 7.19 (dd, J = 8.8, 2.0 Hz, 1H), 7.16 – 7.10 (m, 3H), 6.41 (s, 1H), 3.90 (s, 3H), 1.32 (s, 9H). ^{13}C NMR (101 MHz, CDCl_3) δ 170.6, 152.6, 151.3, 136.3, 136.1, 132.4, 127.3, 126.1, 125.6, 119.8, 118.4, 71.2, 54.7, 34.9, 31.4. HPLC [Daicel Chiraldak AD-H, hexane/*i*-PrOH = 90/10, 210 nm, 1.0 mL/min. t_{R1} = 9.3 min (major), t_{R2} = 14.7 min (minor)]; ee = 99%, $[\alpha]^{20}_{\text{D}} = -6.7$ (c = 0.5, CHCl_3); HRMS (ESI) calcd for $\text{C}_{19}\text{H}_{20}\text{ClNNaO}_5\text{S}$ ($\text{M}+\text{Na}$) $^+$ 432.0648, found 432.0648.

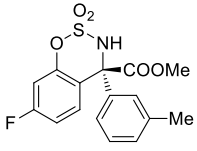
(R)-Ethyl-7-chloro-4-(*m*-tolyl)-3,4-dihydrobenzo[e][1,2,3]oxathiazine-4-carboxylate 2,2-dioxide (3le).



Colorless oil, 54.1 mg, yield: 71%. ^1H NMR (400 MHz, CDCl_3) δ 7.44 (d, J = 8.8 Hz, 1H), 7.32 – 7.16 (m, 3H), 7.13 (d, J = 2.0 Hz, 1H), 7.08 – 6.96 (m, 2H), 6.50 (s, 1H), 4.38 (q, J = 7.2 Hz, 2H), 2.34 (s, 3H), 1.29 (t, J = 7.2 Hz, 3H). ^{13}C NMR (101 MHz, CDCl_3) δ 170.0, 151.4, 139.2, 138.9, 136.3, 132.2, 130.2, 128.8, 128.2, 125.5, 124.7, 119.9, 118.0, 71.1, 64.5, 21.8, 14.1. HPLC [Daicel Chiraldak AD-H, hexane/*i*-PrOH = 90/10, 210 nm, 1.0 mL/min. t_{R1} = 11.0 min (major), t_{R2} = 15.4

min (minor)]; ee = 99%, $[\alpha]^{20}_D = +3.3$ ($c = 0.6$, CHCl_3); HRMS (ESI) calcd for $\text{C}_{17}\text{H}_{17}\text{ClNO}_5\text{S}$ ($\text{M}+\text{H}$) $^+$ 382.0516, found 382.0528.

(R)-methyl-7-fluoro-4-(*m*-tolyl)-3,4-dihydrobenzo[*e*][1,2,3]oxathiazine-4-carboxylate-2,2-dioxide (3me).



Colorless oil, 45.6 mg, yield: 65%. ^1H NMR (400 MHz, CDCl_3) δ 7.46 (dd, $J = 8.0, 6.0$ Hz, 1H), 7.26 (t, $J = 7.6$ Hz, 1H), 7.23 – 7.16 (m, 1H), 7.08 – 6.99 (m, 2H), 6.98 – 6.92 (m, 1H), 6.85 (dd, $J = 8.4, 2.4$ Hz, 1H), 6.46 (s, 1H), 3.90 (s, 3H), 2.34 (s, 3H). ^{13}C NMR (101 MHz, CDCl_3) δ 170.7, 163.2 (d, $J = 250.9$ Hz), 151.8, 139.1, 138.9, 132.6 (d, $J = 9.2$ Hz), 130.3, 128.9, 128.1, 124.7, 115.4, 113.0 (d, $J = 21.6$ Hz), 107.2 (d, $J = 25.4$ Hz), 71.2, 54.8, 21.8. HPLC [Daicel Chiralpak AD-H, hexane/*i*-PrOH = 90/10, 210 nm, 1.0 mL/min. $t_{\text{R}1} = 10.4$ min (major), $t_{\text{R}2} = 13.1$ min (minor)]; ee = 98%, $[\alpha]^{20}_D = -3.6$ ($c = 0.4$, CHCl_3); HRMS (ESI) calcd for $\text{C}_{16}\text{H}_{14}\text{FNNaO}_5\text{S}$ ($\text{M}+\text{Na}$) $^+$ 374.0474, found 374.0494.

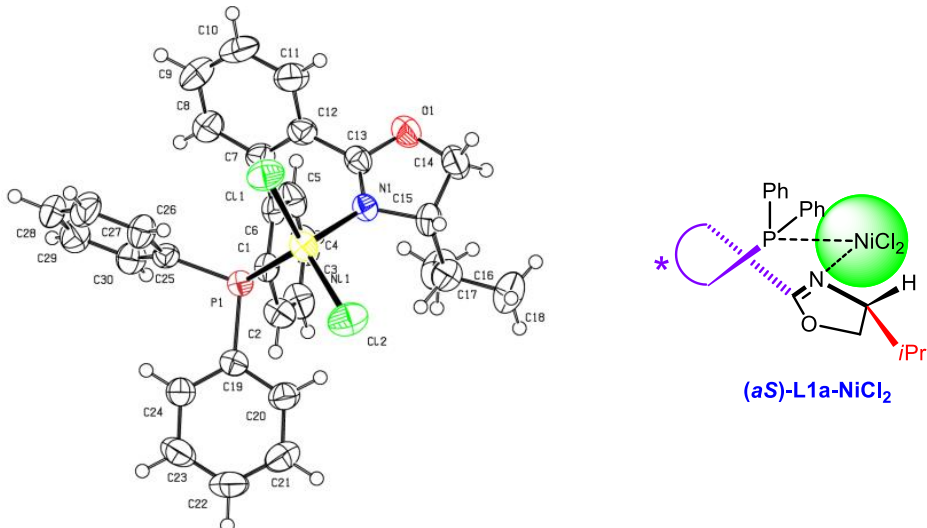
Gram scale reaction: To a 100 ml flask was charged with $\text{Ni}(\text{ClO}_4)_2 \cdot 6\text{H}_2\text{O}$ (100.0 mg, 0.273 mmol, 0.050 equiv), **L1a** (184.0 mg, 0.410 mmol, 0.075 equiv) and unpurified TFE (27.3 mL). The solution was stirred at 60 °C for 0.5 h, then substrate **1a** (1.00 g, 5.46 mmol, 1.0 equiv) and phenylboronic acid (1.00 g, 8.19 mmol, 1.5 equiv) were added into the flask. Another portion of TFE (27.3 mL) was added to the flask. After stirring at 60 °C for 48 h in air, the reaction mixture was cooled to room temperature and the solvent was removed by rotary evaporation. The residue was purified by column chromatography on silica gel (petroleum ether/EtOAc = 5/1) to give the desired product **3aa** as a white solid (1.31 g). The yield is 92% and ee is 95%.

5. Computational Details and Two Plausible Reaction Mechanisms.

All computations were carried out using the WB97XD method, as implemented in the Gaussian 09 software package.⁷ For nickel the GEN basis set with the associated effective Core Potential was employed.⁸ All other atoms were modeled at the 6-31G(d,p) level of theory.⁹

Geometry optimizations were performed with the account of the solvent effects (SMD, 2,2,2-Trifluoroethanol) without applying any geometry Constraints (C1 symmetry).

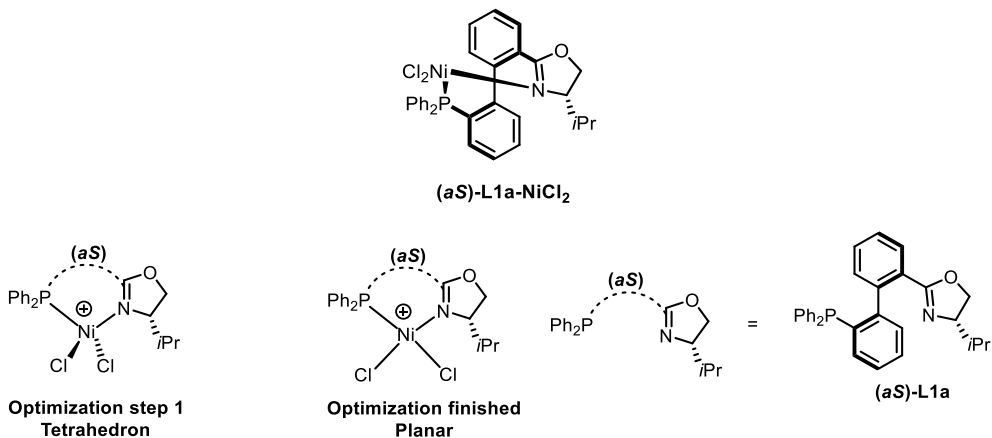
Based on our previous results, ligands exist as an equilibrium mixture of diastereomers in solution due to rotation around the internal bond of the biphenyl groups.¹⁰ Interestingly, when these ligands coordinate to palladium or iridium, only one of two possible diastereomeric complexes is formed. When nickel coordinates with **L1a**, two possible configurations of the Ni(II) complex can form: (*aS*)-**L1a-Ni(II)** and (*aR*)-**L1a-Ni(II)**. The formation of (*aR*)-**L1a-Ni(II)** is disfavored due to the steric hindrance of the *i*Pr group and the anion coordinated to Ni(II). However, the coordination behavior of the *tropos* phosphine-oxazoline biphenyl-Ni(II) complex in solvent could not be detected by NMR. The *tropos* phosphine-oxazoline biphenyl-Ni(II) complex was crystallized from EtOAc and X-ray diffraction analysis showed that its axial chirality has an *S* configuration and the coordination configuration is tetrahedron.

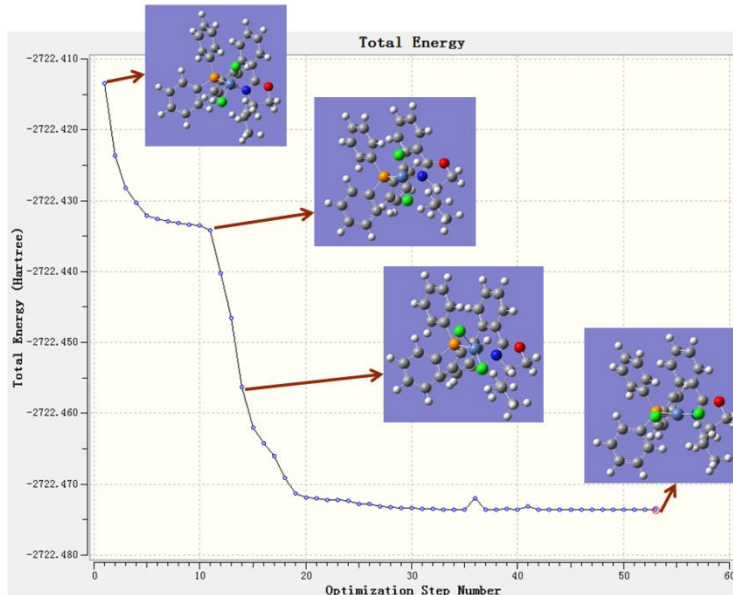


The calculations show that the configuration of the catalyst transforms from tetrahedron to planar in solution (Figure S1). The configuration is most likely different in solution and in the solid state. Reported DFT calculations also show that the configuration of Ni(II) in solution is planar.¹¹

Energies and Free Energies of Computed Structures

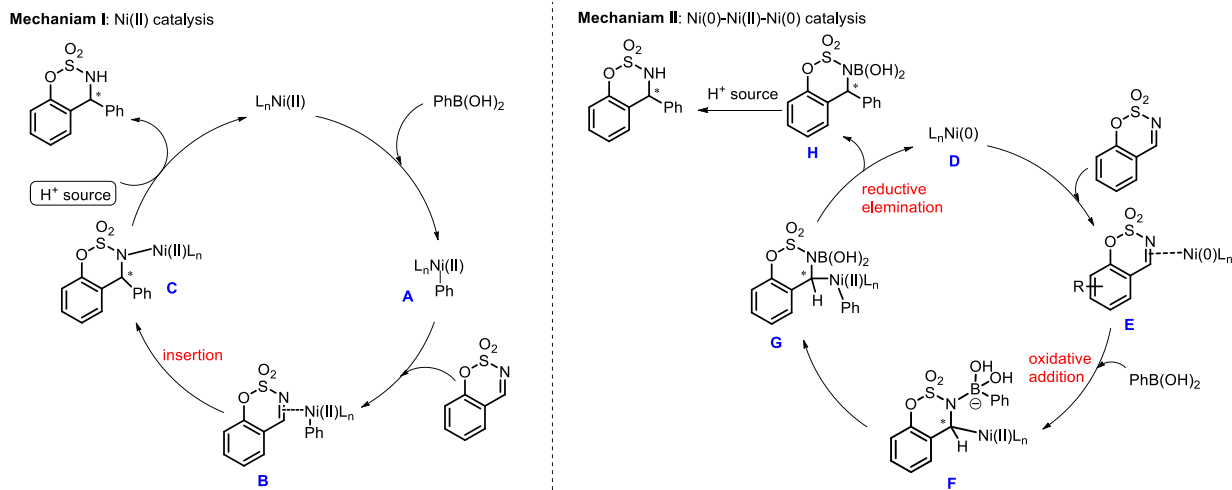
Figure S1. Optimization of (aS)-L1a-NiCl₂ in TFE.





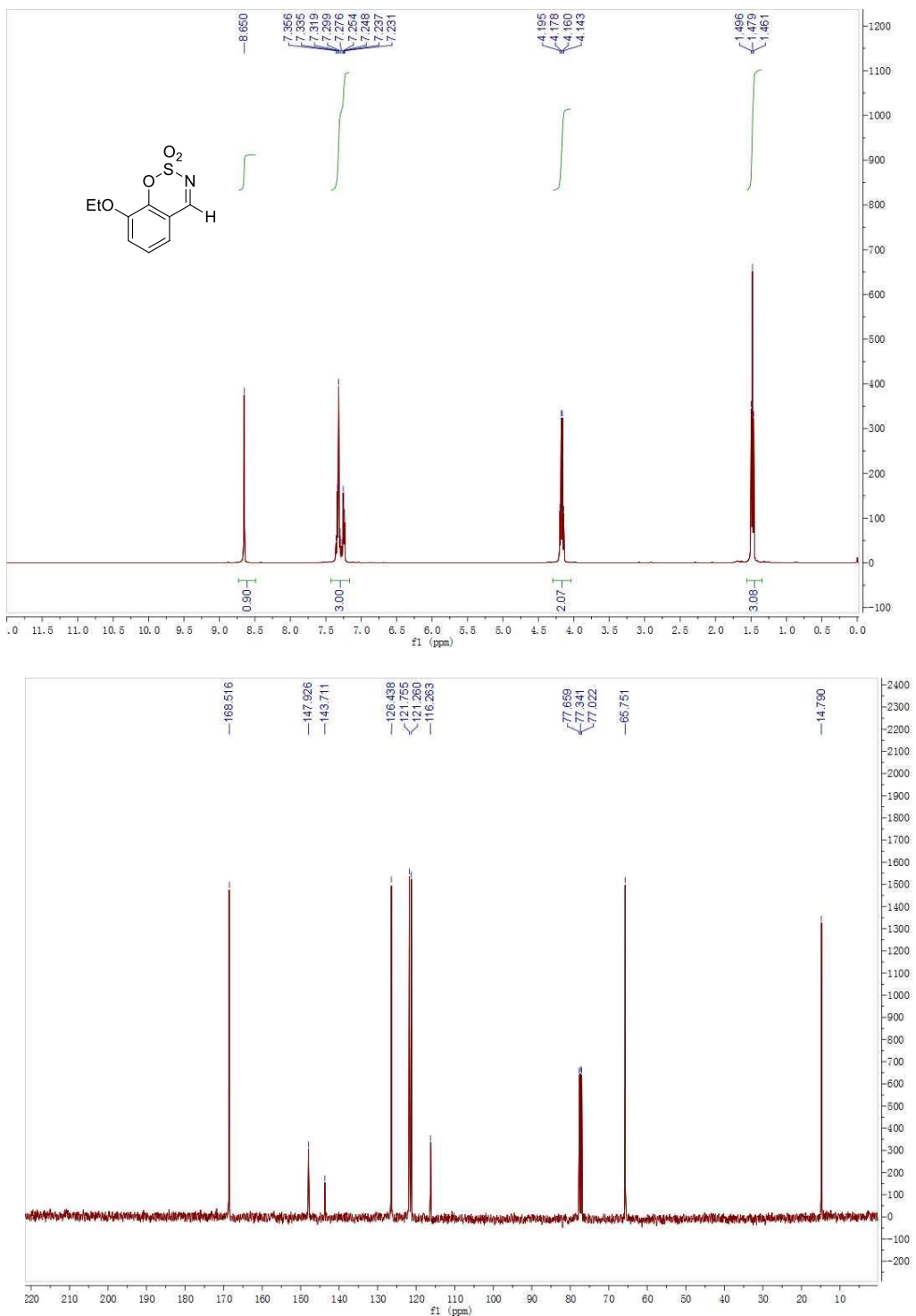
Compound	ZPVE Corrected Energy, a.u.	Free Energy (333 K), a.u.
(aS)-L1a-NiCl ₂	-2721.959189	-2722.036586

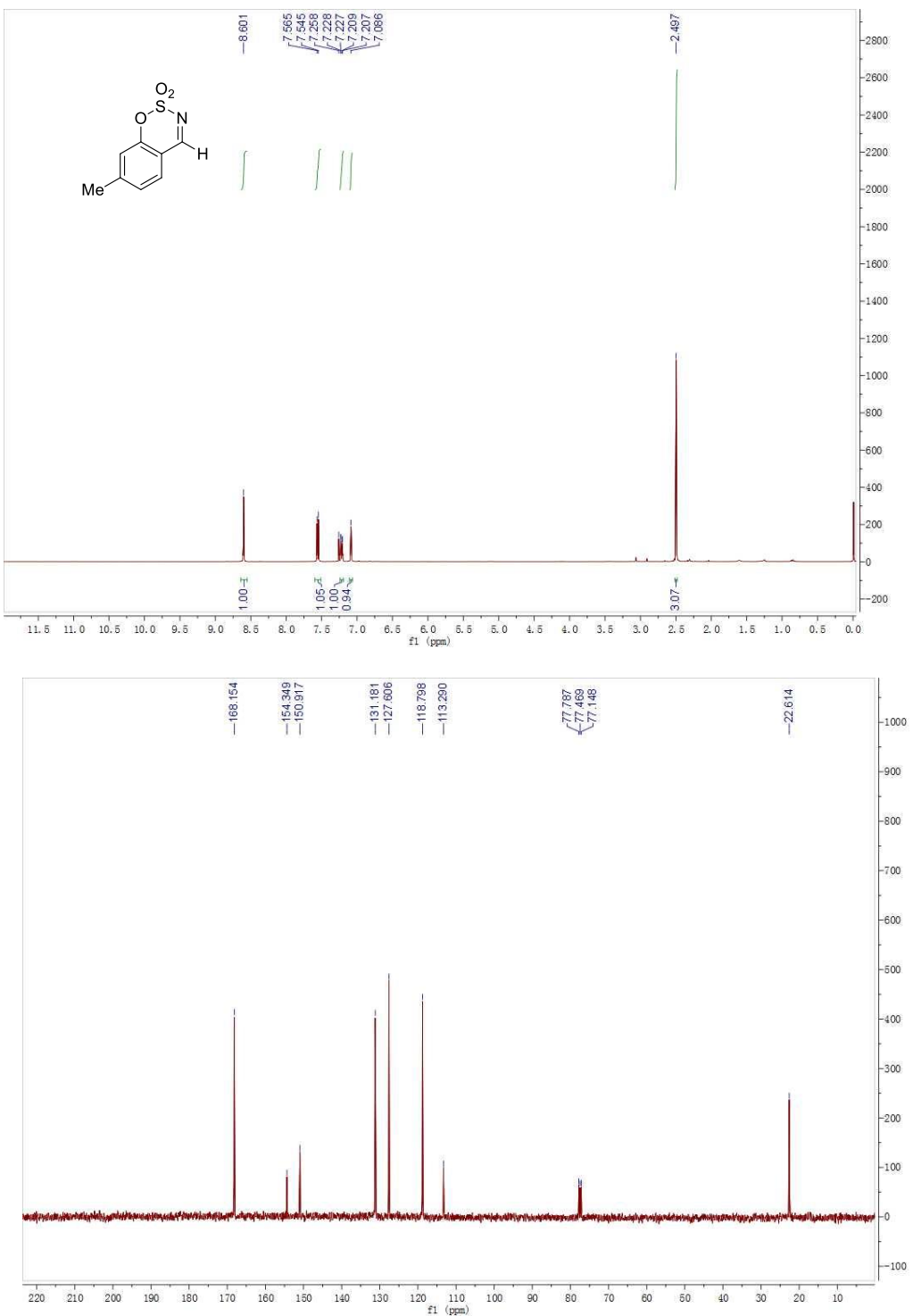
Scheme S1. Two plausible reaction mechanisms.

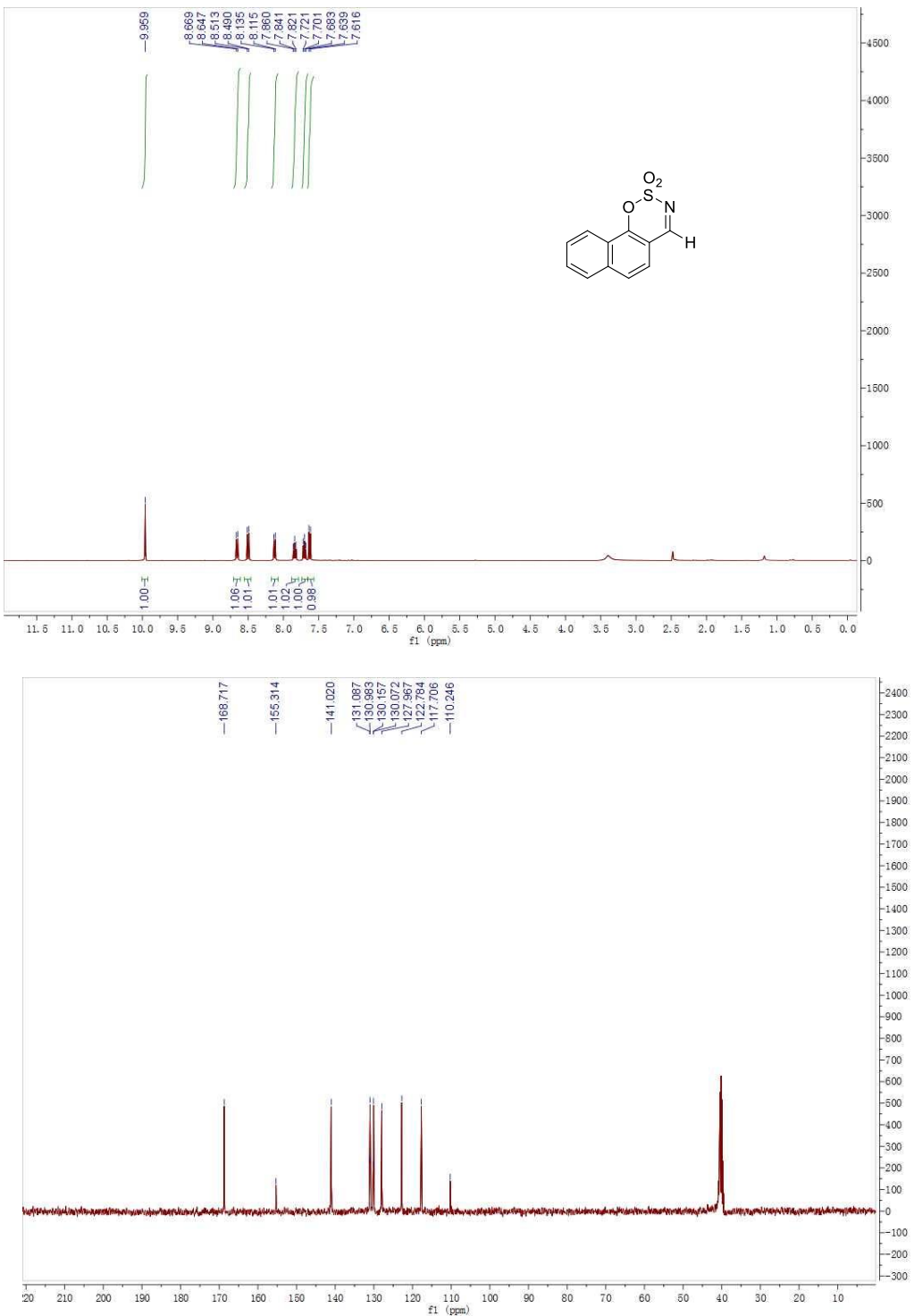


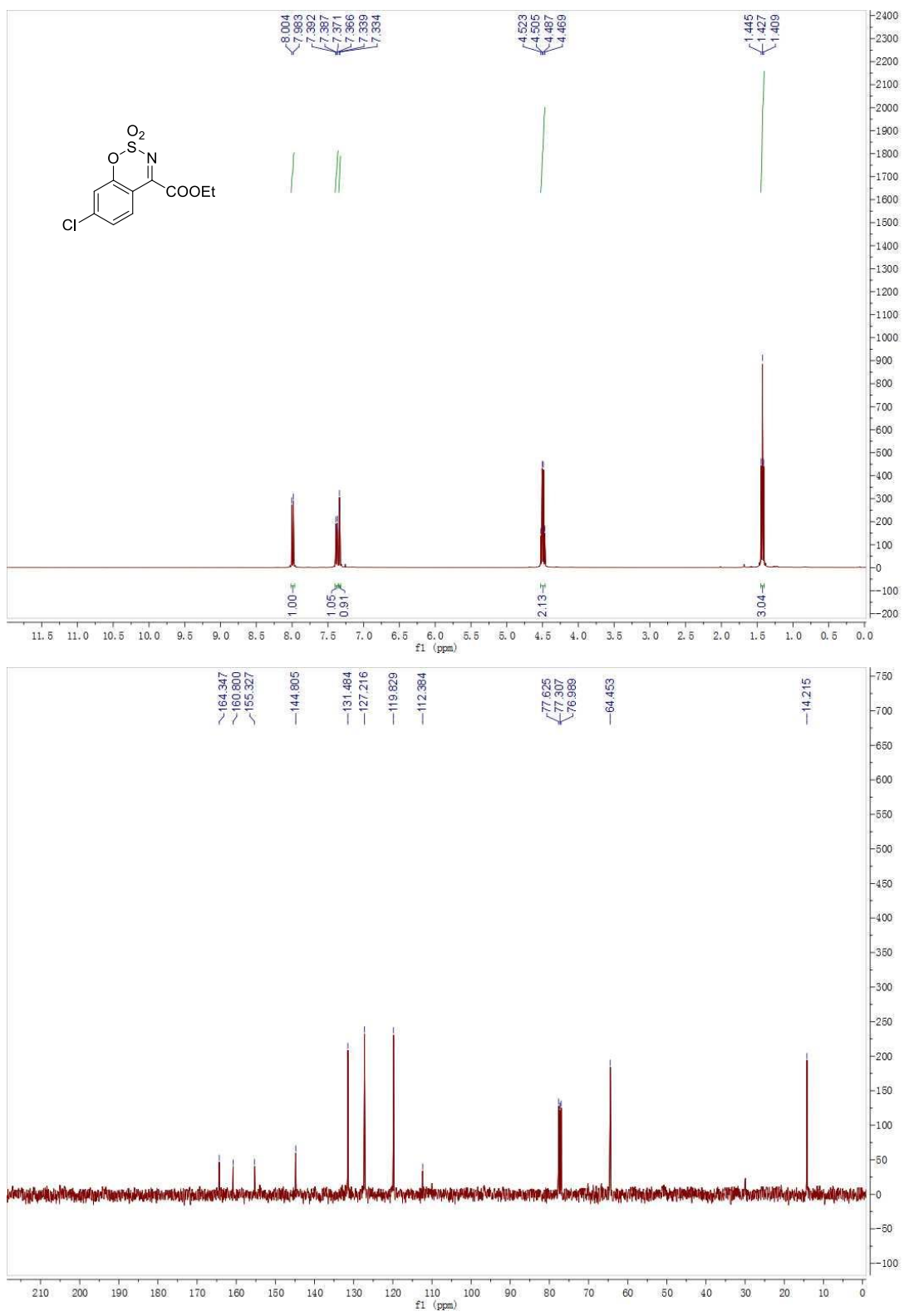
In mechanism I, as the first step, the cationic Ni(II)-**L1a** complex was converted to the Ph-Ni(II) intermediate **A** after transmetalation of phenylboronic acid. Then the substrate coordinates with nickel and the phenyl group inserts to the C=N bond. Finally a proton from the solvent transfers to the nitrogen atom to form the product following the release of the catalyst. According to reported additions of organoboron reagents to unsaturated compounds,¹² Mechanism II starts with the coordination of the substrate with Ni(0)-**L1a** (**E**). The phenylboronic acid then coordinates with the N atom of the substrate and followed by the oxidative addition to generate Ni(II)-intermediate **F**. Then the phenyl group transfers to nickel to form **G**. The catalyst **D** regenerates through reductive elimination of intermediate **G** with the formation of product-boronic acid species **H**. Protonation of **H** generates the desired product.

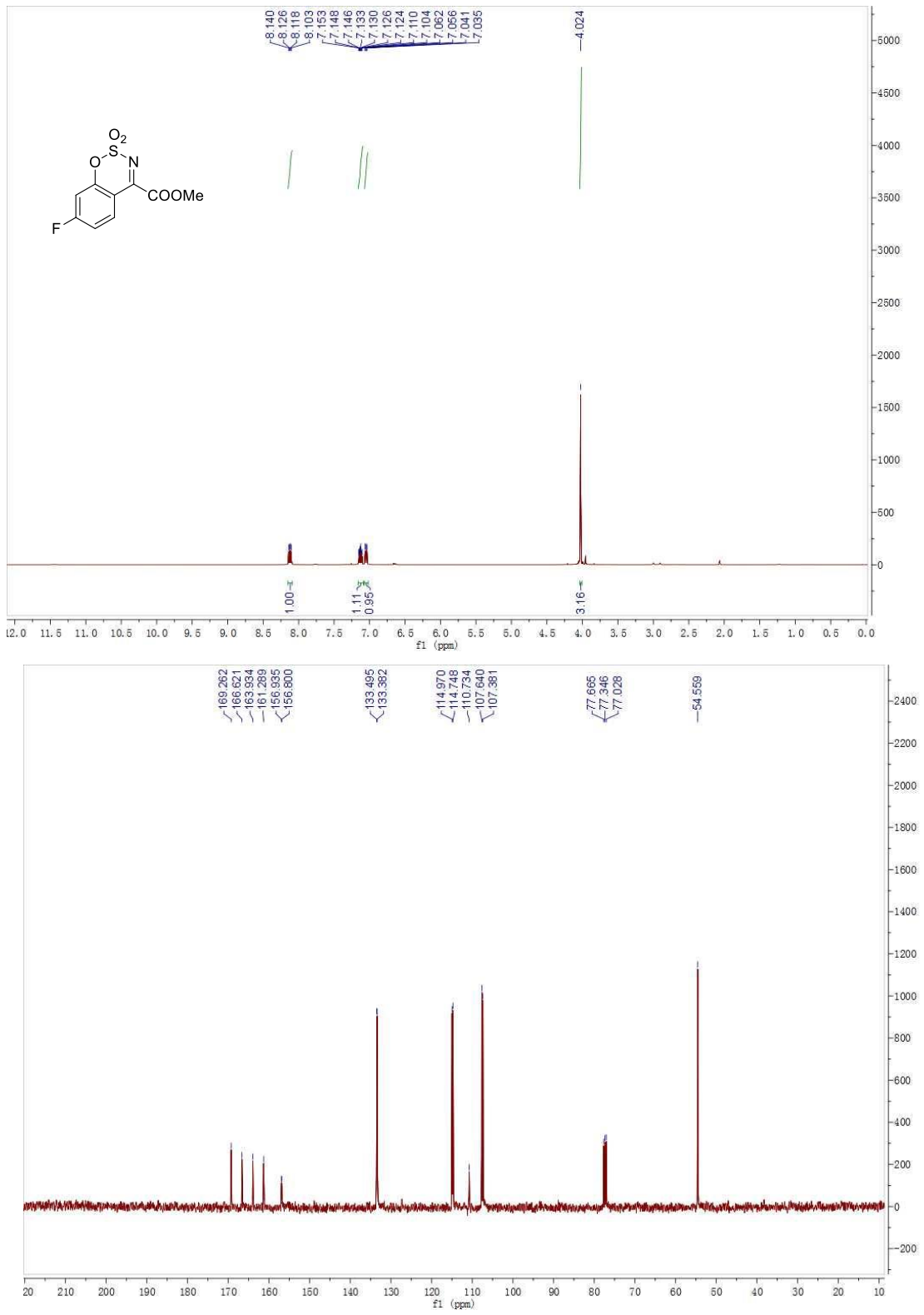
6. NMR Spectra

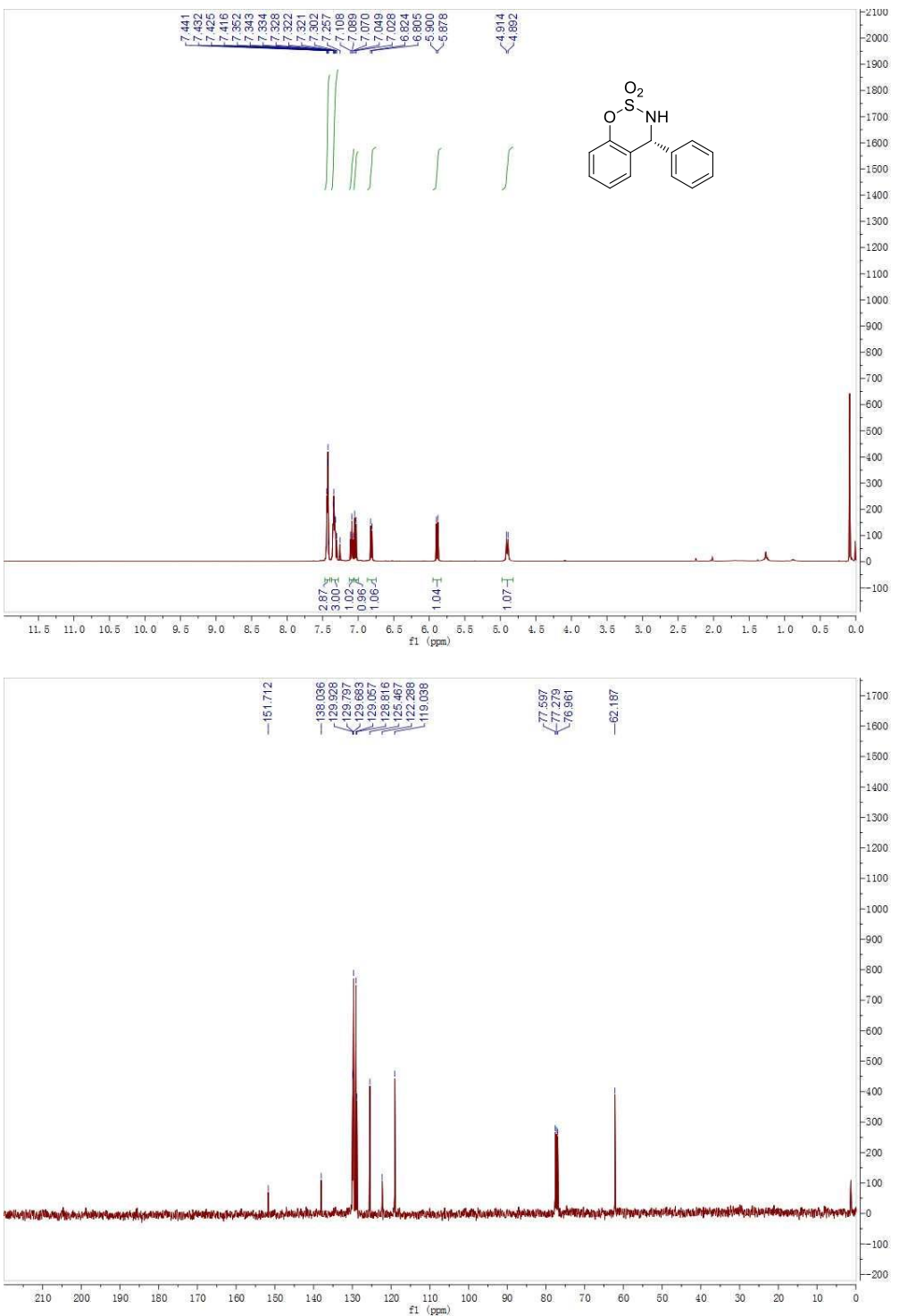


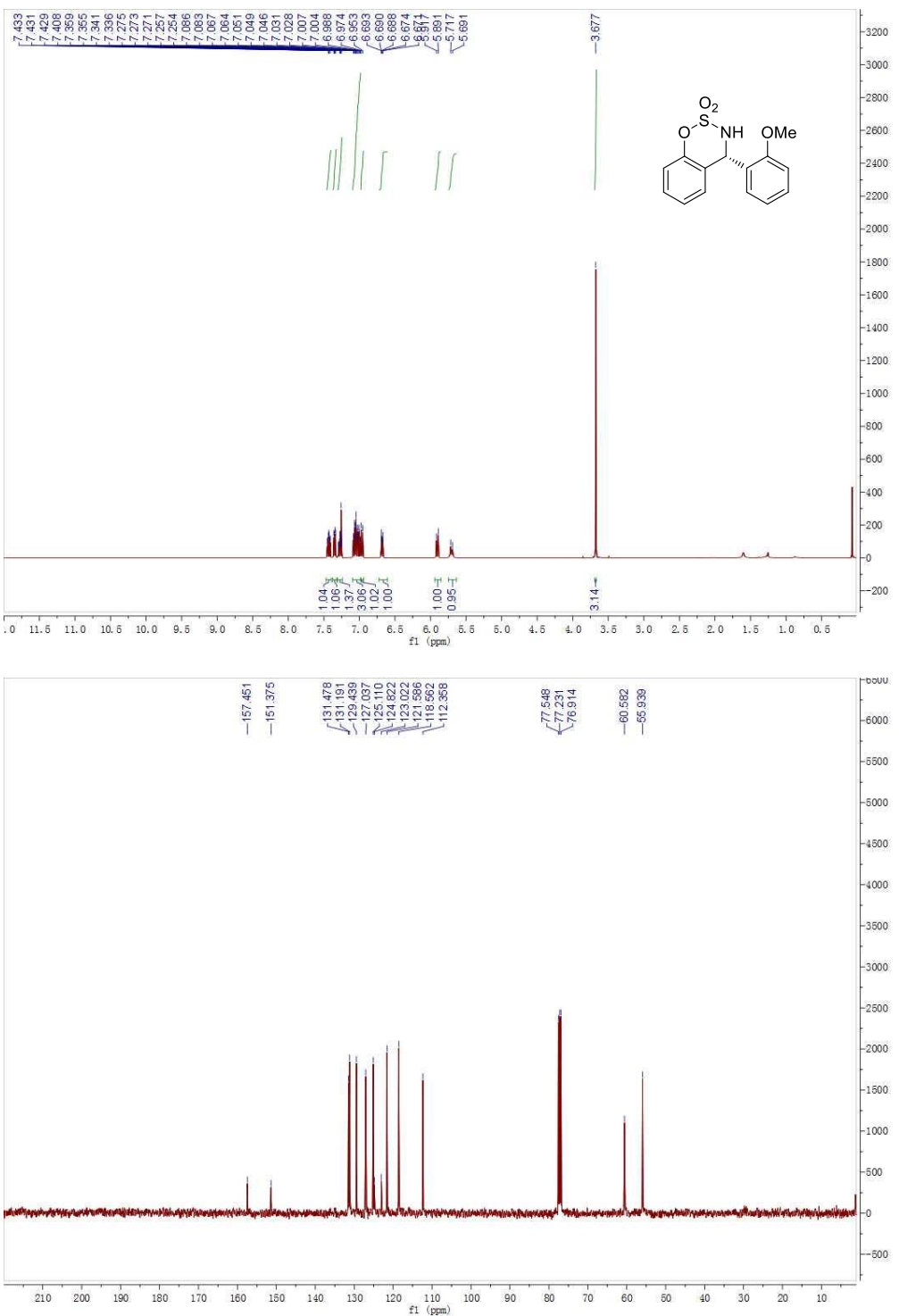


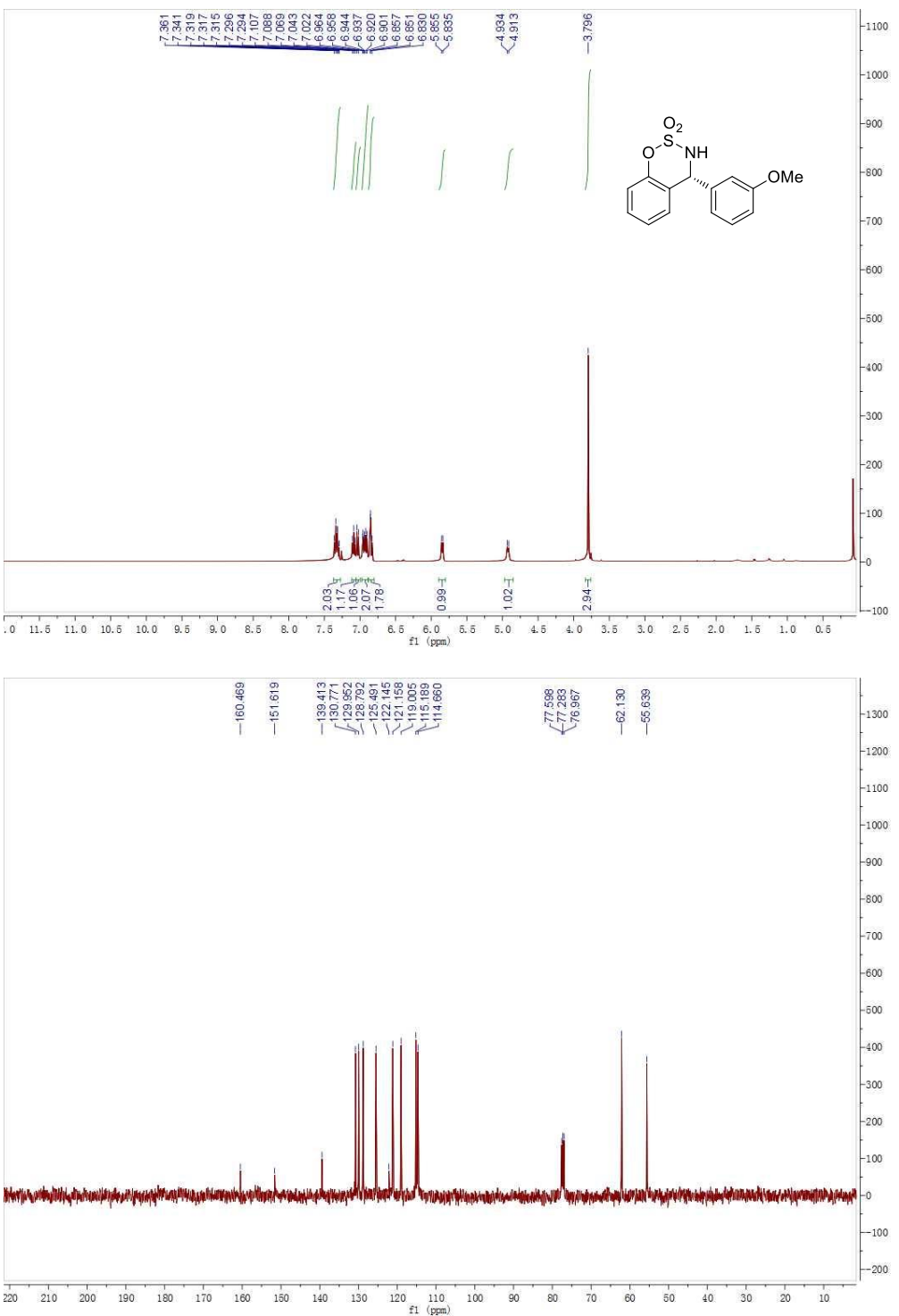


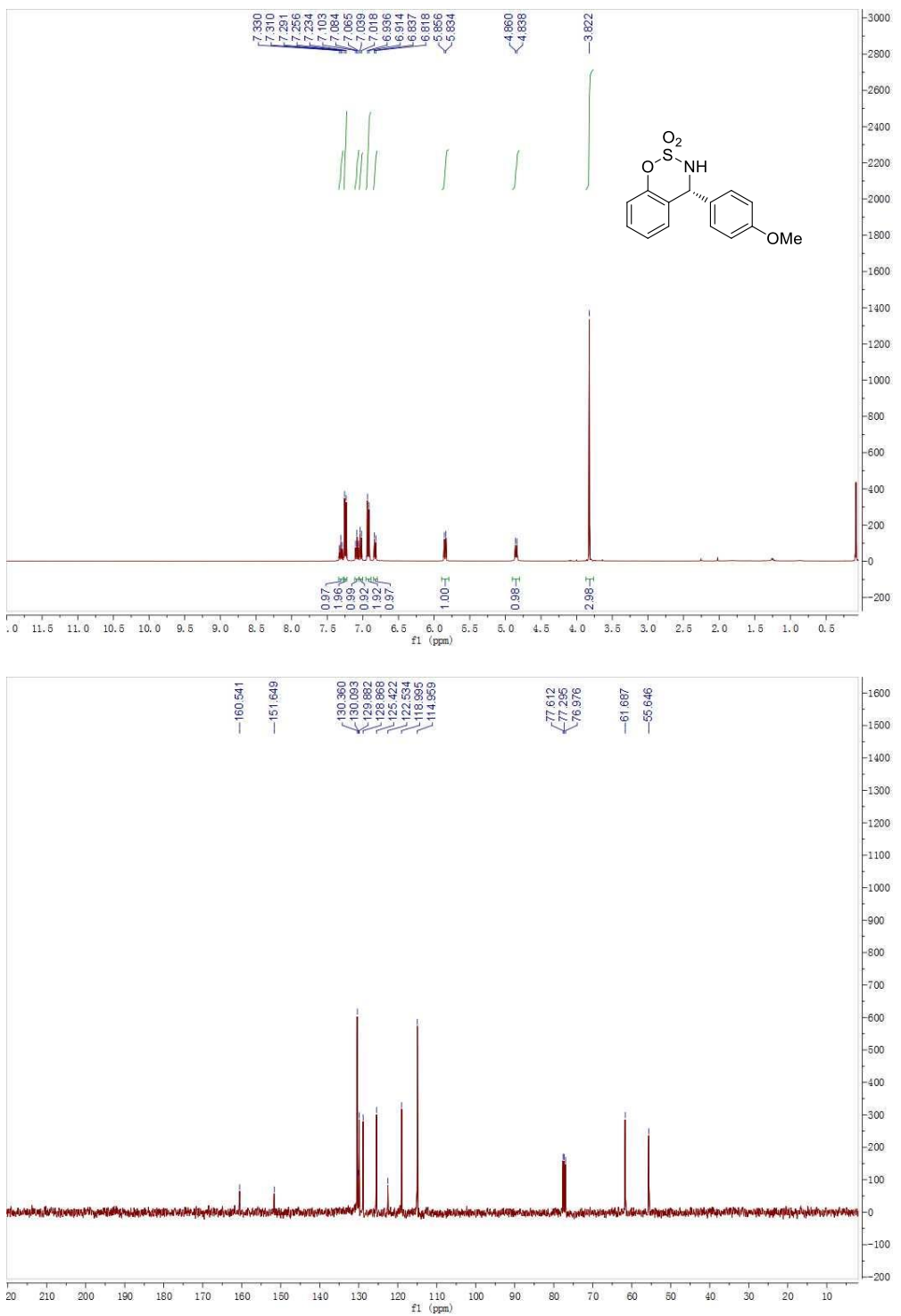


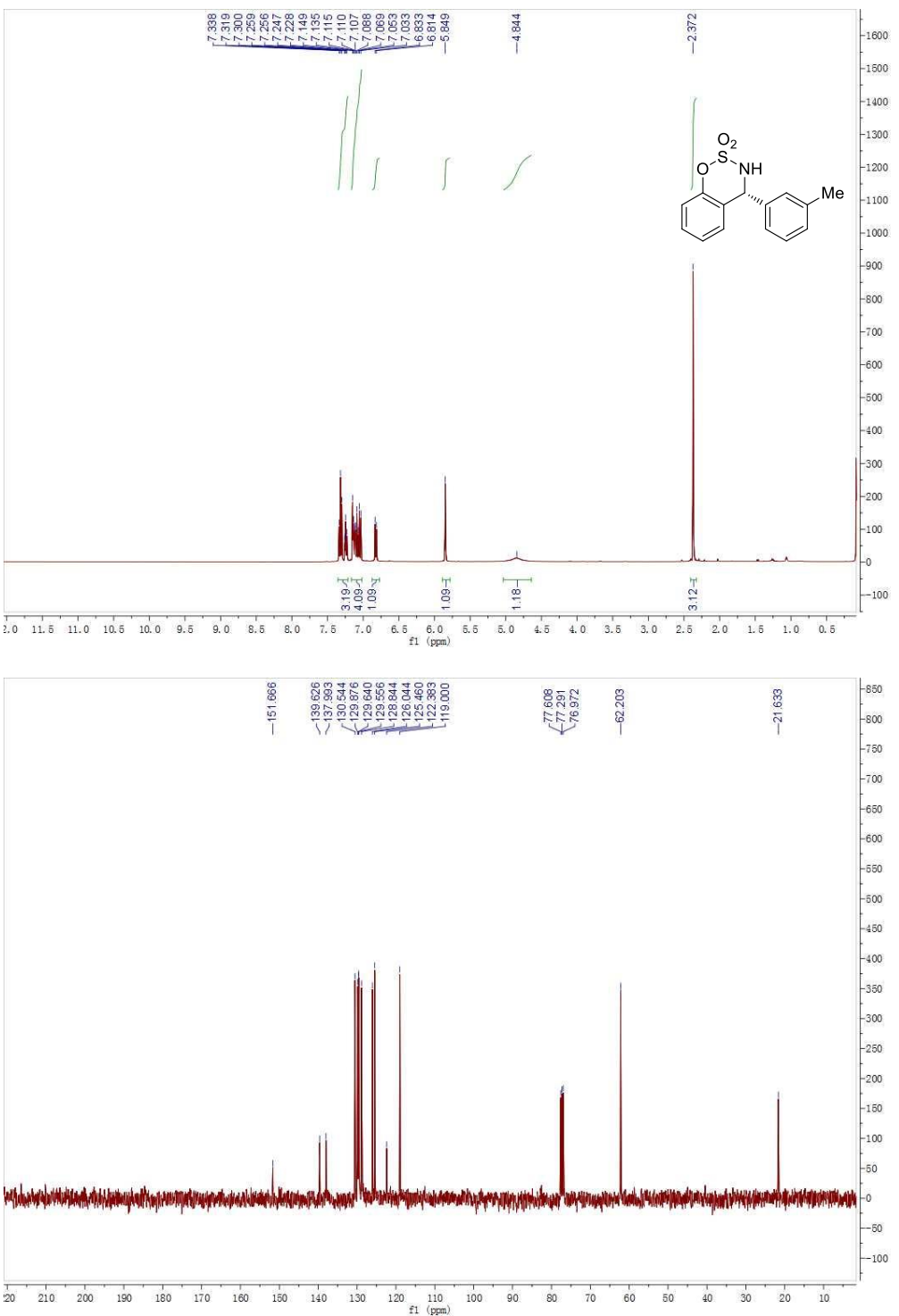


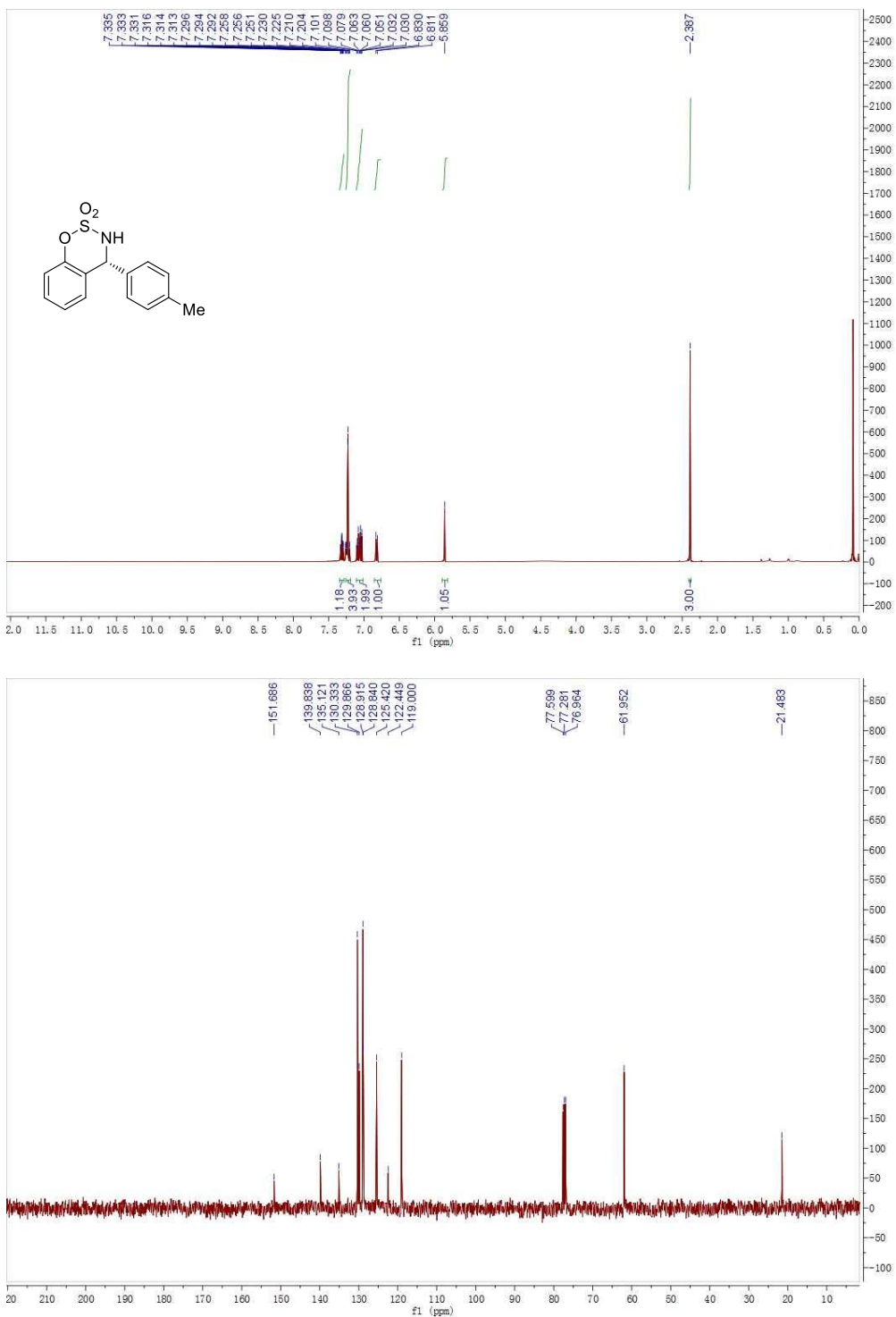


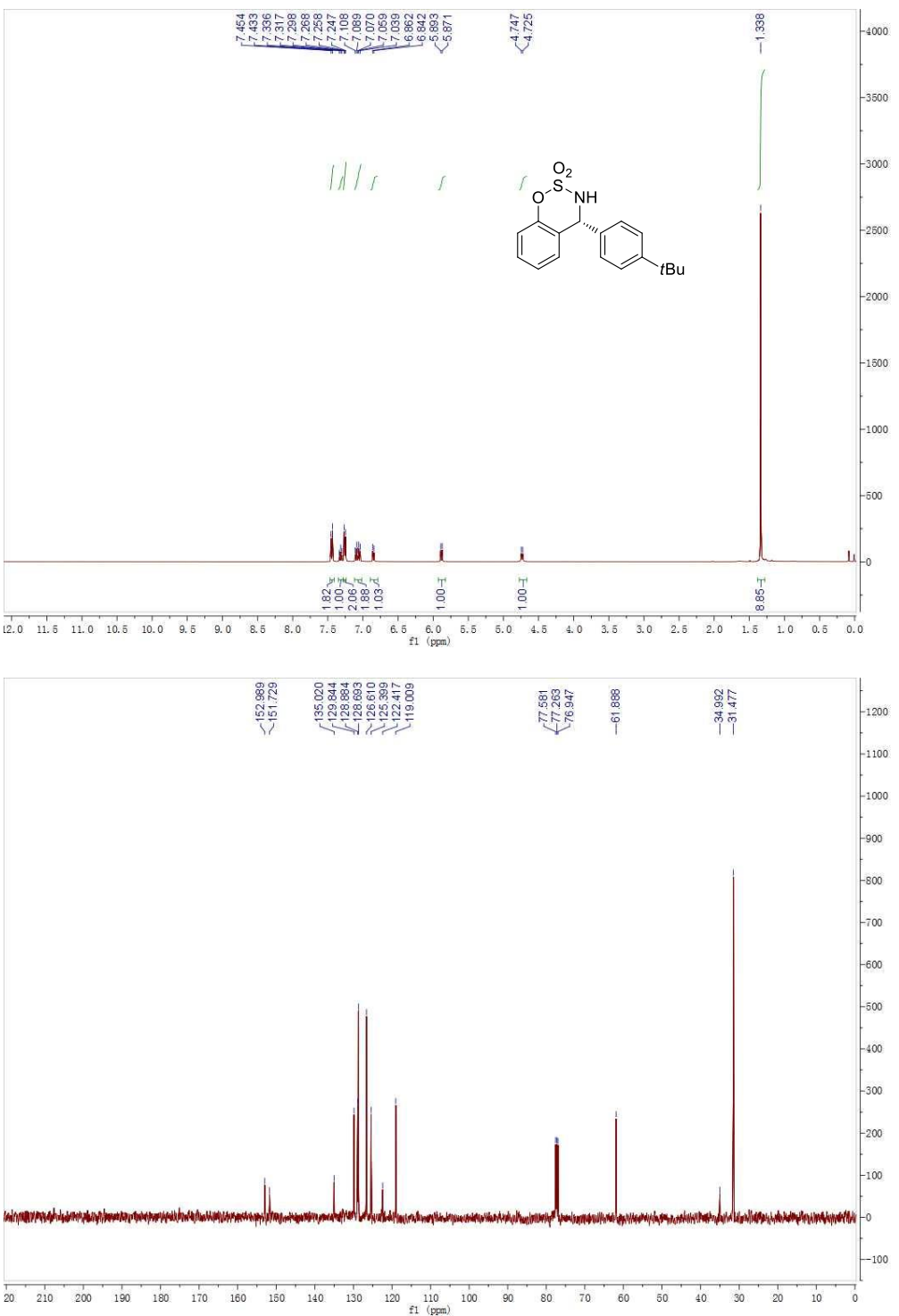


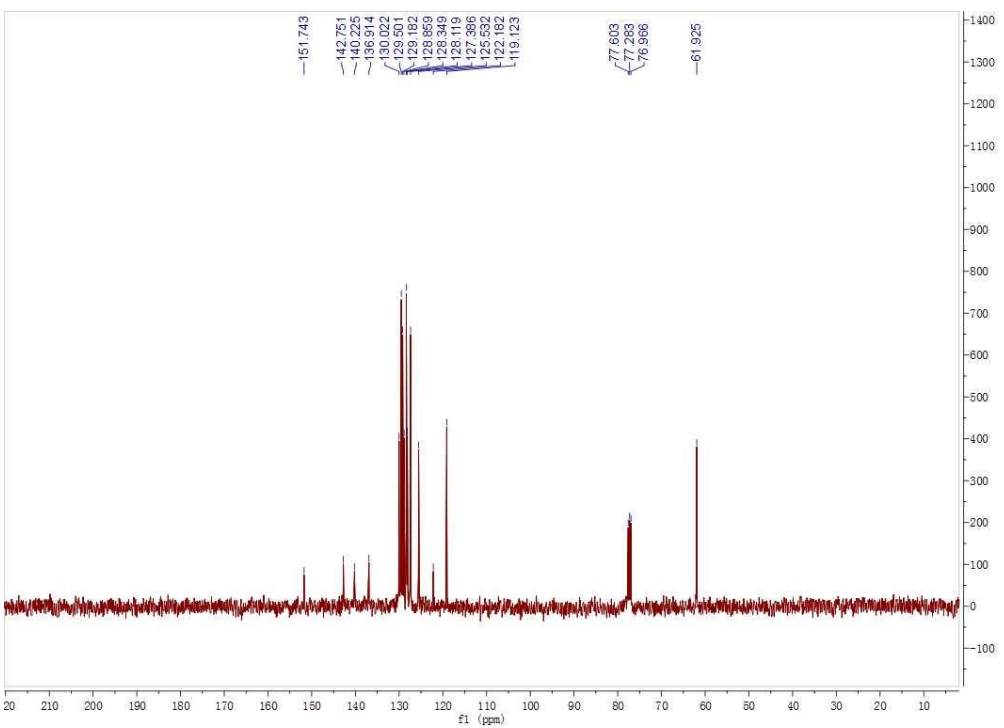
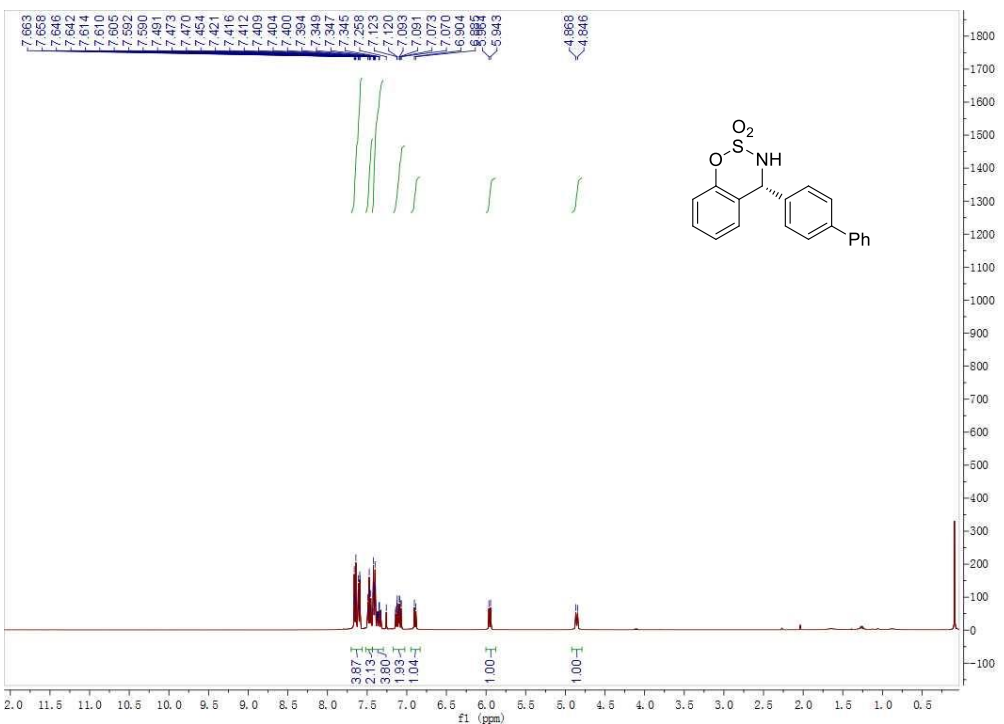


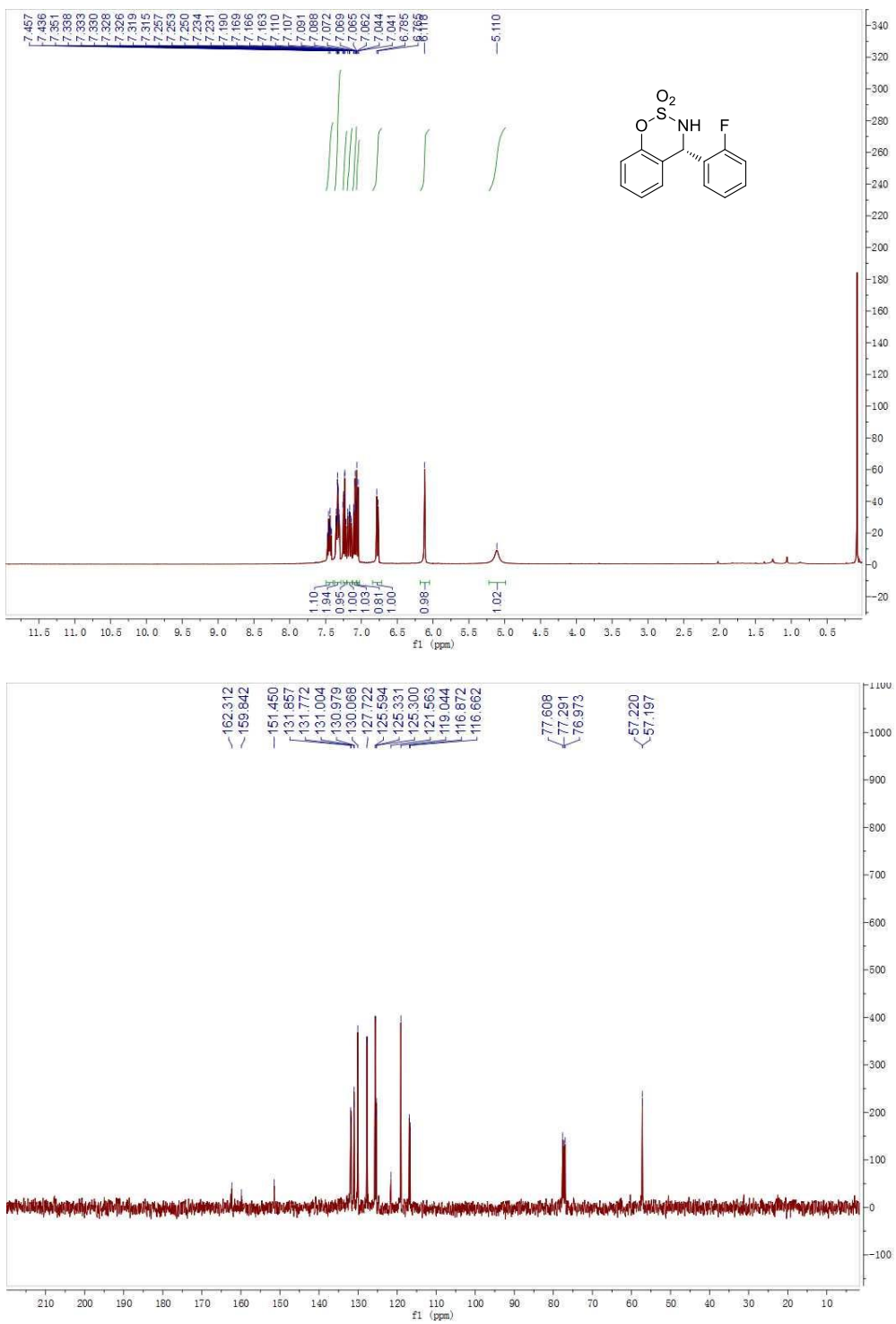


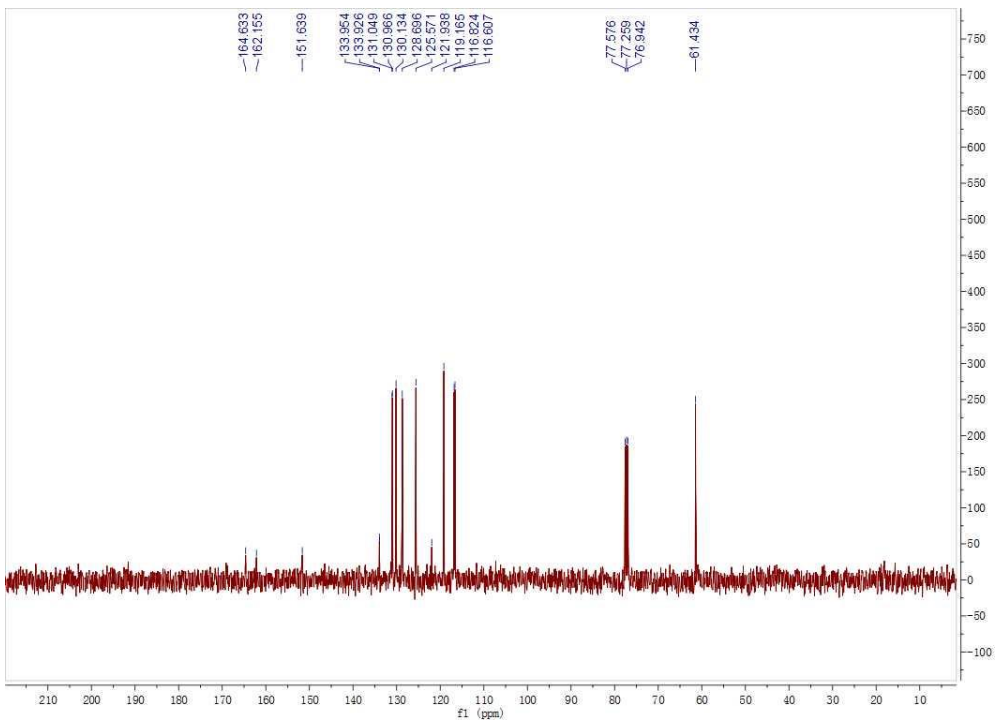
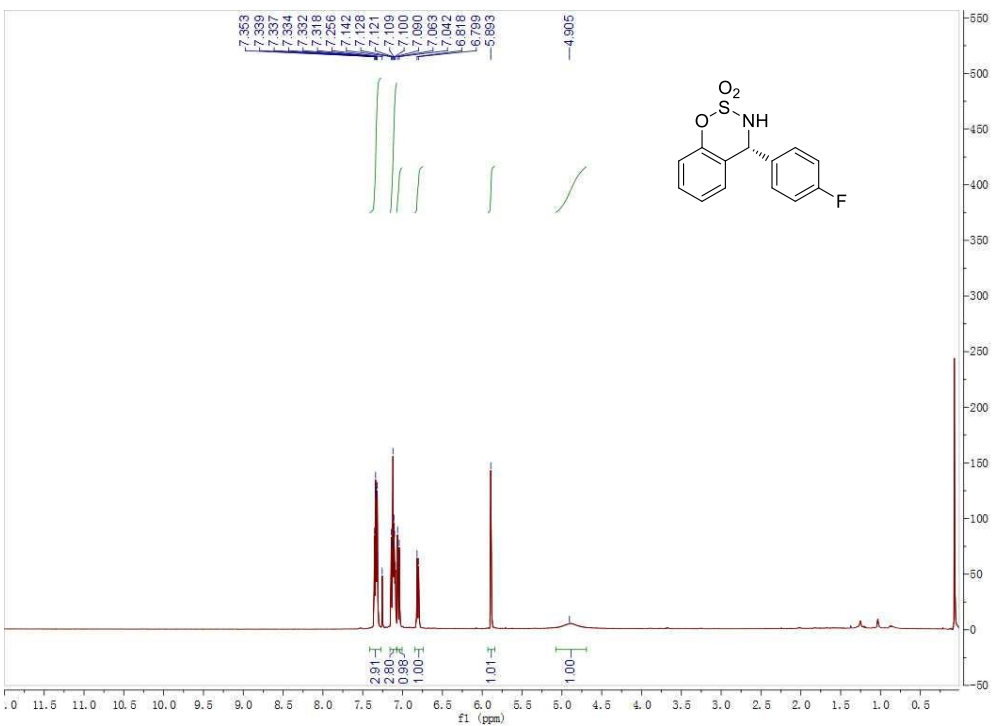


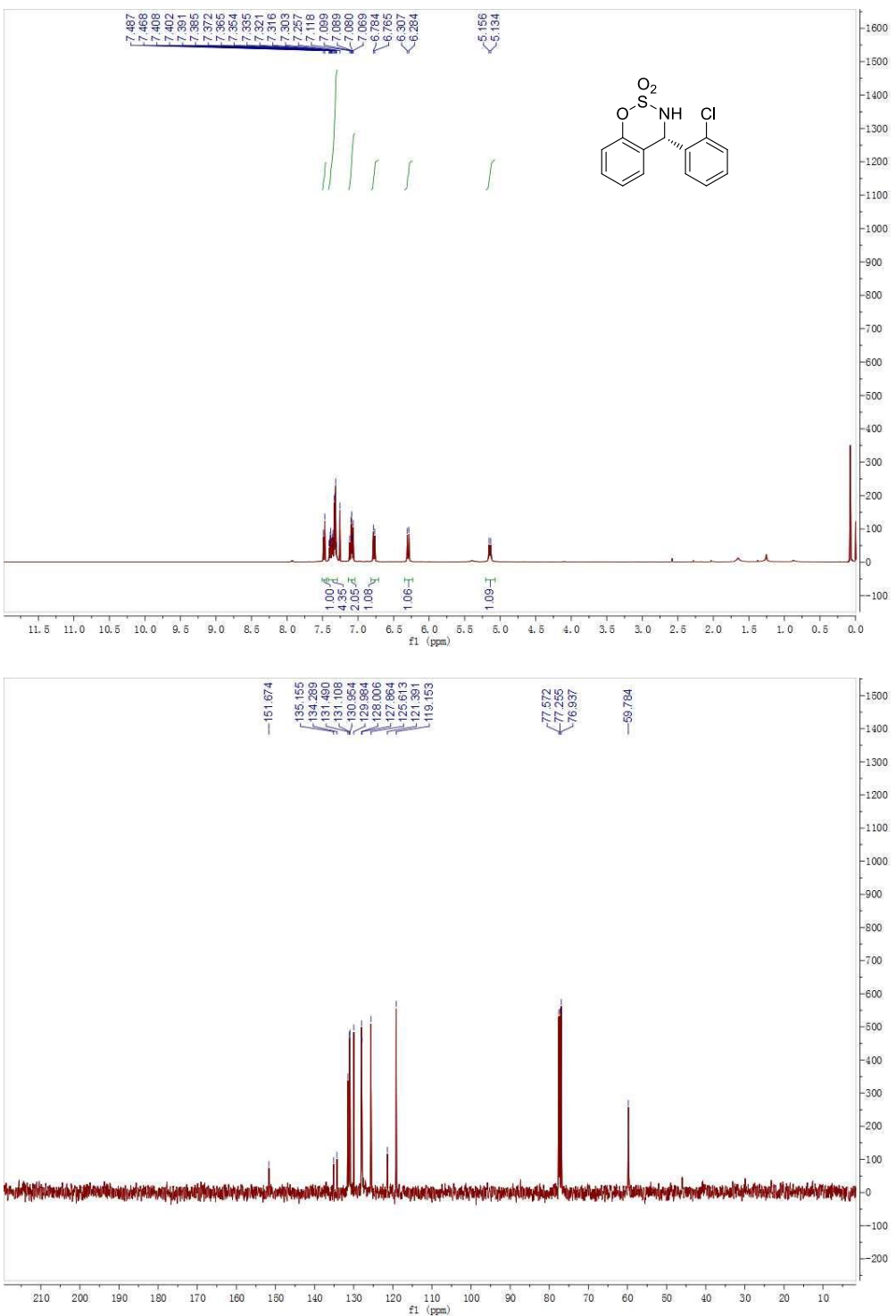


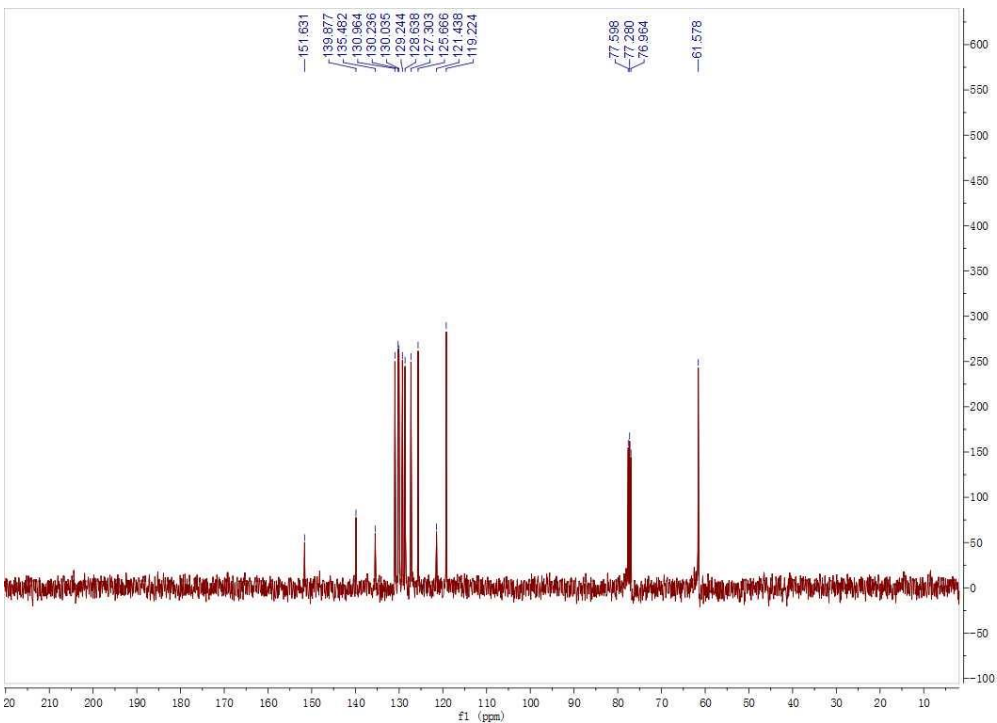
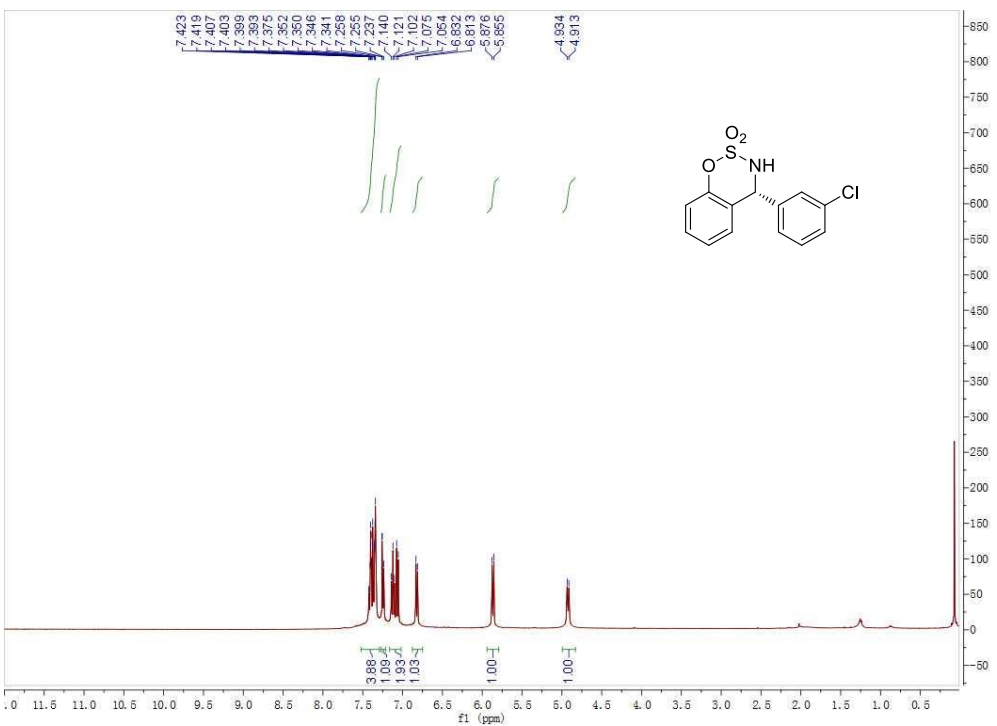


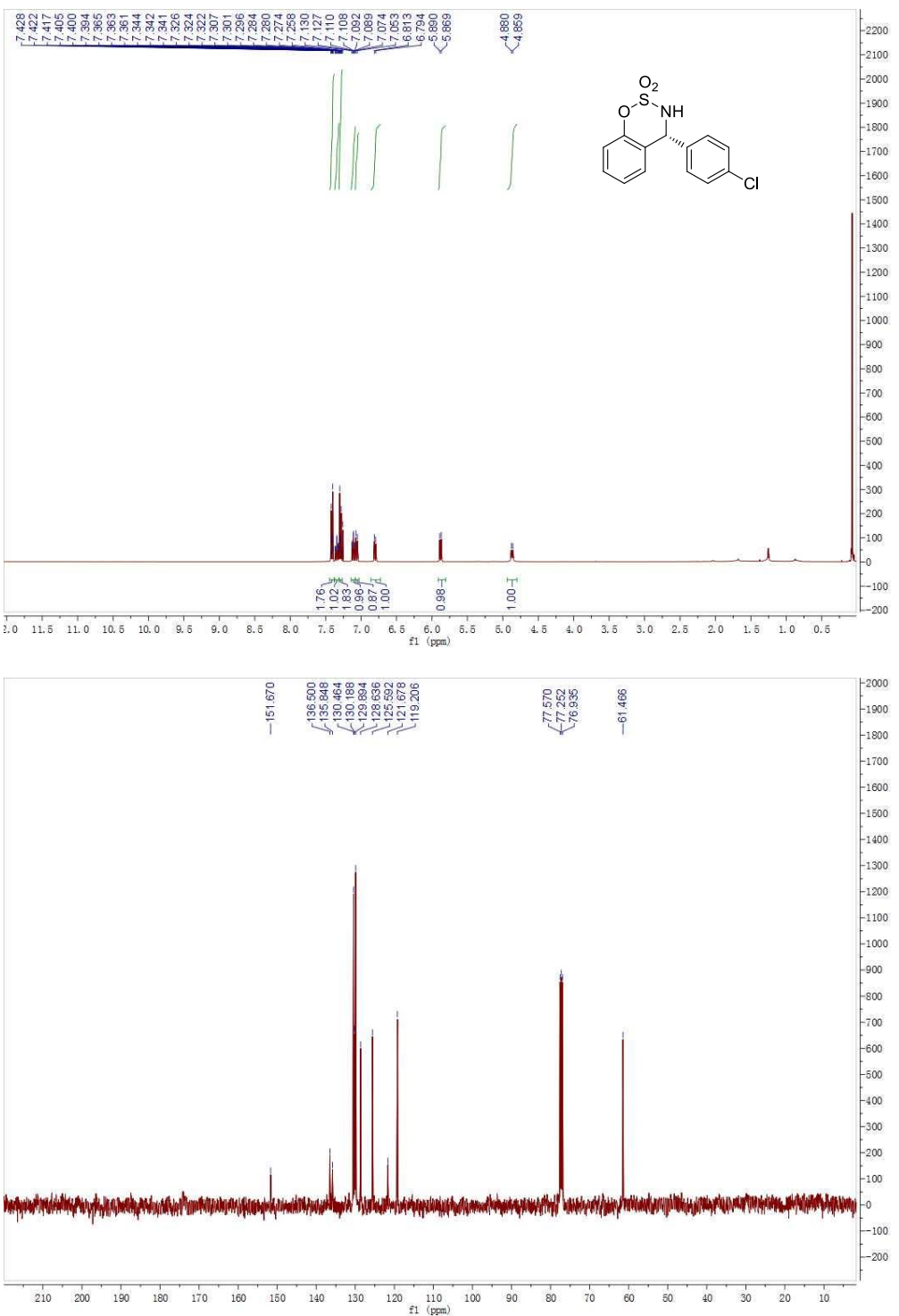


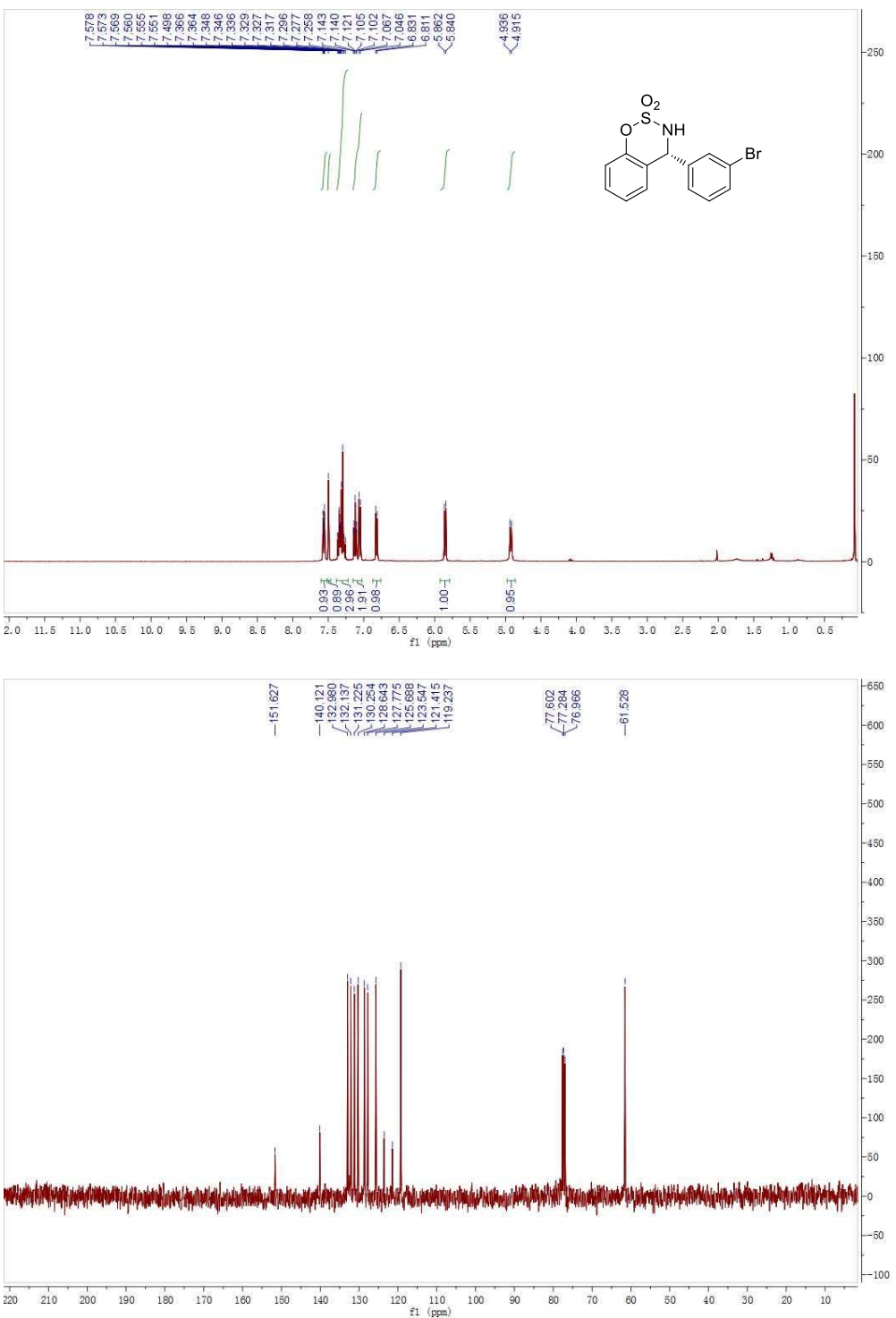


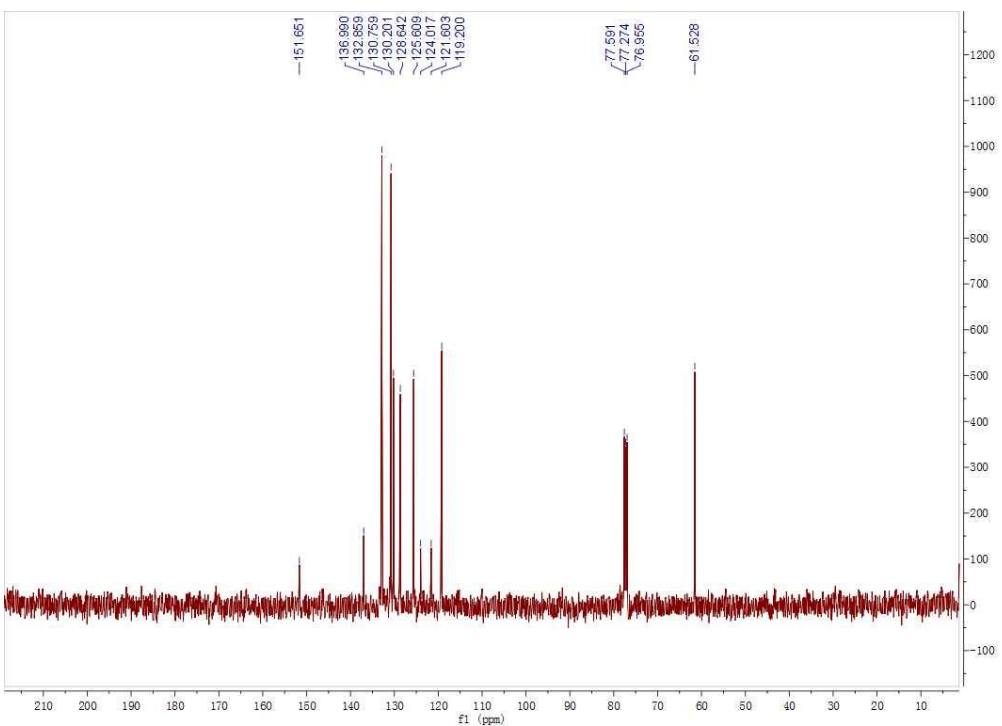
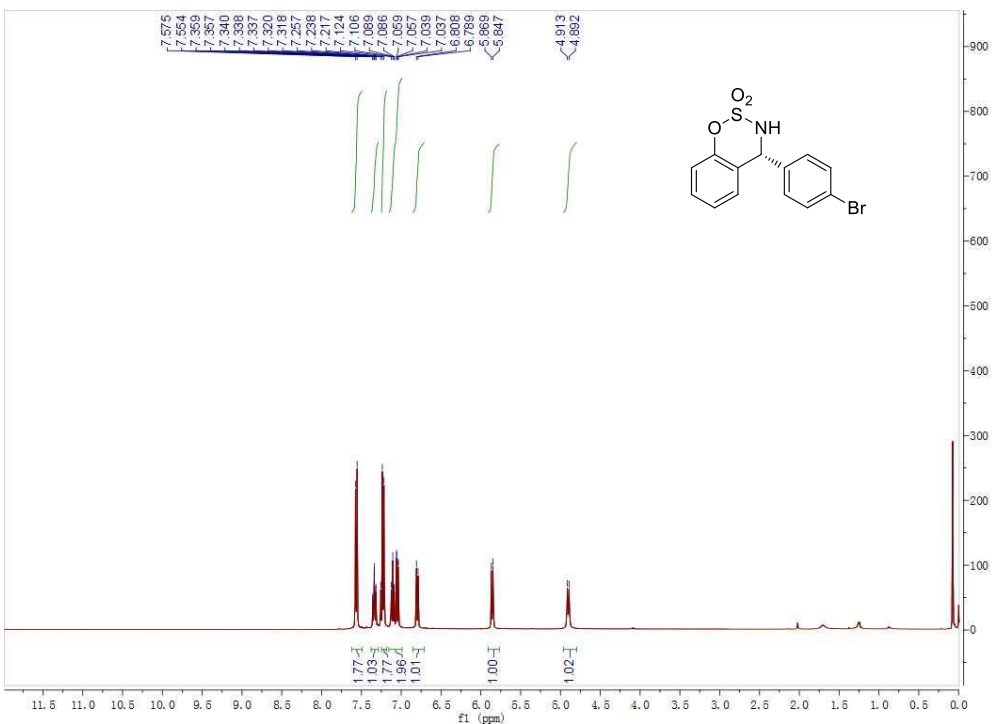


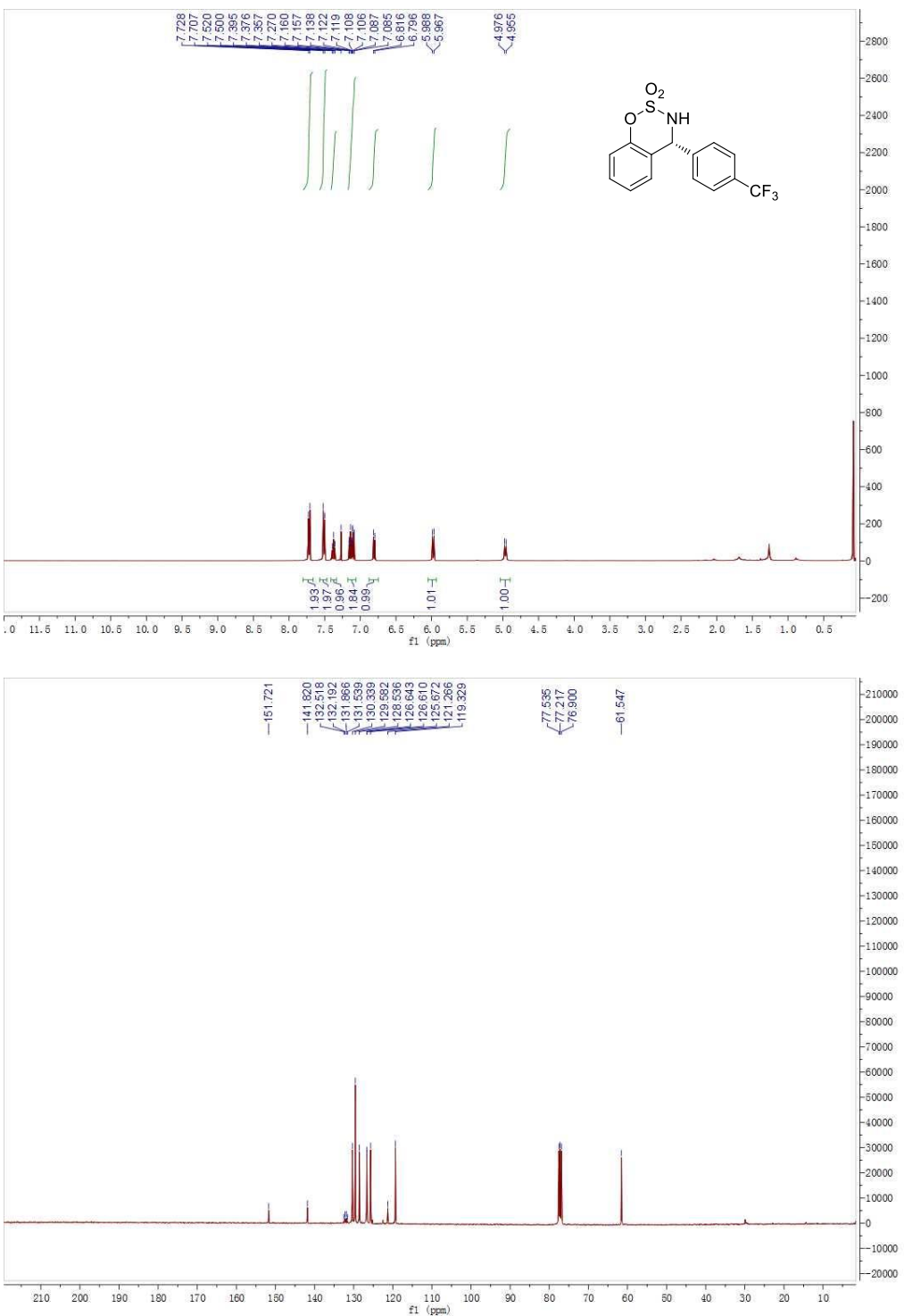


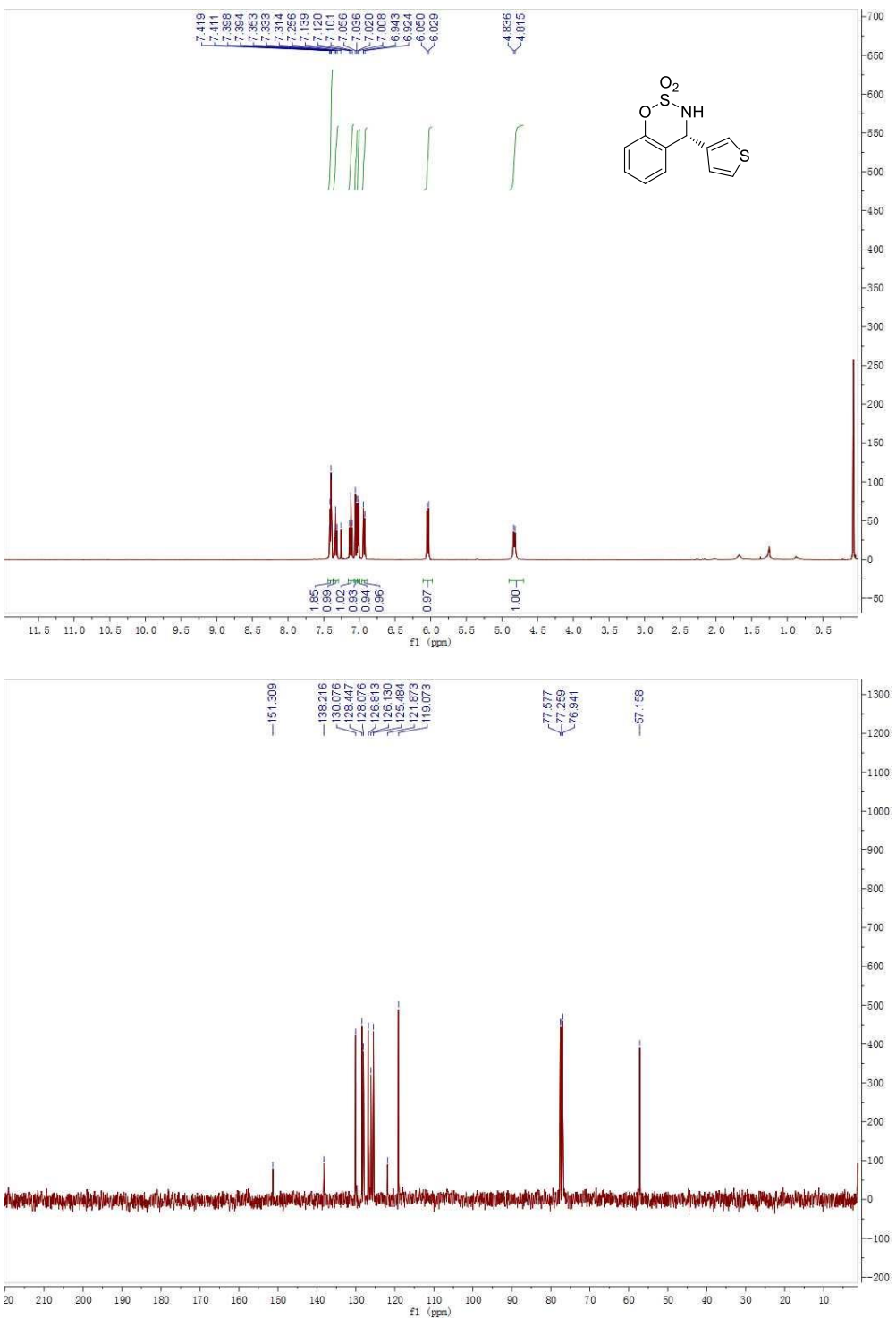


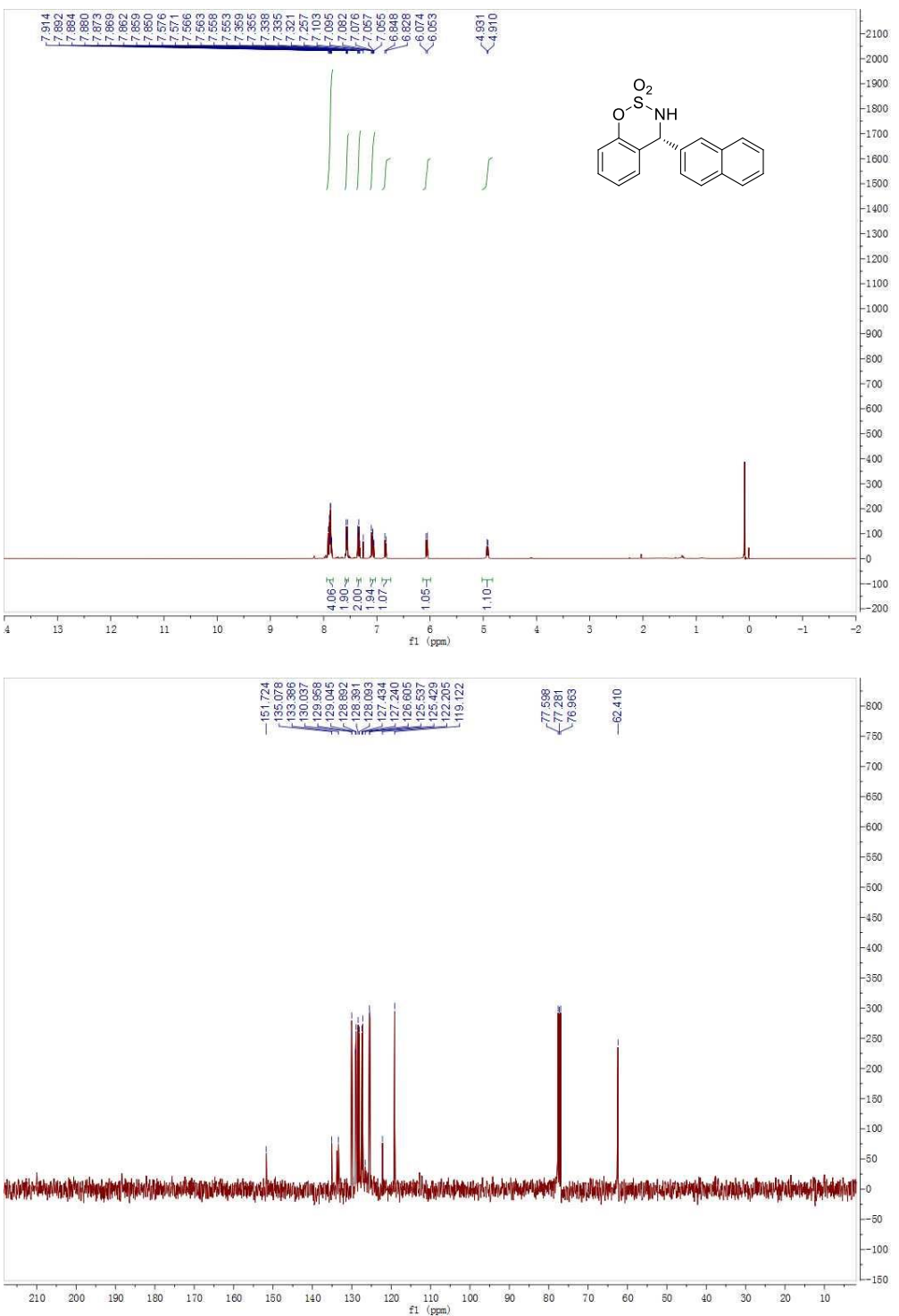


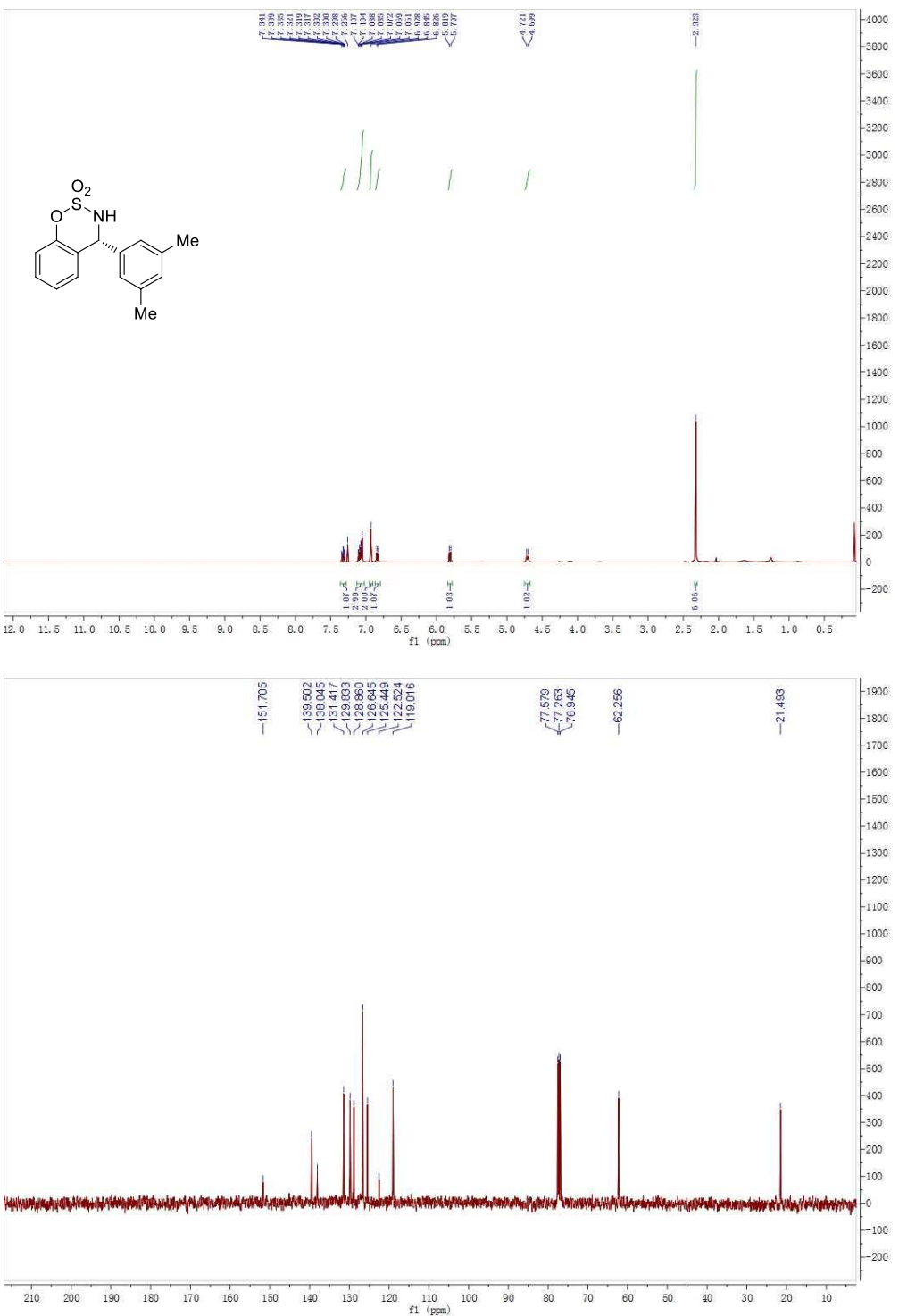


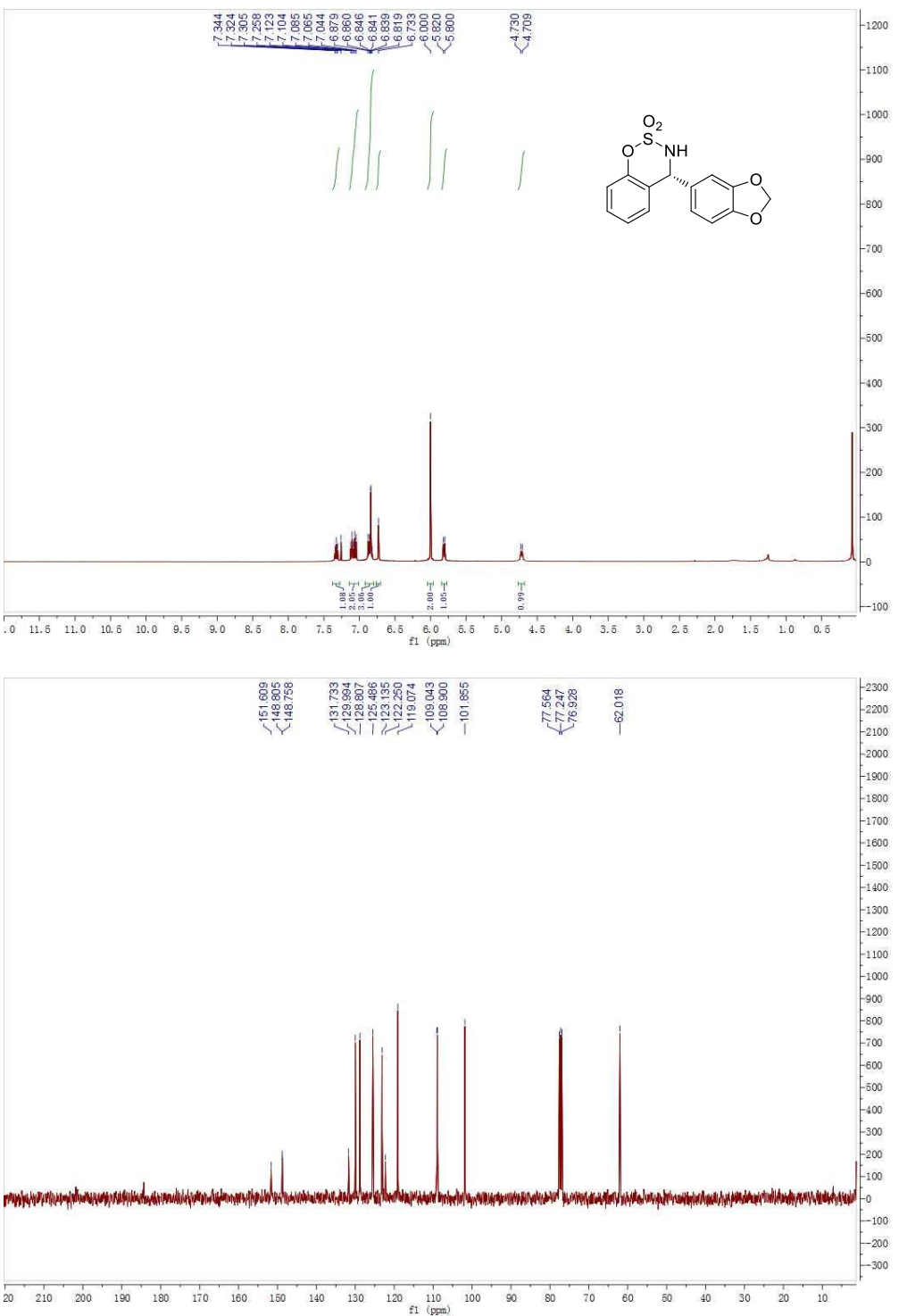


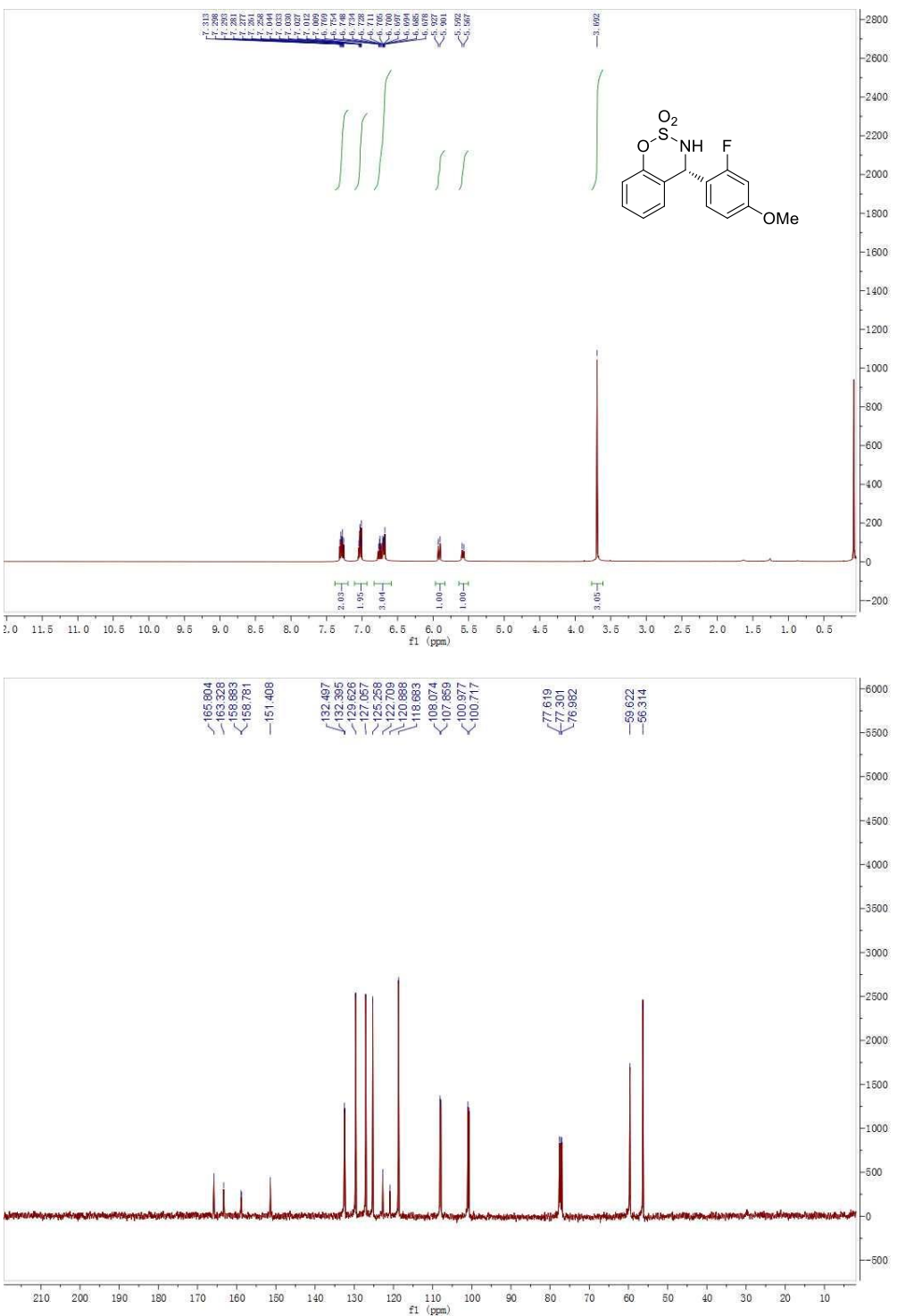


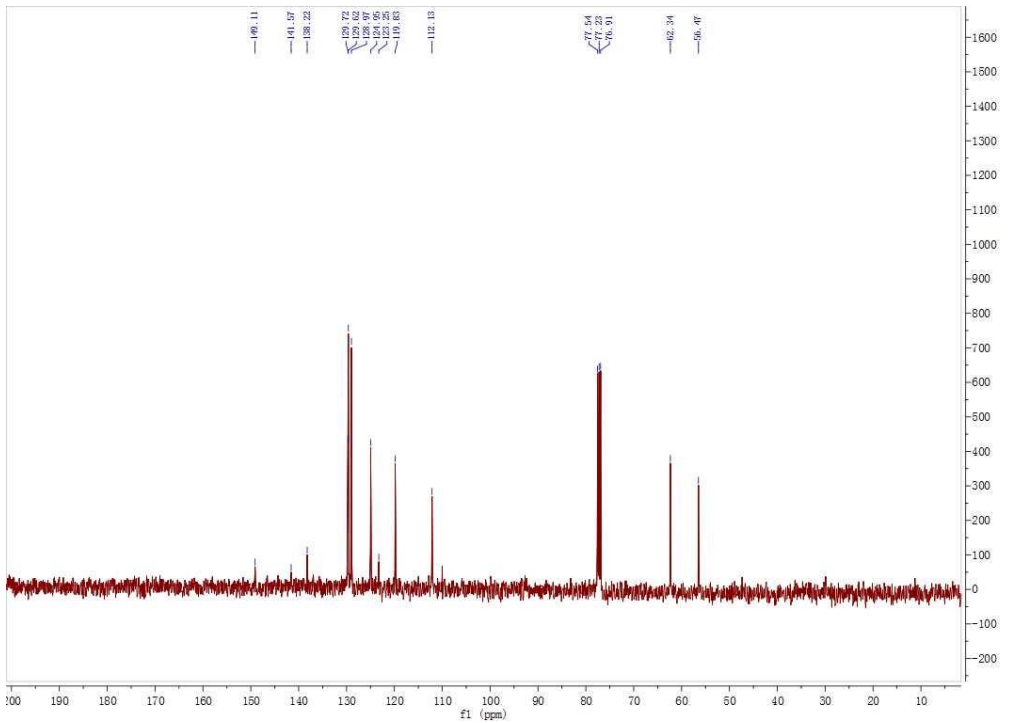
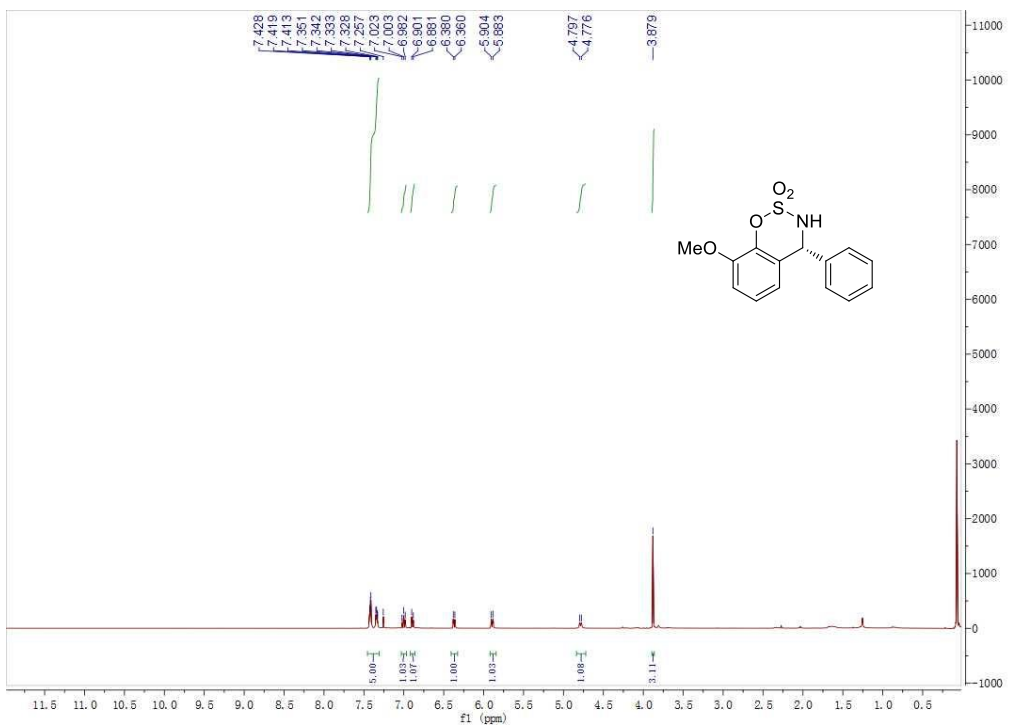


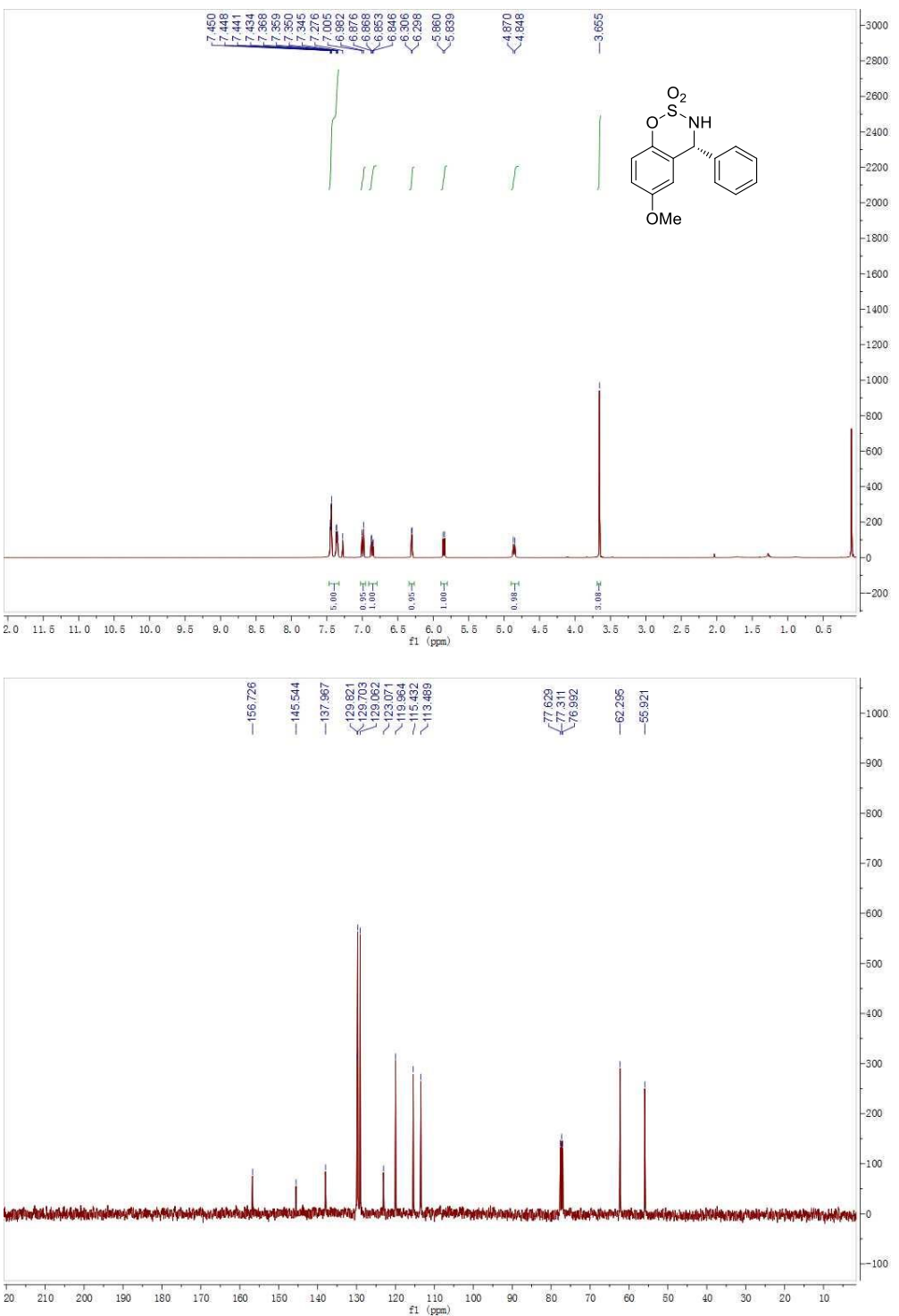


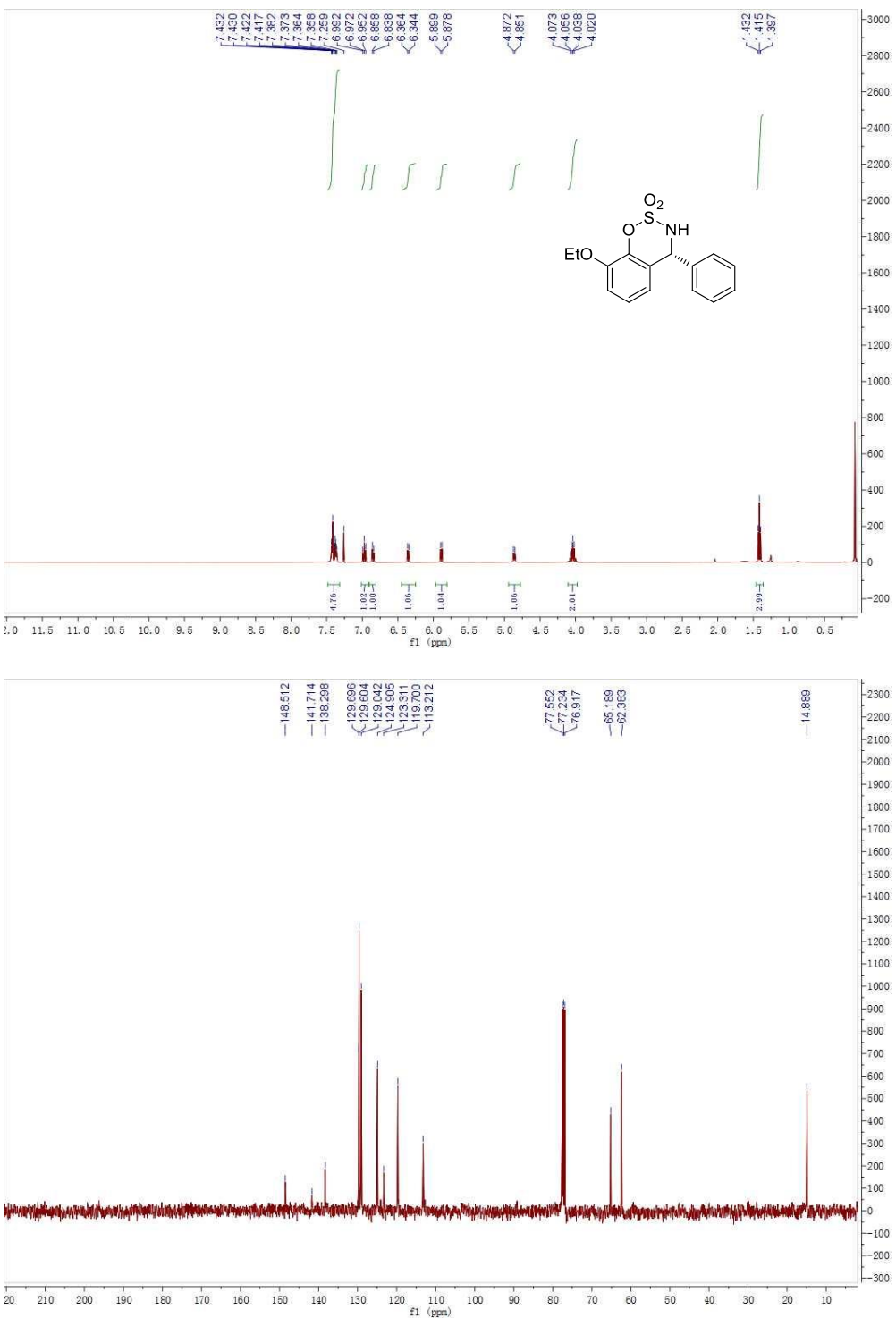


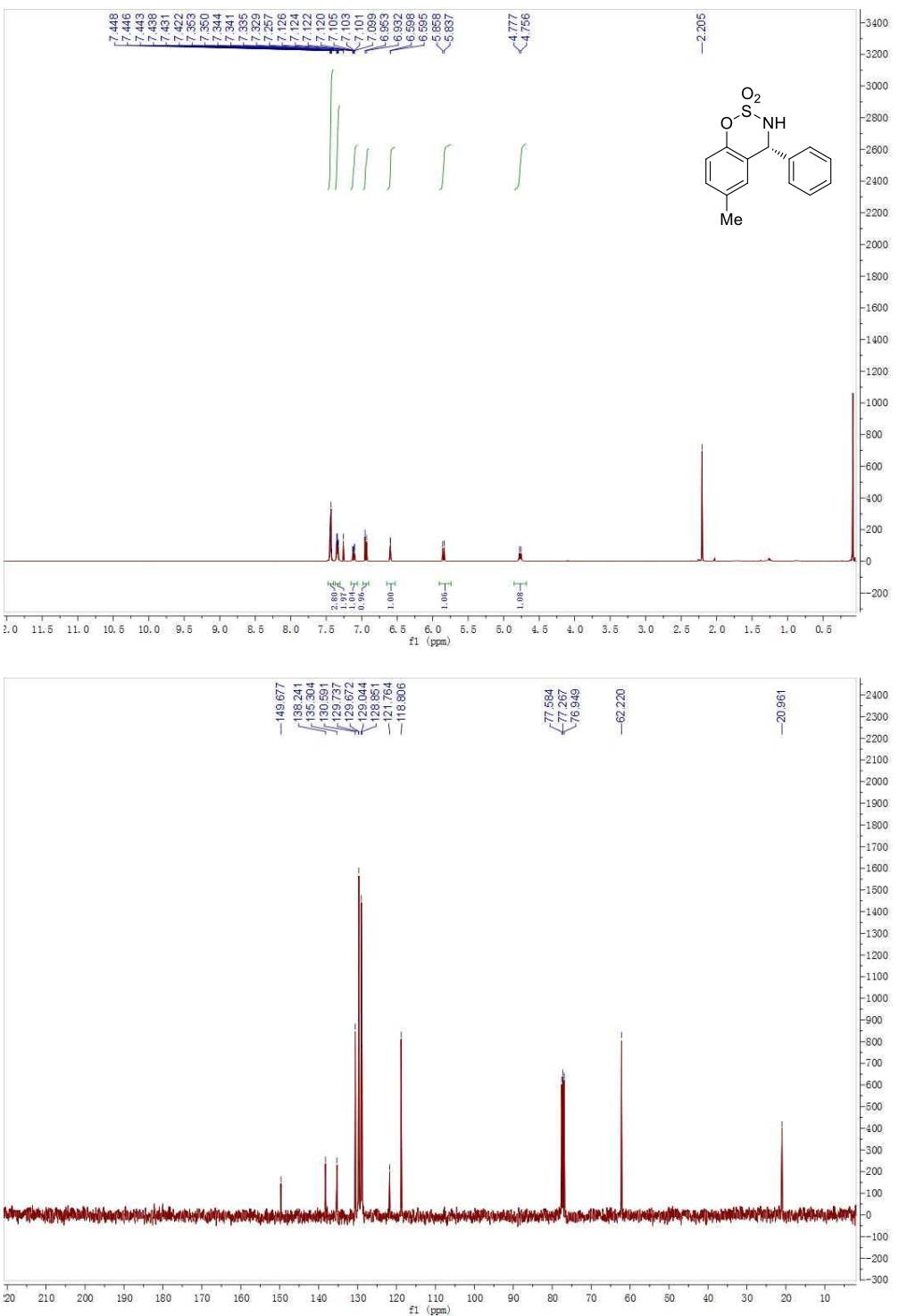


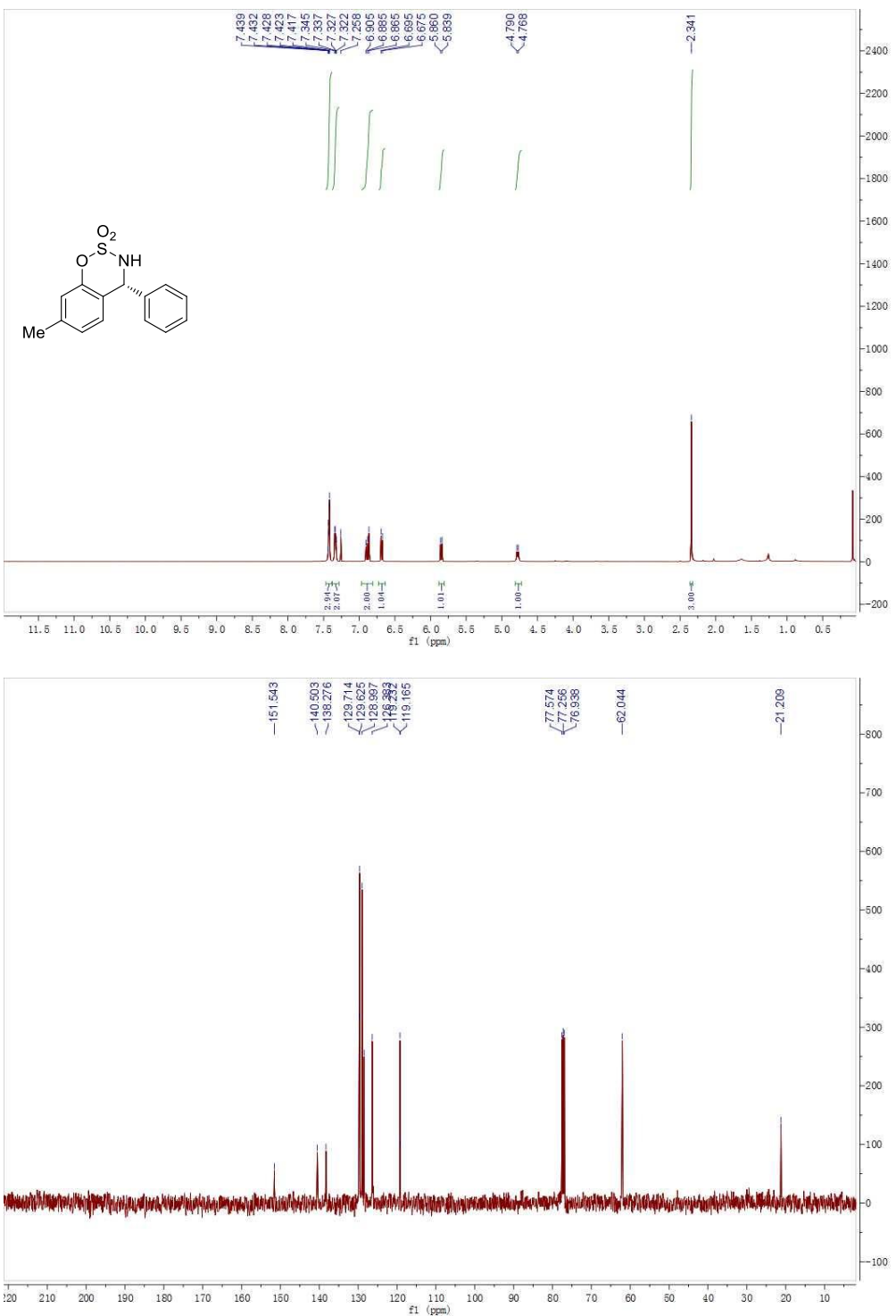


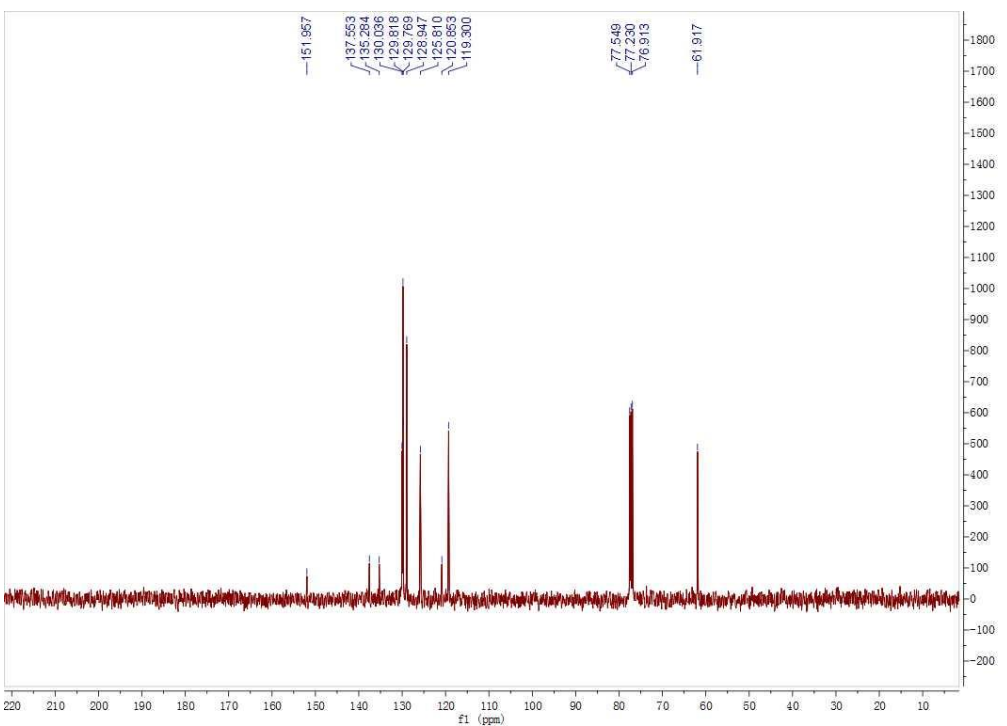
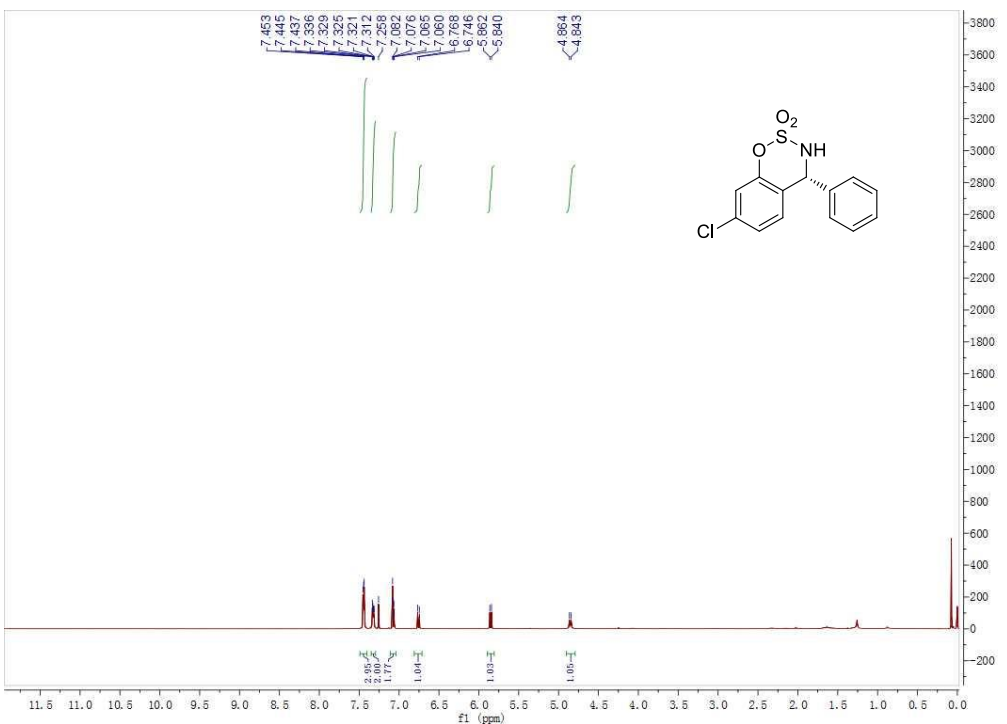


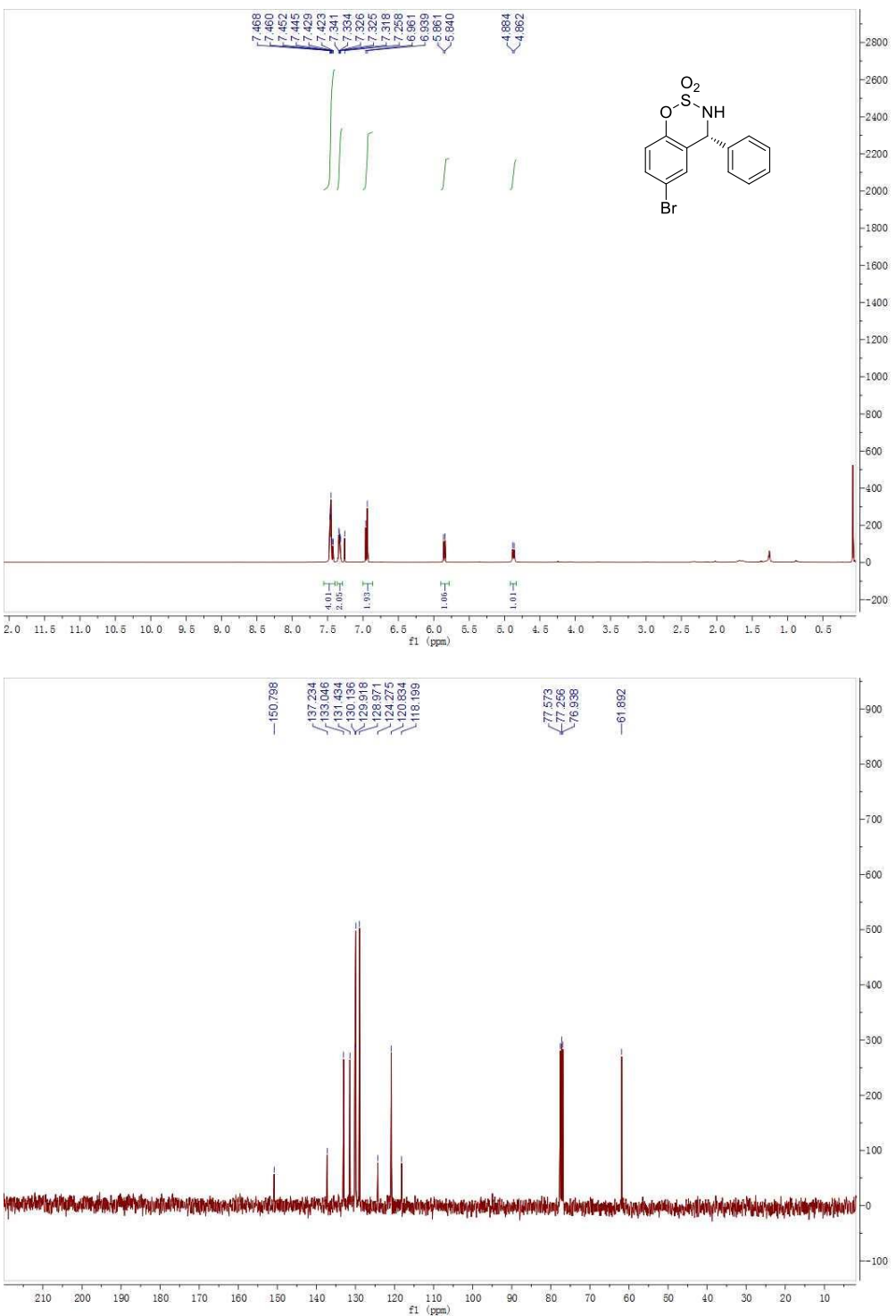


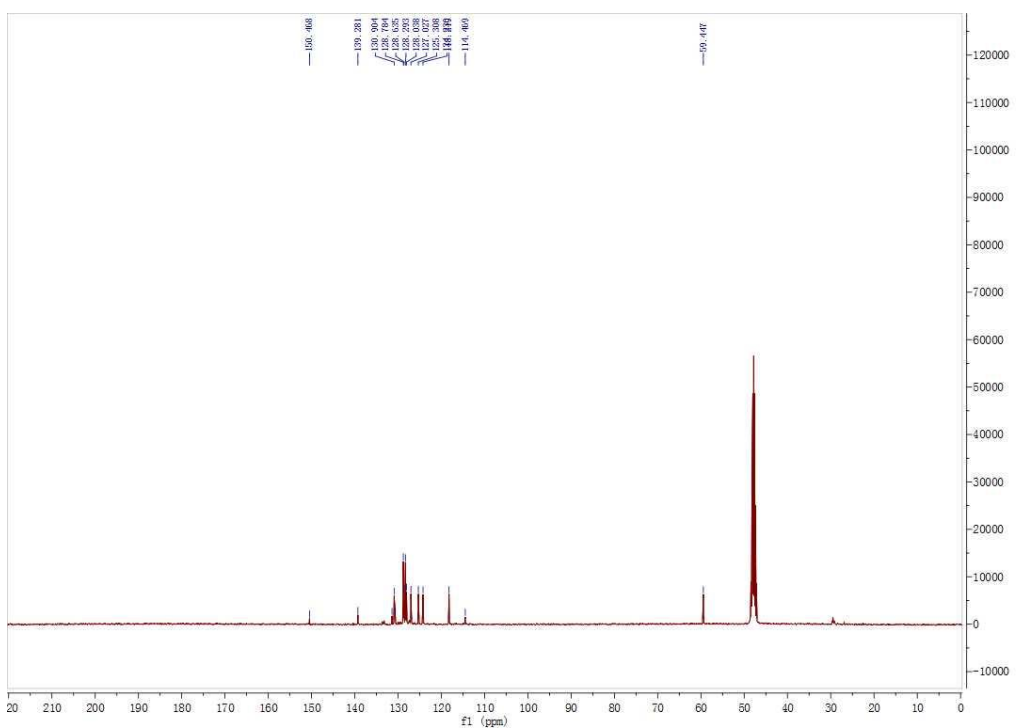
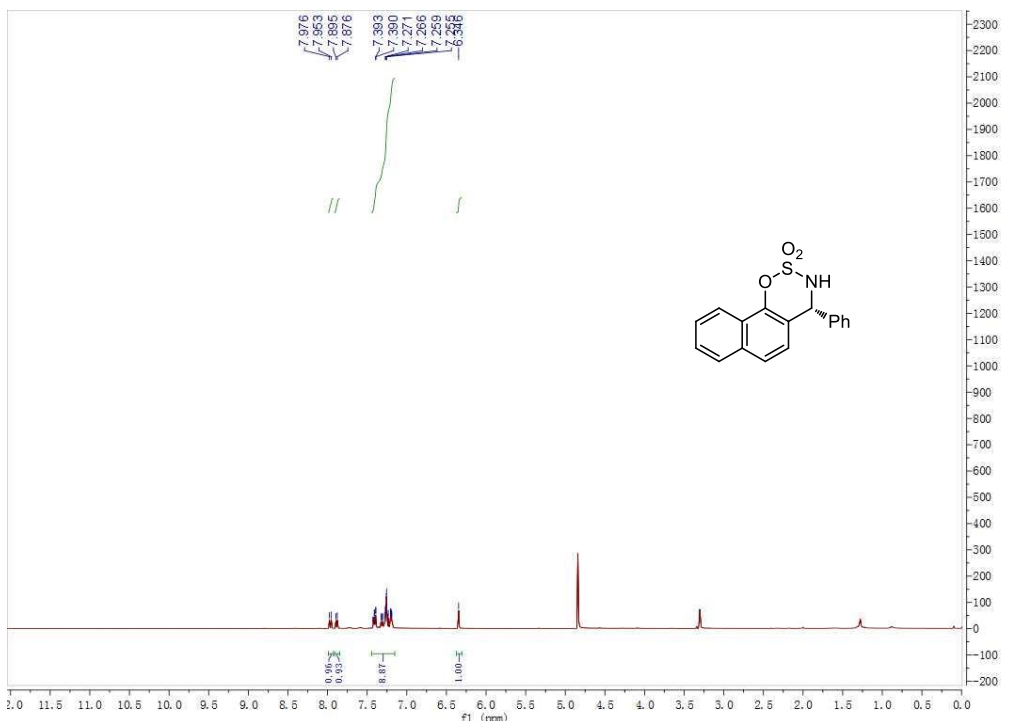


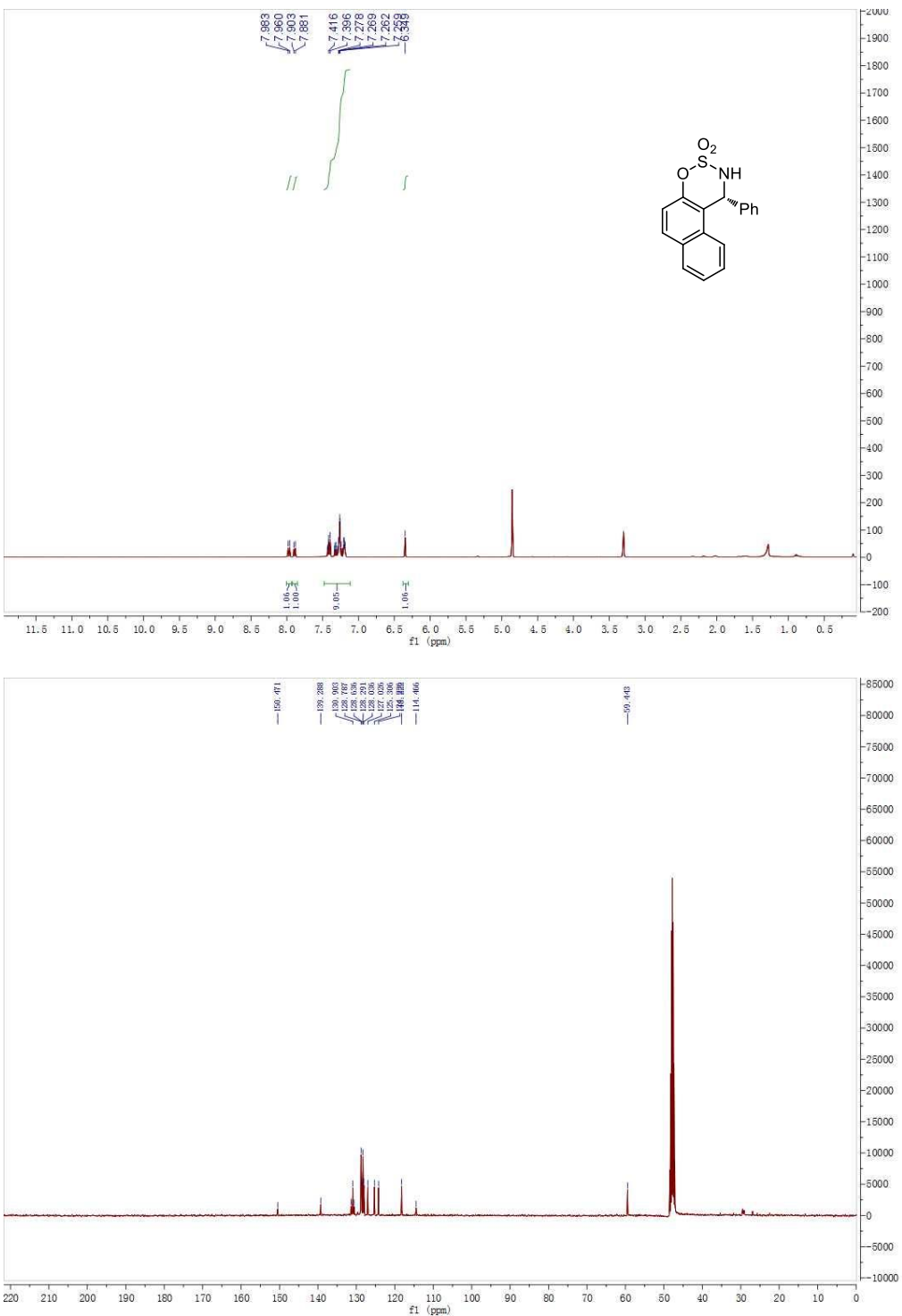


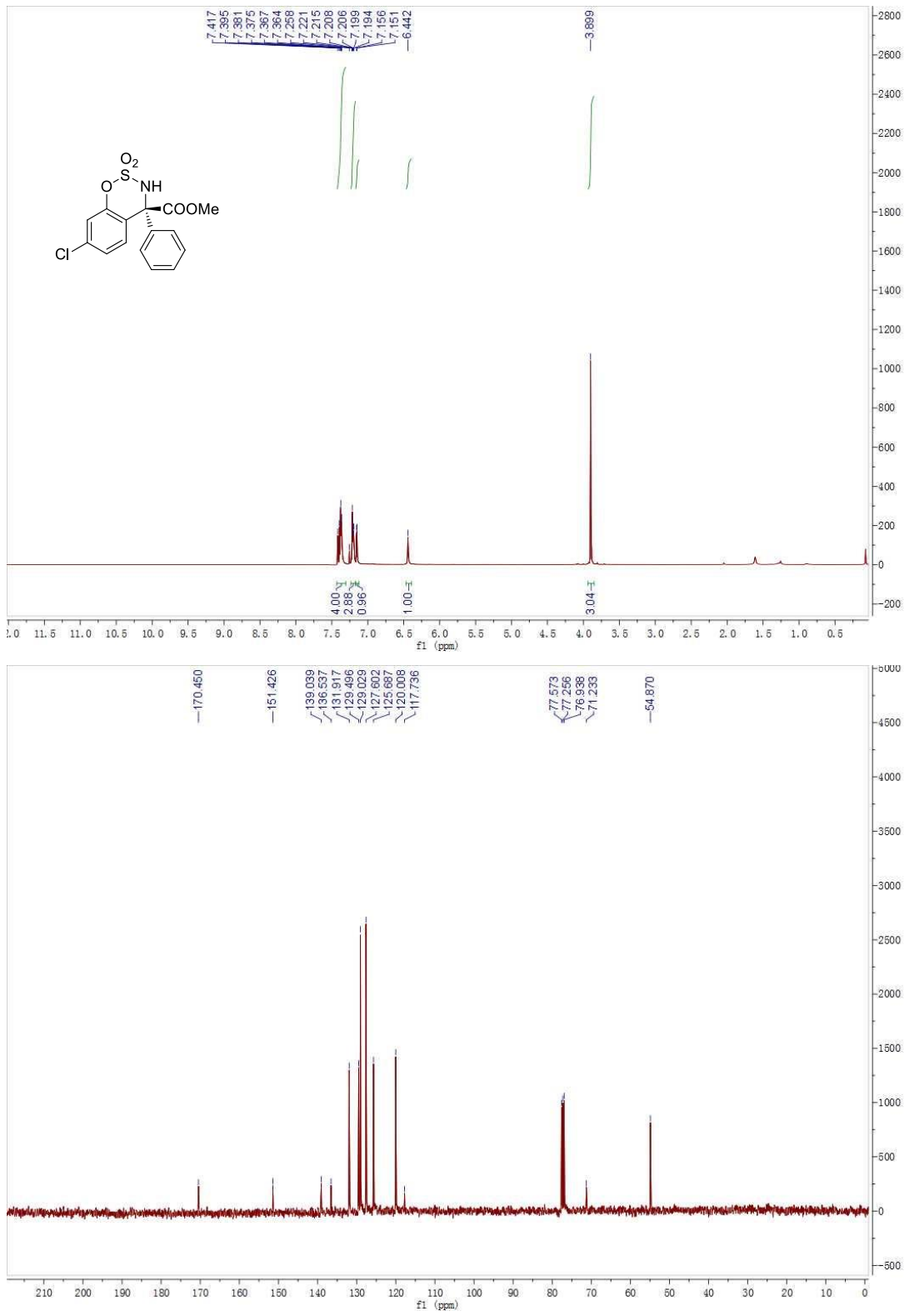


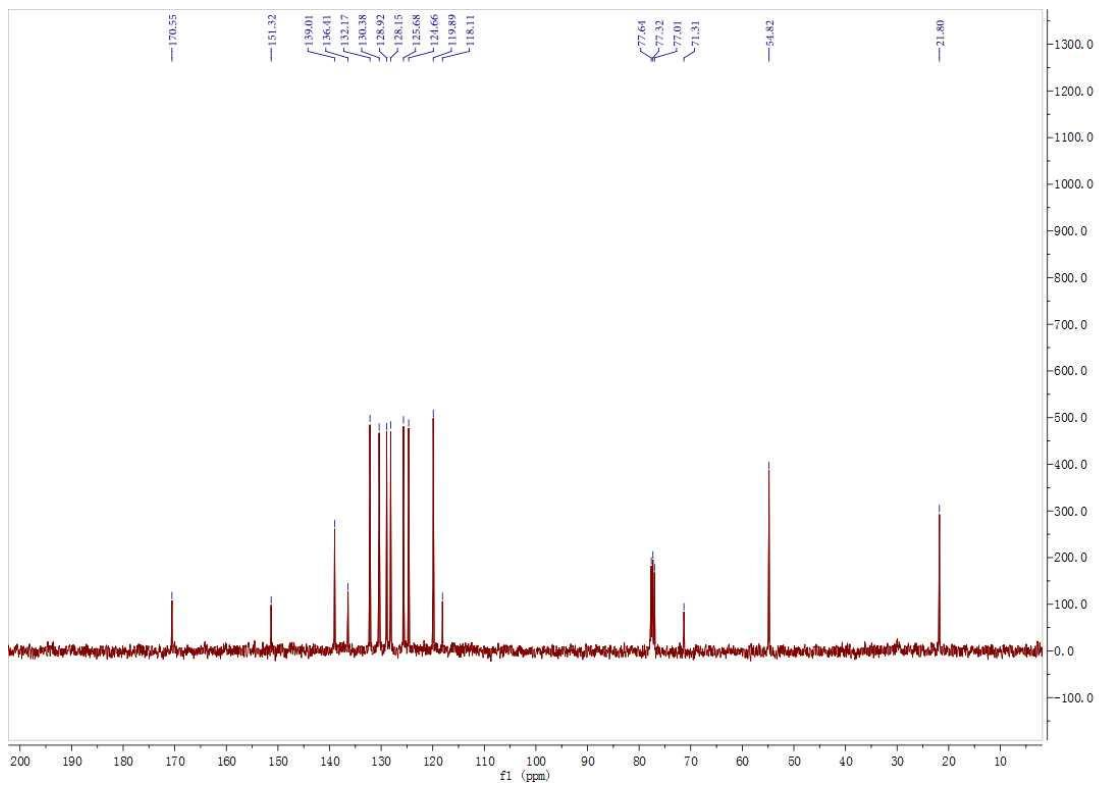
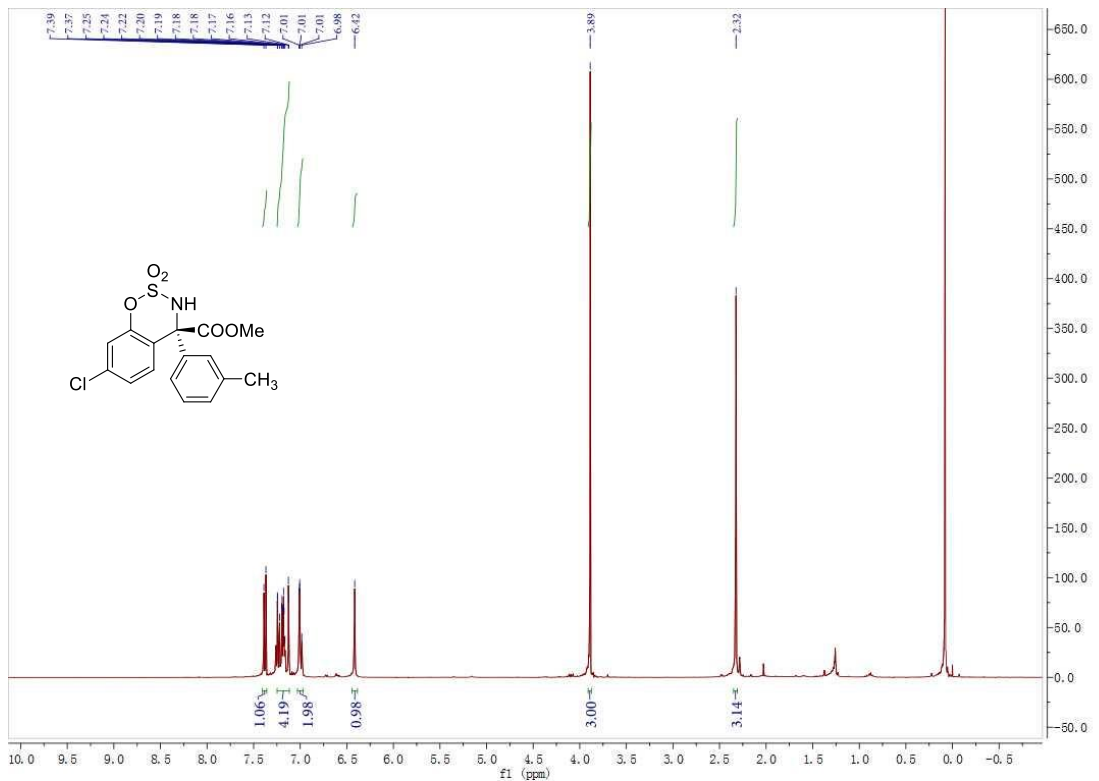


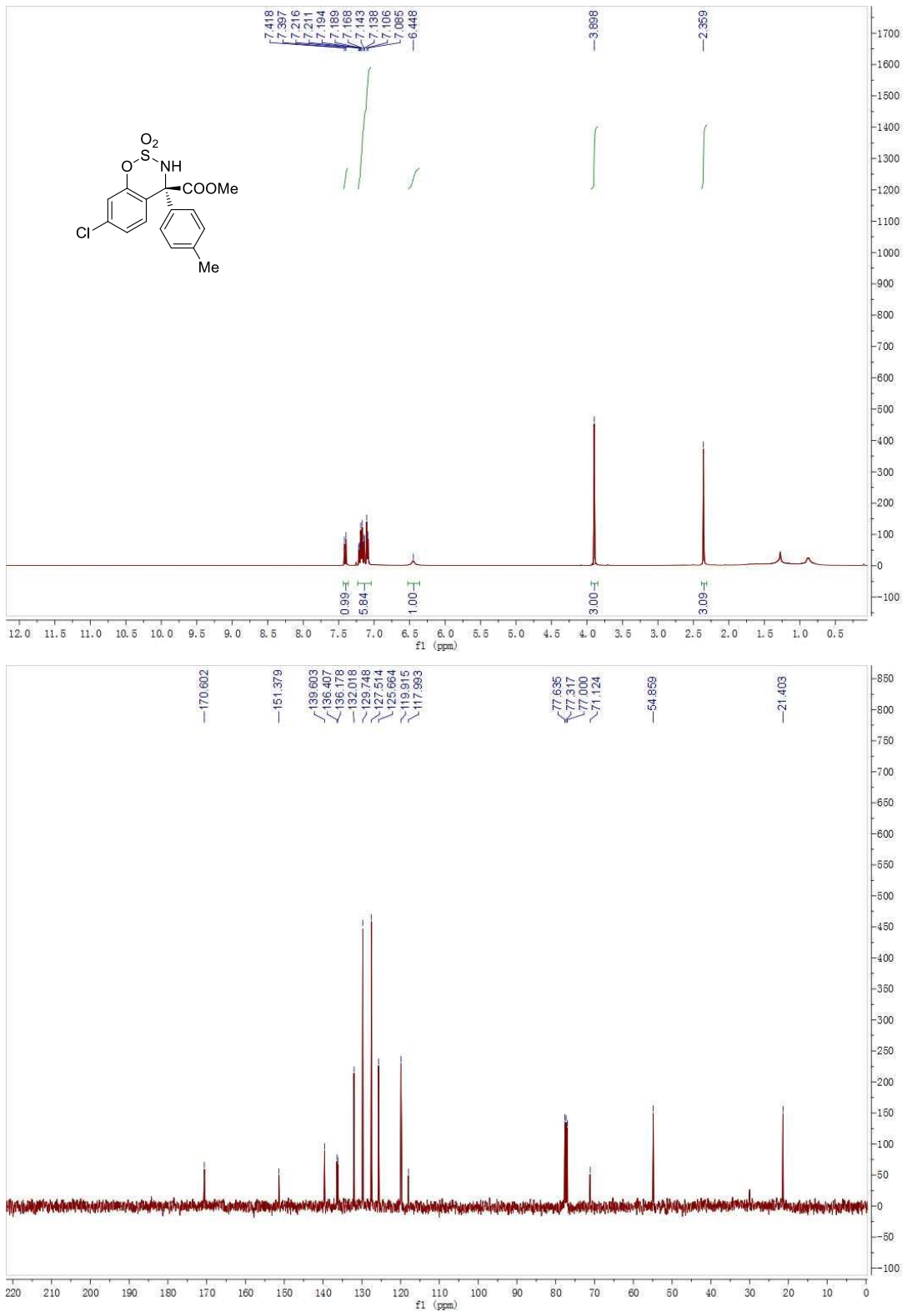


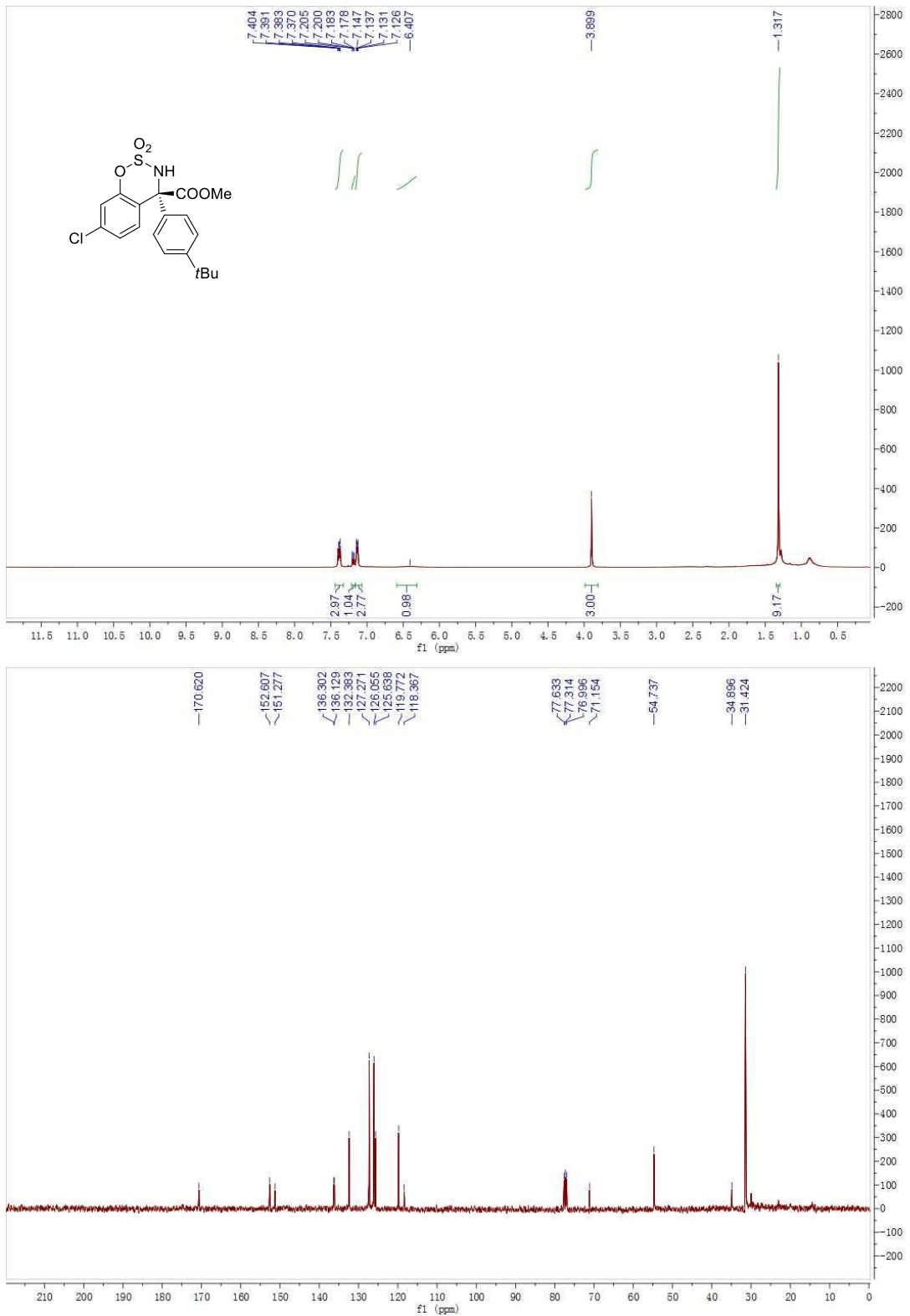


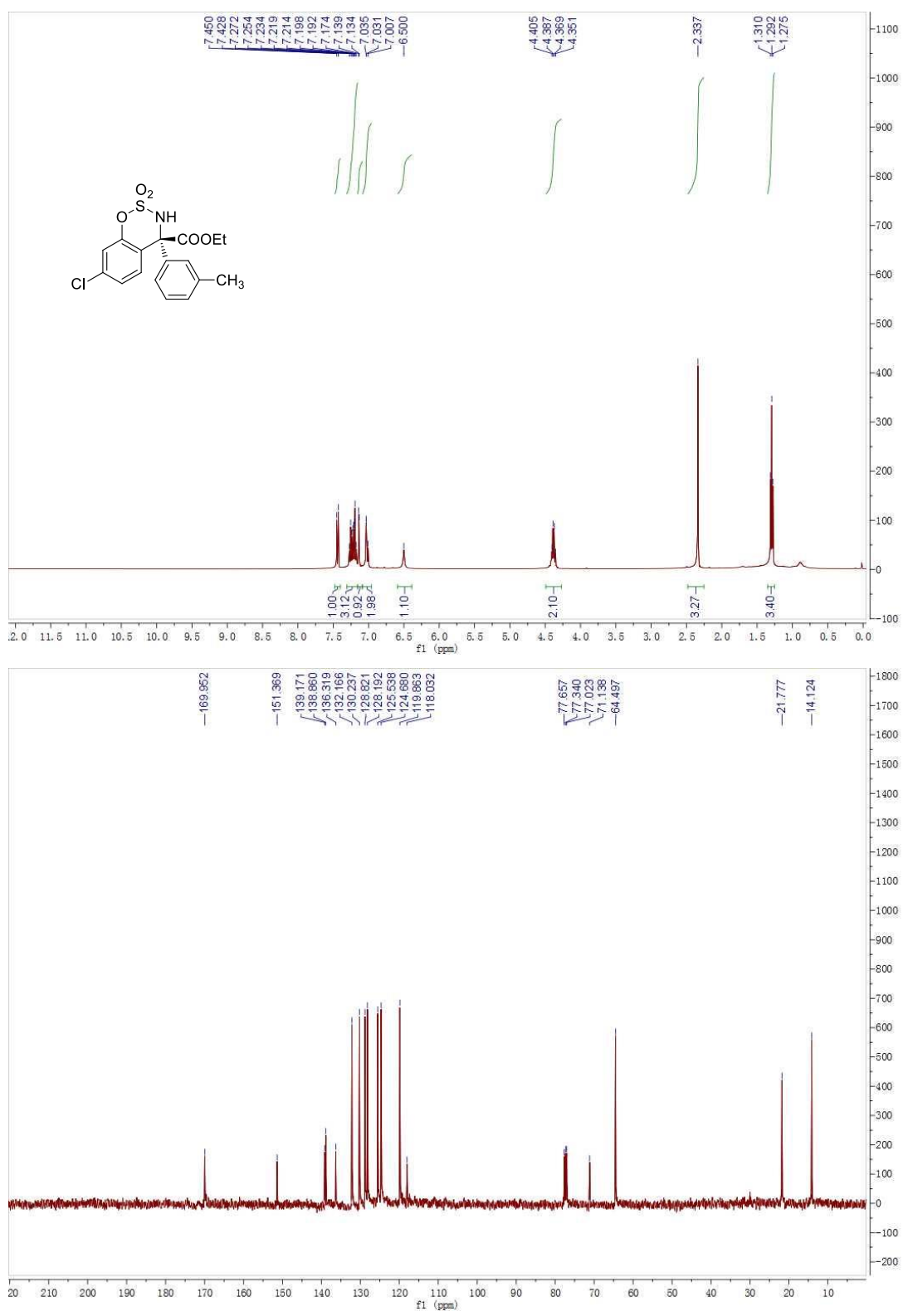


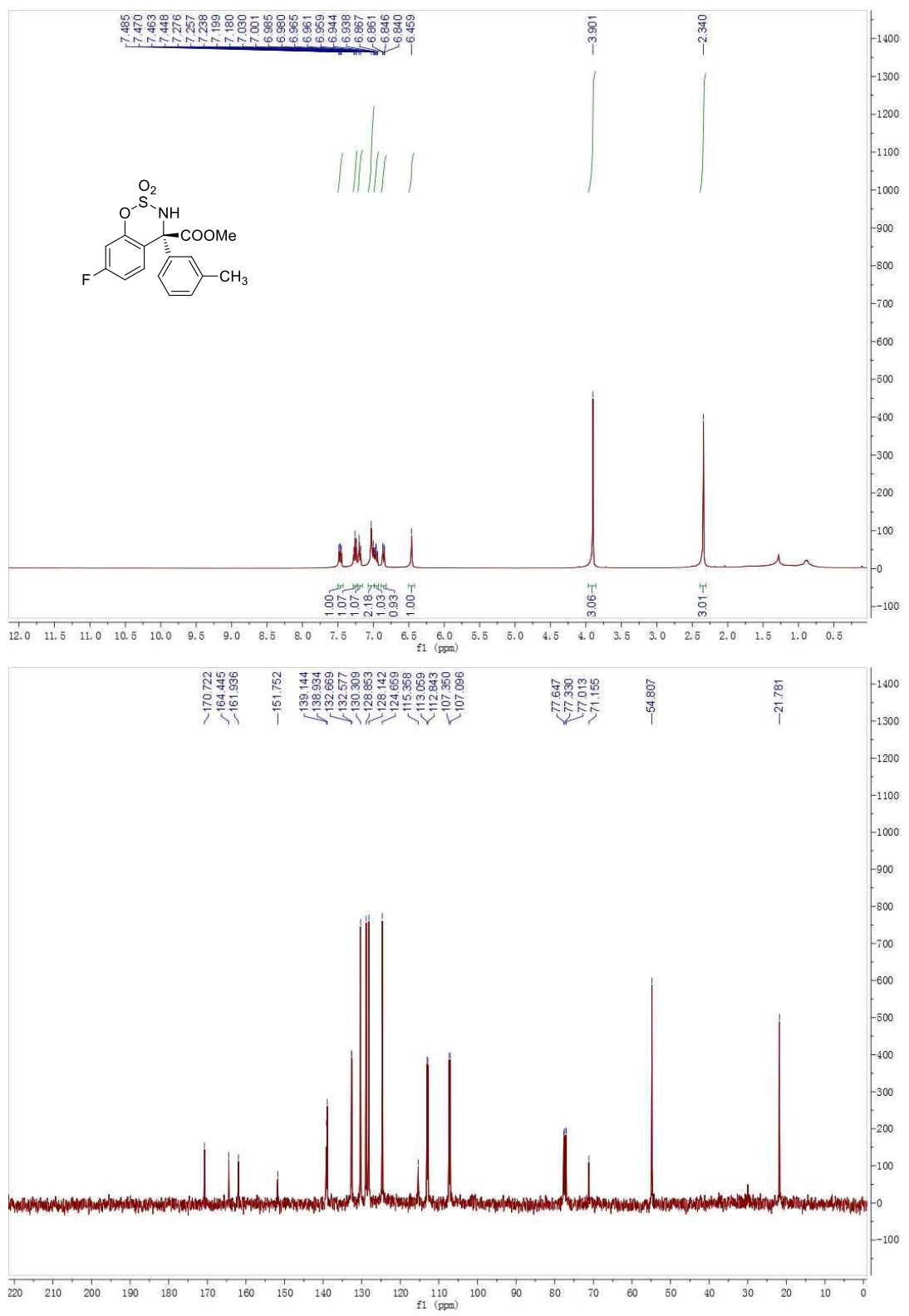




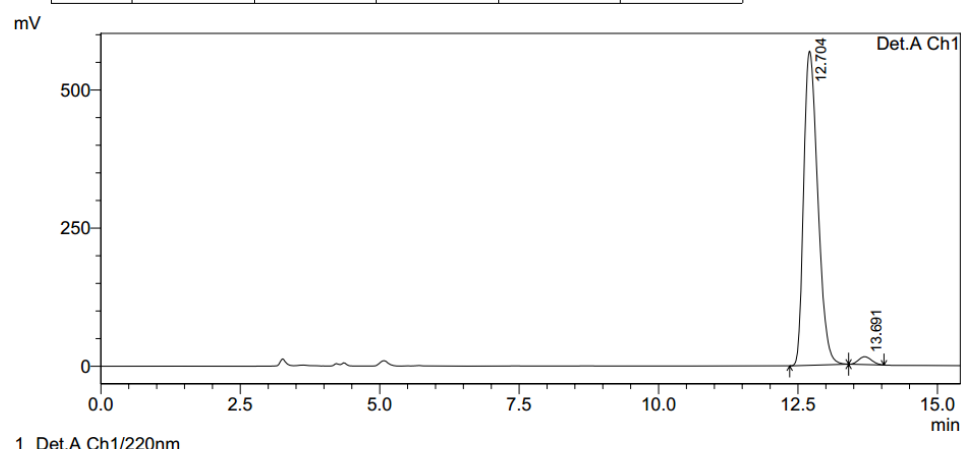
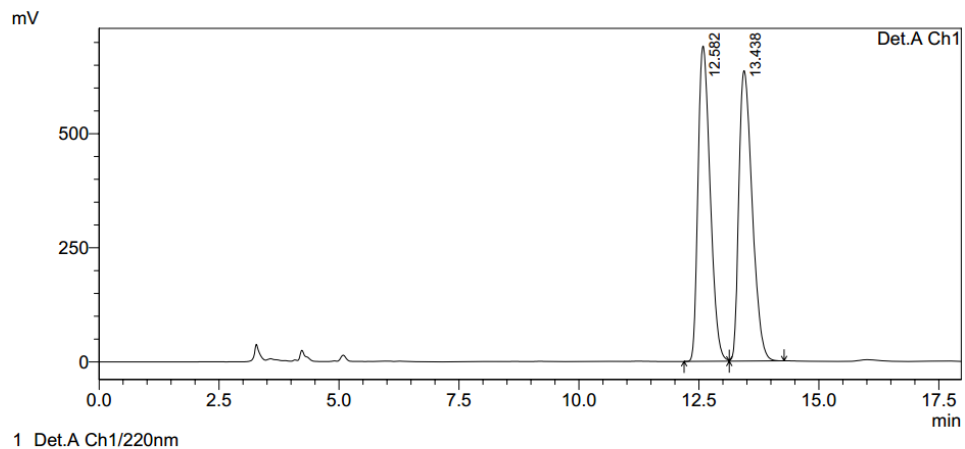
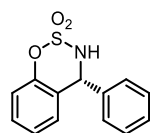


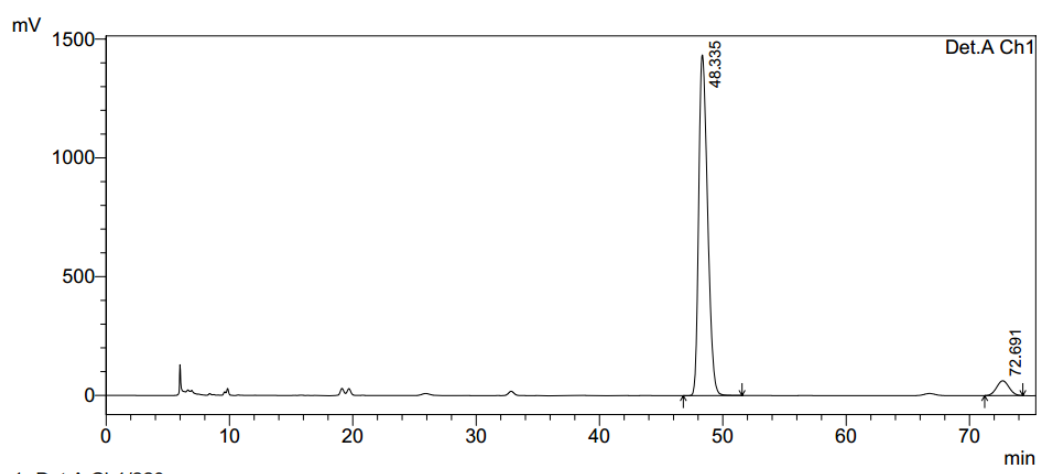
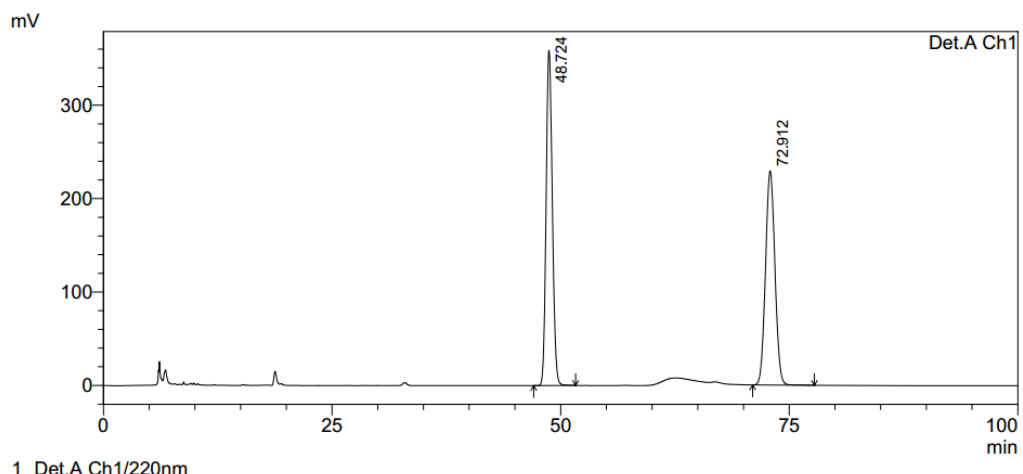
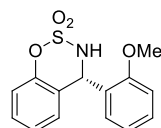


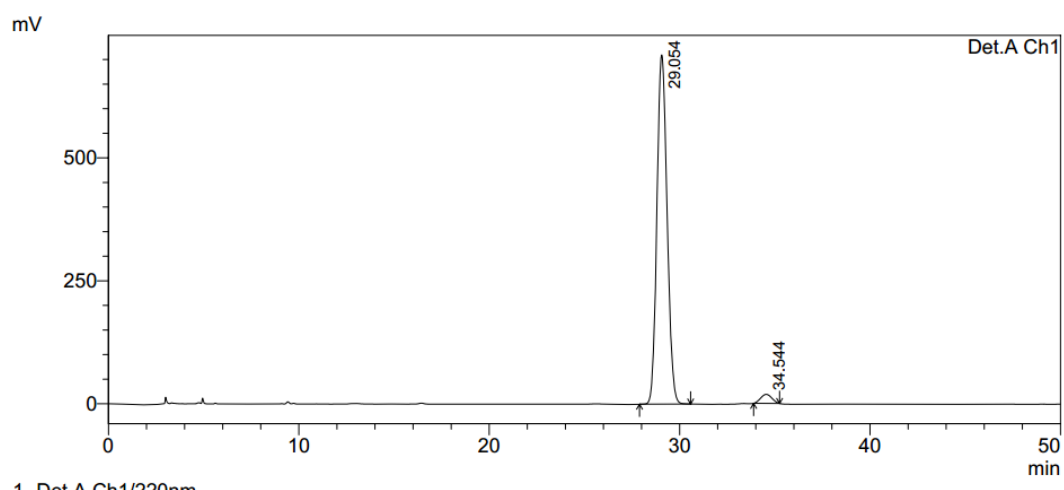
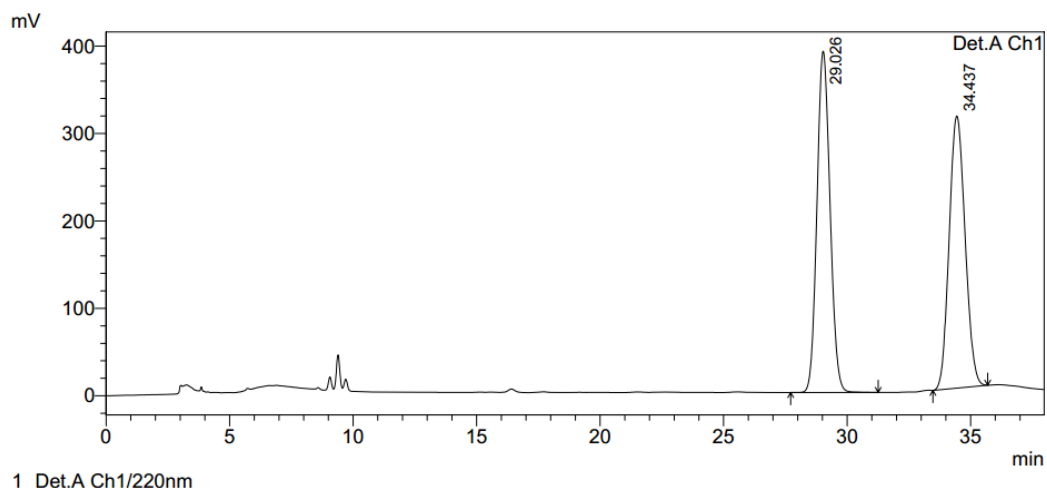
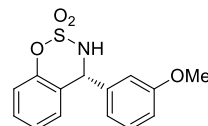


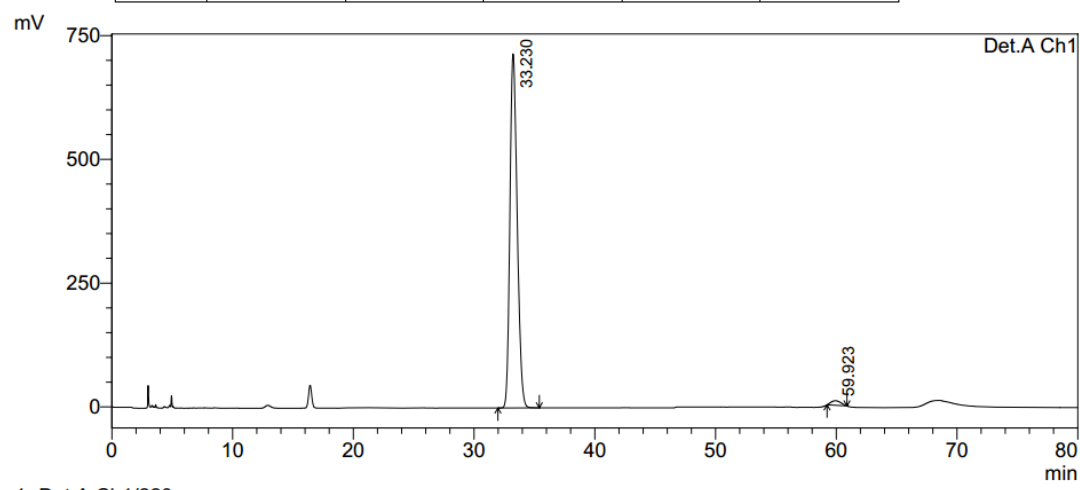
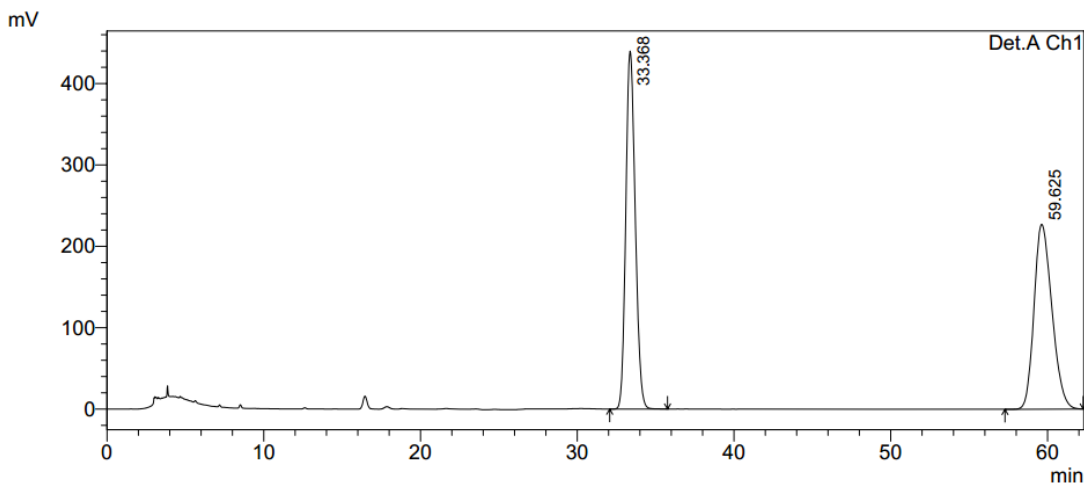
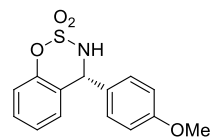


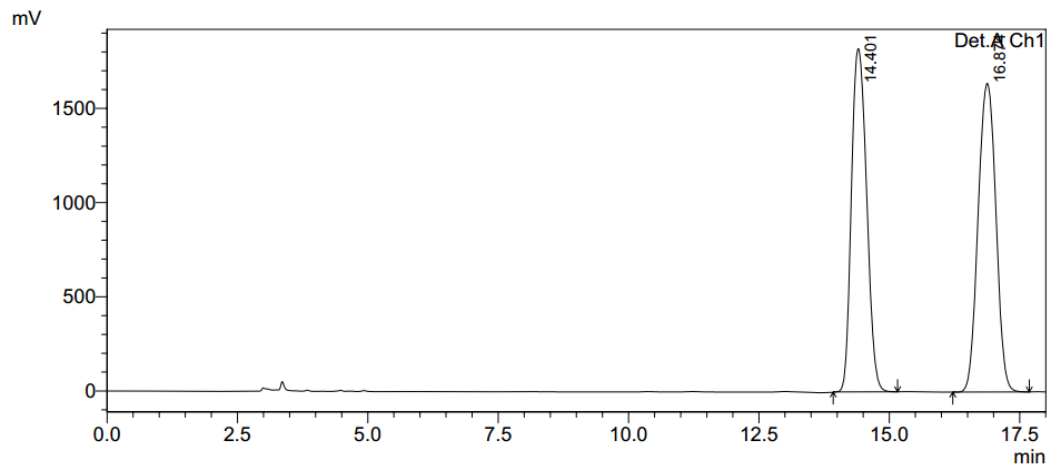
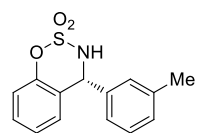
7. HPLC Spectra of Products









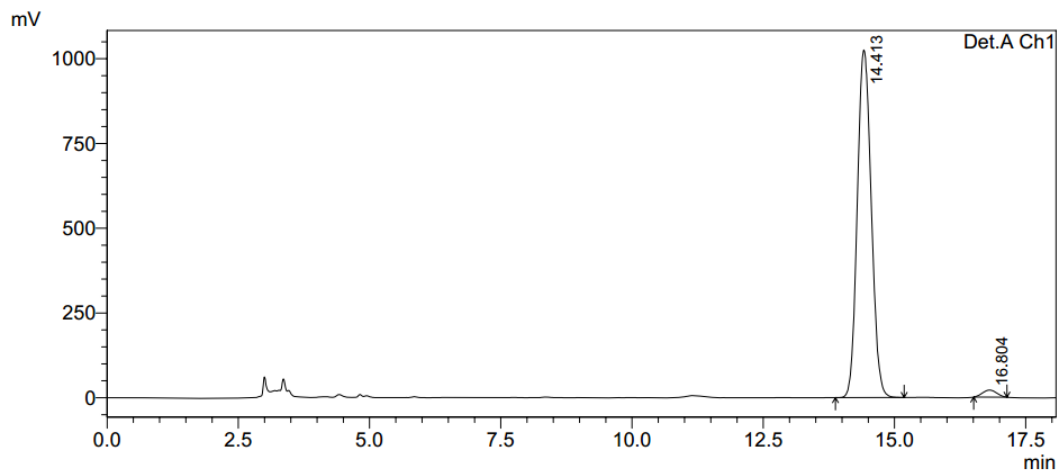


Detector A Ch1 220nm

PeakTable

Detector A Ch1 220nm

Peak#	Ret. Time	Area	Height	Area %	Height %
1	14.401	36973901	1822793	48.756	52.664
2	16.874	38860297	1638387	51.244	47.336
Total		75834198	3461181	100.000	100.000

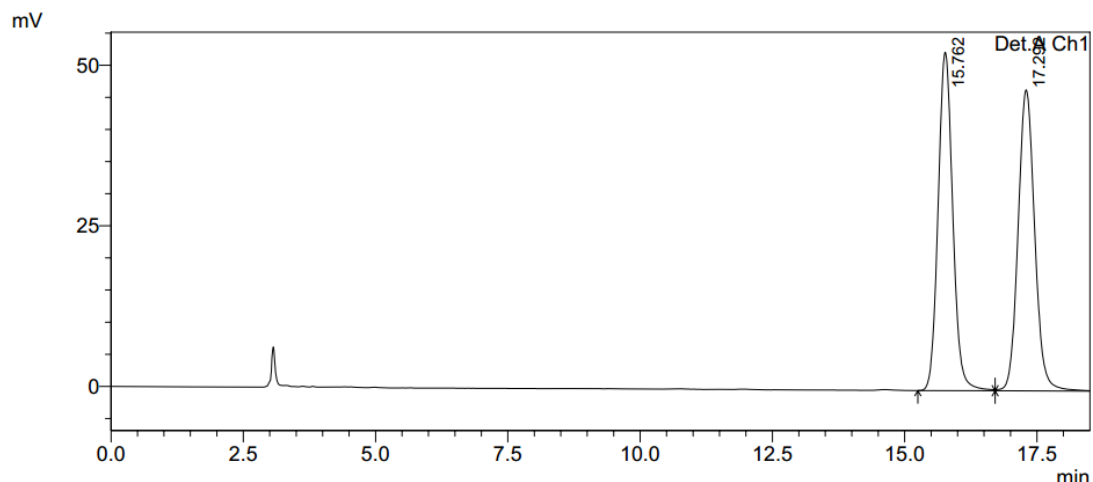
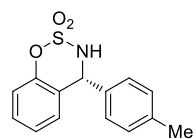


Detector A Ch1 220nm

PeakTable

Detector A Ch1 220nm

Peak#	Ret. Time	Area	Height	Area %	Height %
1	14.413	18975772	1025635	97.975	98.000
2	16.804	392221	20929	2.025	2.000
Total		19367993	1046563	100.000	100.000

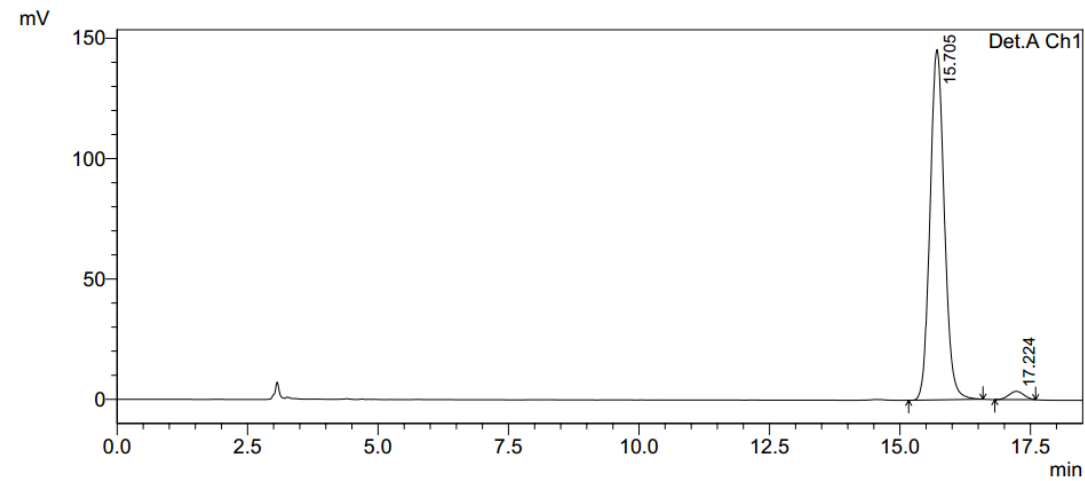


1 Det.A Ch1/220nm

PeakTable

Detector A Ch1 220nm

Peak#	Ret. Time	Area	Height	Area %	Height %
1	15.762	1013160	52692	49.844	52.933
2	17.292	1019522	46853	50.156	47.067
Total		2032682	99545	100.000	100.000

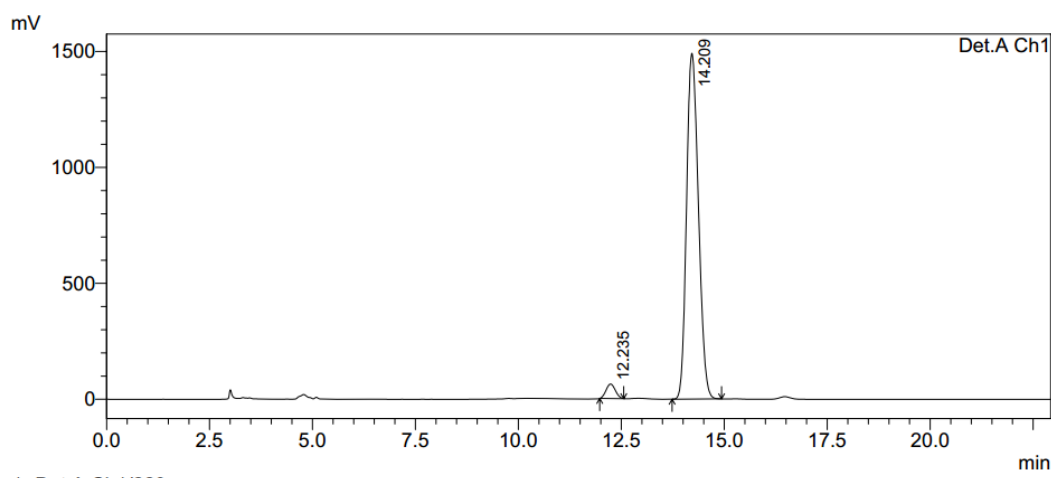
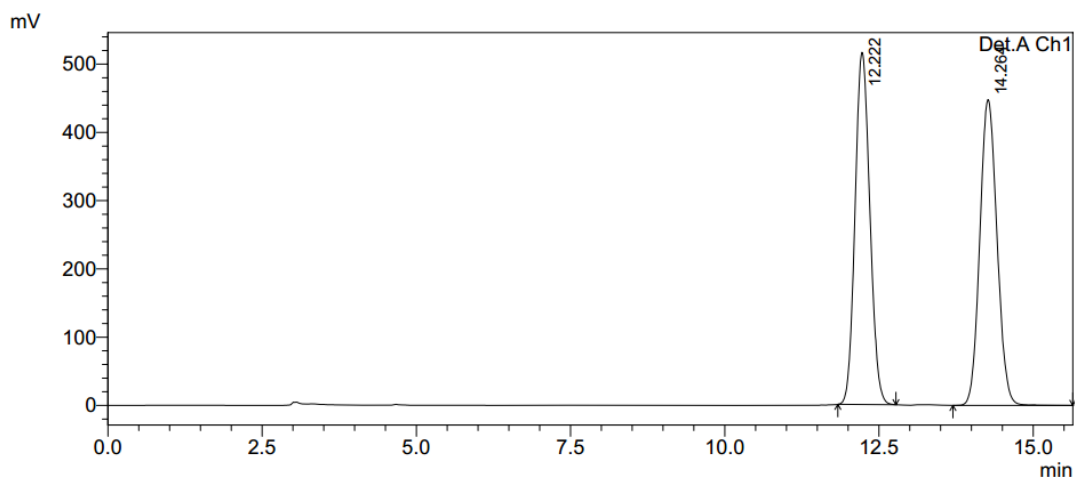
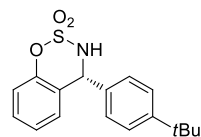


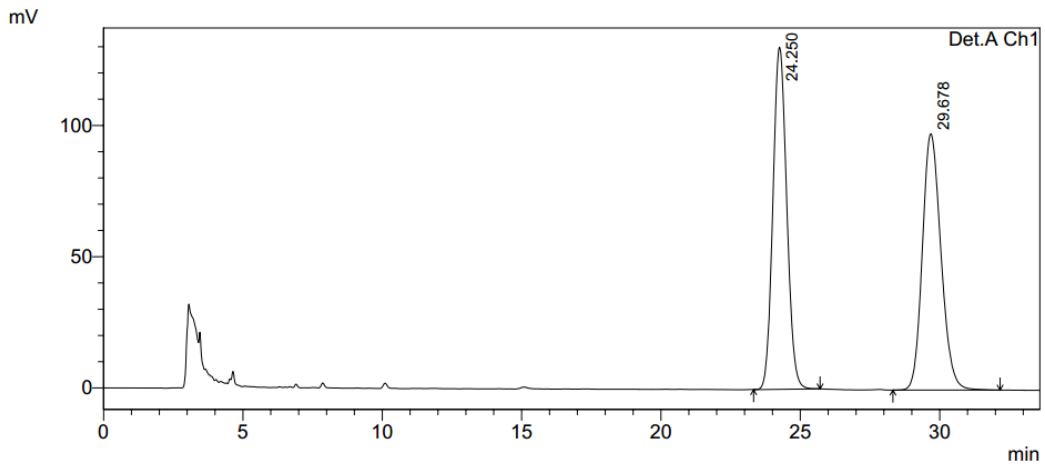
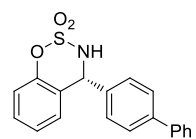
1 Det.A Ch1/220nm

PeakTable

Detector A Ch1 220nm

Peak#	Ret. Time	Area	Height	Area %	Height %
1	15.705	2772630	145592	97.581	97.694
2	17.224	68740	3437	2.419	2.306
Total		2841370	149029	100.000	100.000

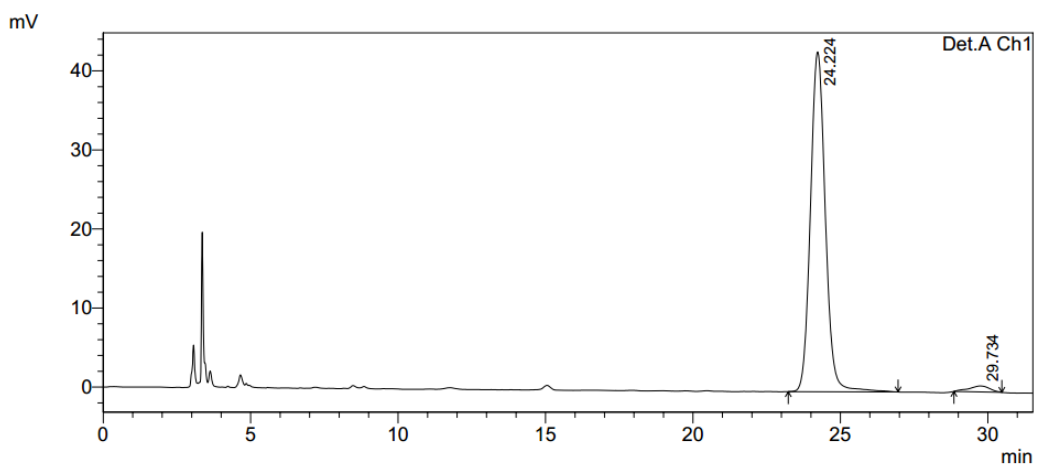




Detector A Ch1 220nm

PeakTable

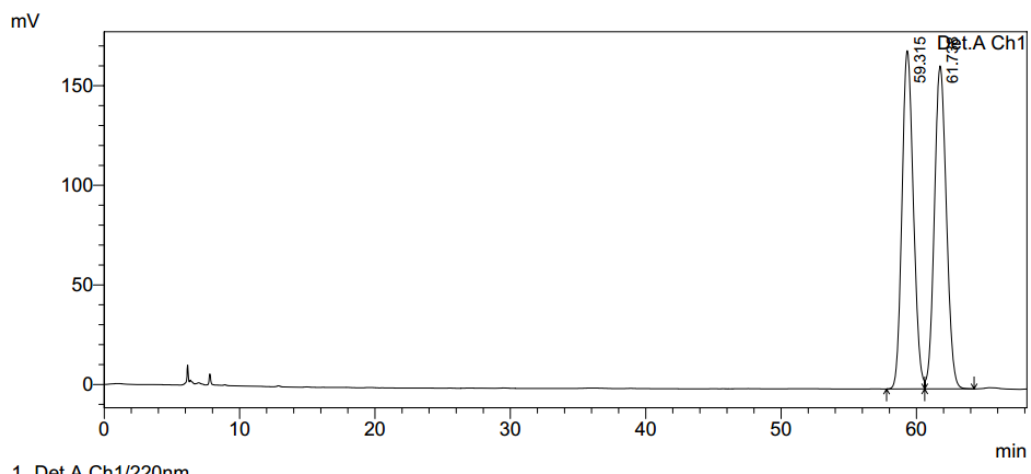
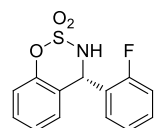
Detector A Ch1 220nm					
Peak#	Ret. Time	Area	Height	Area %	Height %
1	24.250	4487720	130397	49.756	57.181
2	29.678	4531795	97647	50.244	42.819
Total		9019515	228043	100.000	100.000



Detector A Ch1 220nm

PeakTable

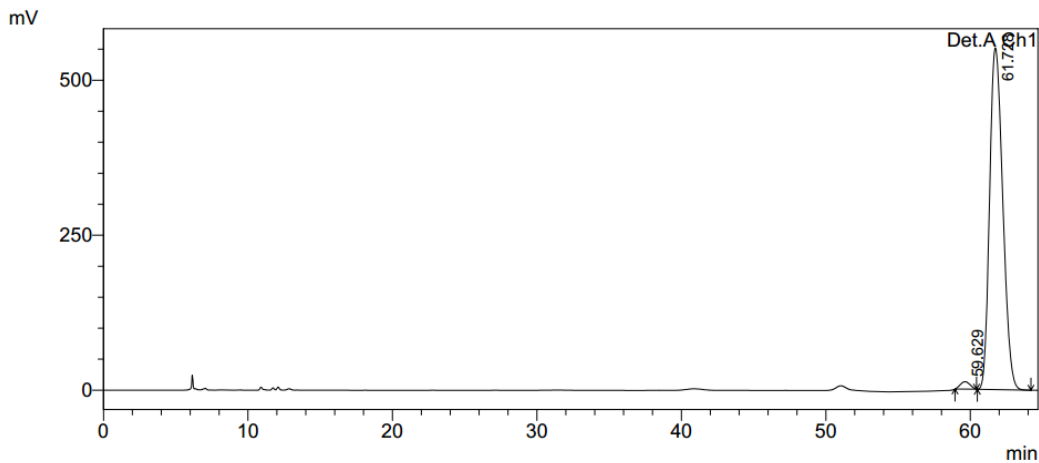
Detector A Ch1 220nm					
Peak#	Ret. Time	Area	Height	Area %	Height %
1	24.224	1509301	42990	97.645	98.300
2	29.734	36408	744	2.355	1.700
Total		1545709	43734	100.000	100.000



PeakTable

Detector A Ch1 220nm

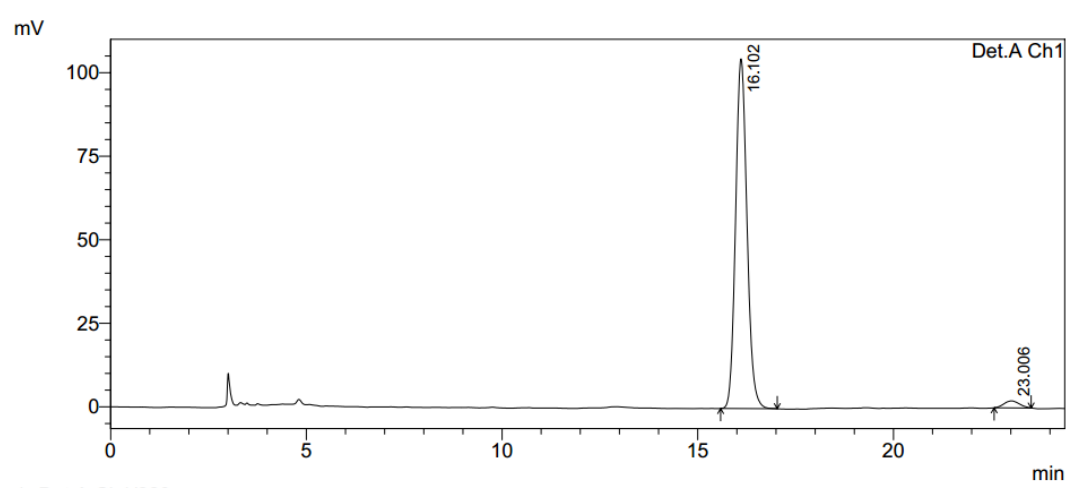
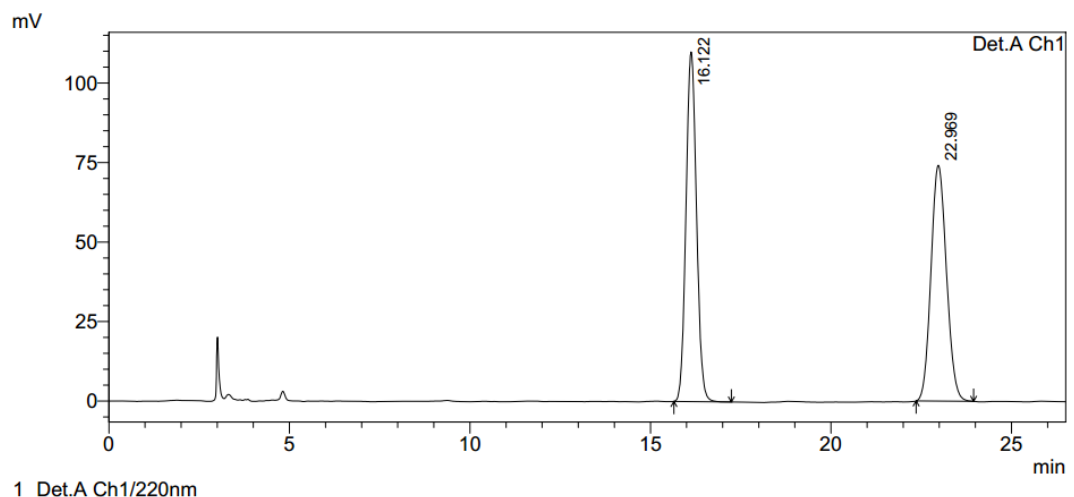
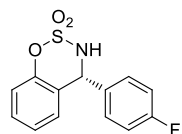
Peak#	Ret. Time	Area	Height	Area %	Height %
1	59.315	9924832	169864	49.883	51.154
2	61.738	9971316	162198	50.117	48.846
Total		19896148	332062	100.000	100.000

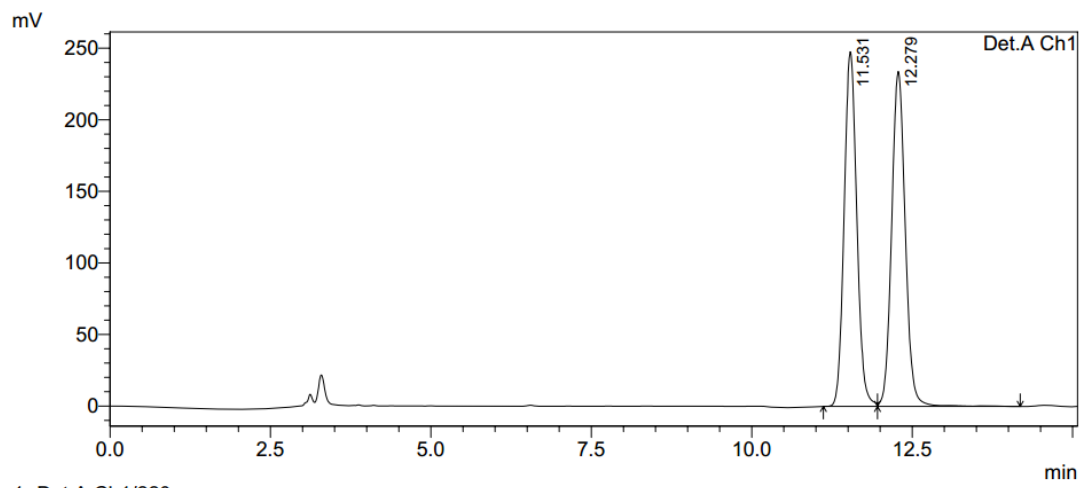
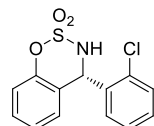


PeakTable

Detector A Ch1 220nm

Peak#	Ret. Time	Area	Height	Area %	Height %
1	59.629	564173	11994	1.594	2.129
2	61.728	34833641	551351	98.406	97.871
Total		35397814	563345	100.000	100.000

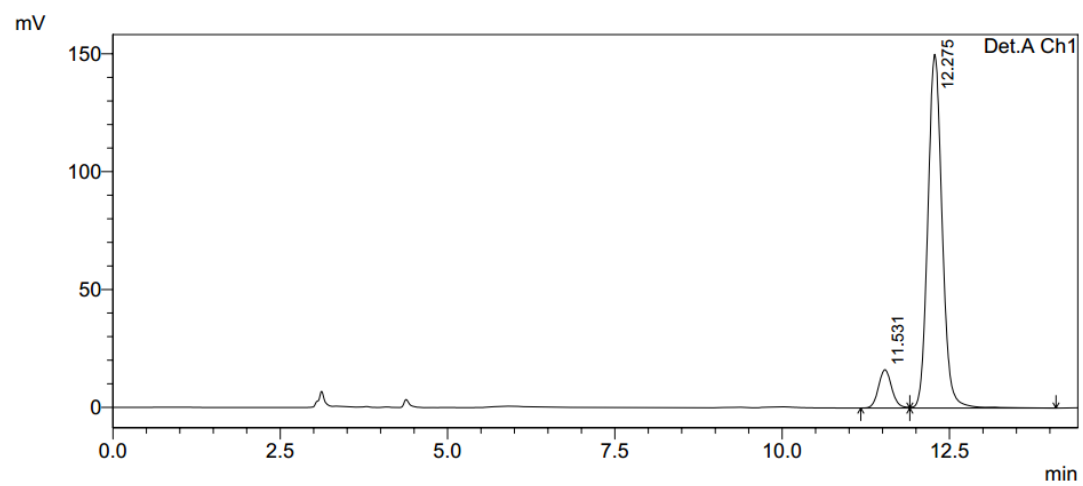




PeakTable

Detector A Ch1 220nm

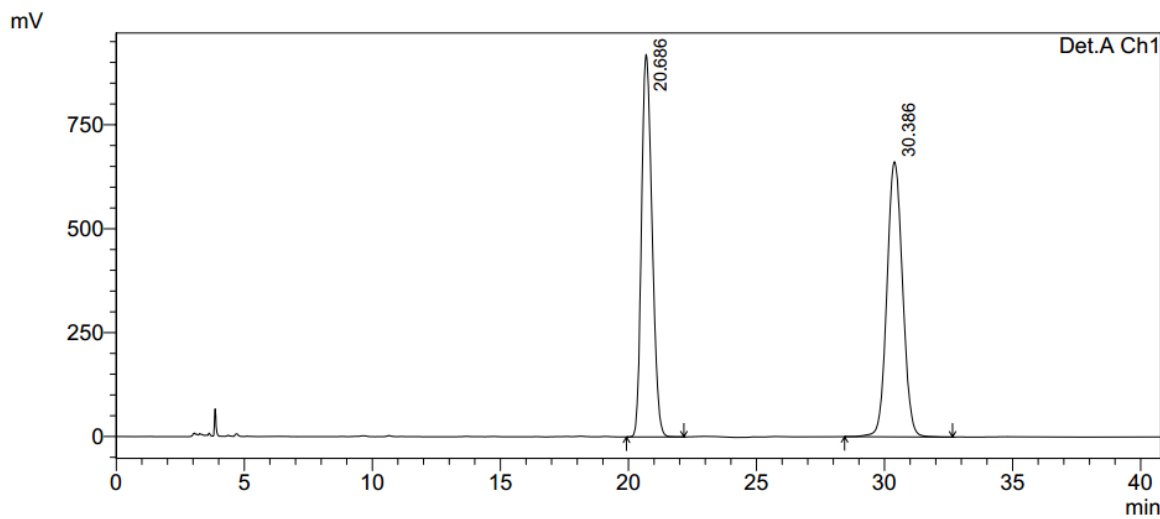
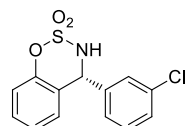
Peak#	Ret. Time	Area	Height	Area %	Height %
1	11.531	3391231	247750	49.625	51.429
2	12.279	3442461	233982	50.375	48.571
Total		6833692	481732	100.000	100.000



PeakTable

Detector A Ch1 220nm

Peak#	Ret. Time	Area	Height	Area %	Height %
1	11.531	224808	16298	9.159	9.796
2	12.275	2229638	150075	90.841	90.204
Total		2454445	166373	100.000	100.000

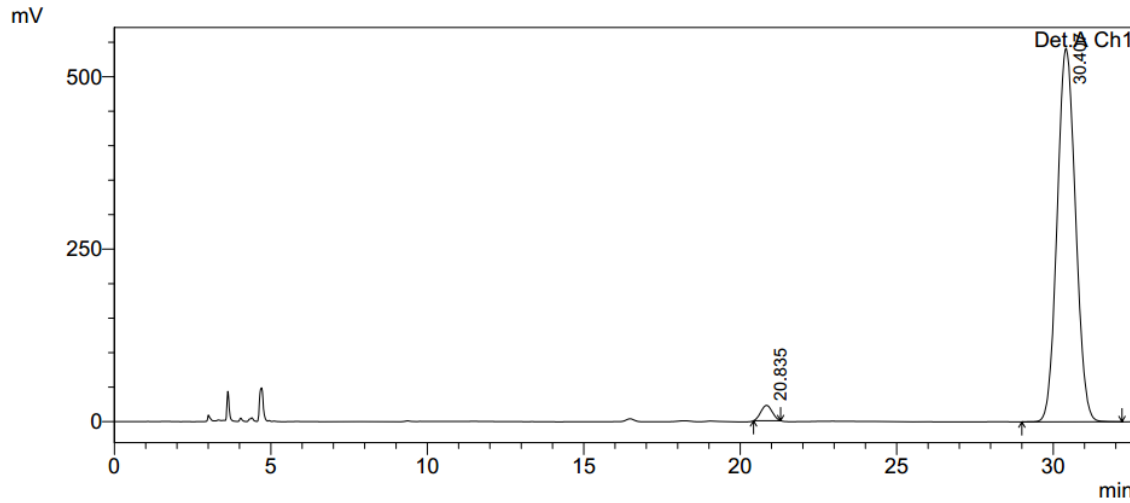


1 Det.A Ch1/220nm

PeakTable

Detector A Ch1 220nm

Peak#	Ret. Time	Area	Height	Area %	Height %
1	20.686	26407135	920389	48.507	58.170
2	30.386	28033204	661844	51.493	41.830
Total		54440339	1582233	100.000	100.000

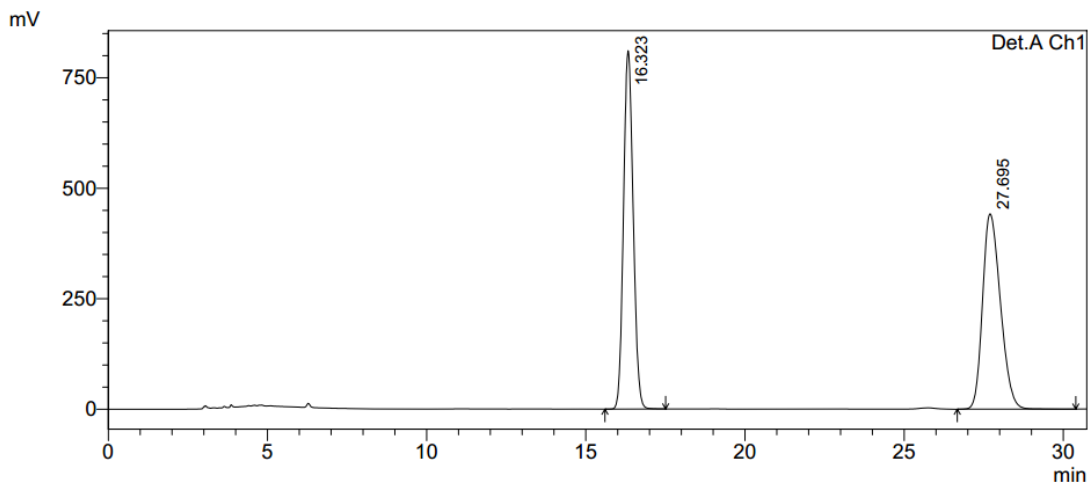
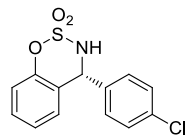


1 Det.A Ch1/220nm

PeakTable

Detector A Ch1 220nm

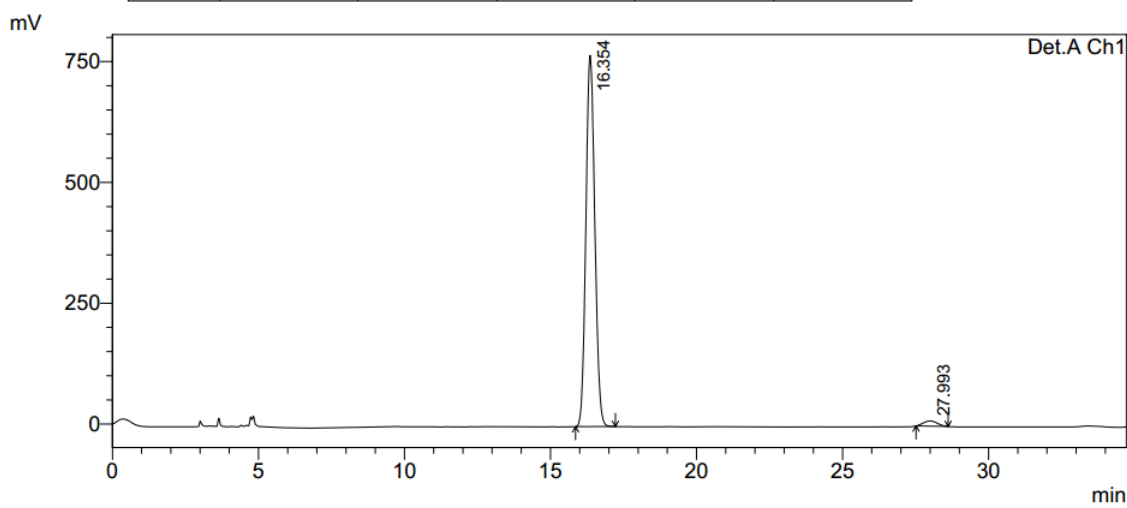
Peak#	Ret. Time	Area	Height	Area %	Height %
1	20.835	559861	22197	2.475	3.938
2	30.407	22061232	541435	97.525	96.062
Total		22621094	563632	100.000	100.000



PeakTable

Detector A Ch1 220nm

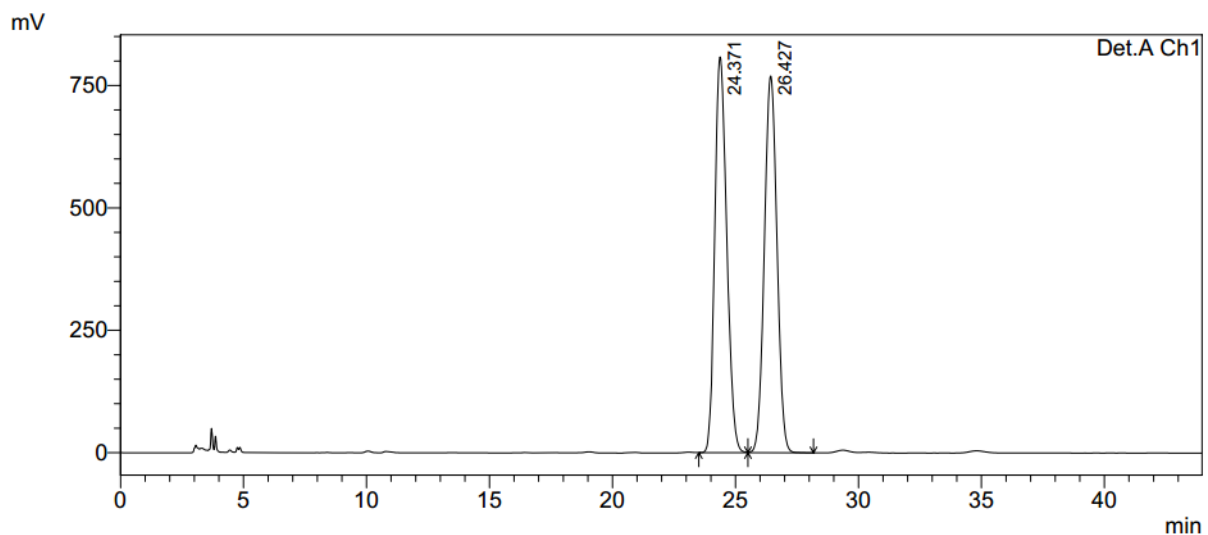
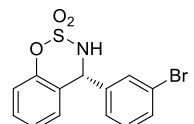
Peak#	Ret. Time	Area	Height	Area %	Height %
1	16.323	17137501	810824	49.907	64.728
2	27.695	17201181	441836	50.093	35.272
Total		34338682	1252659	100.000	100.000



PeakTable

Detector A Ch1 220nm

Peak#	Ret. Time	Area	Height	Area %	Height %
1	16.354	16262081	768152	97.857	98.622
2	27.993	356165	10734	2.143	1.378
Total		16618245	778887	100.000	100.000

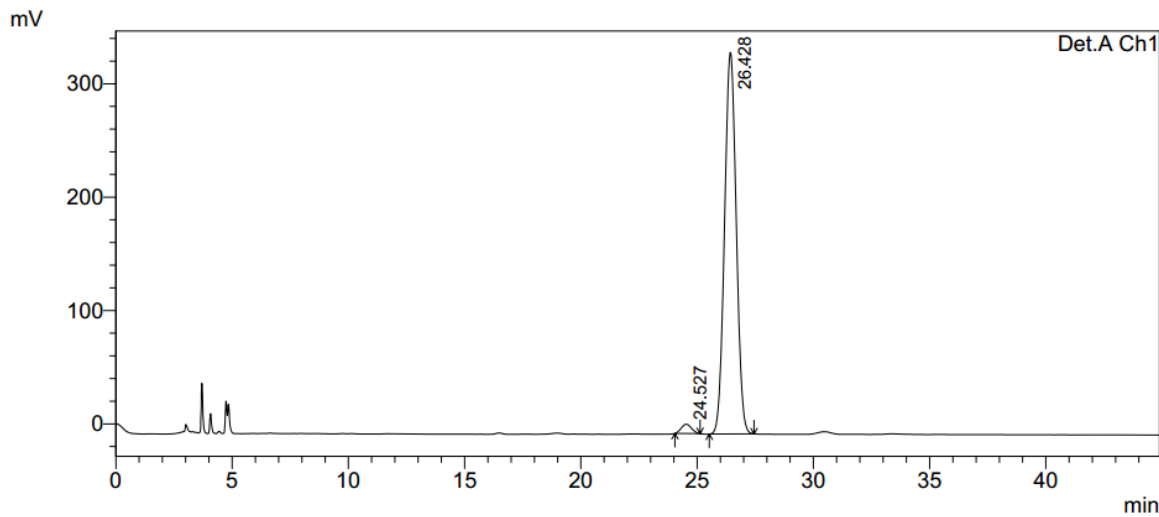


1 Det.A Ch1/220nm

PeakTable

Detector A Ch1 220nm

Peak#	Ret. Time	Area	Height	Area %	Height %
1	24.371	27290940	808414	49.904	51.230
2	26.427	27395463	769583	50.096	48.770
Total		54686402	1577997	100.000	100.000

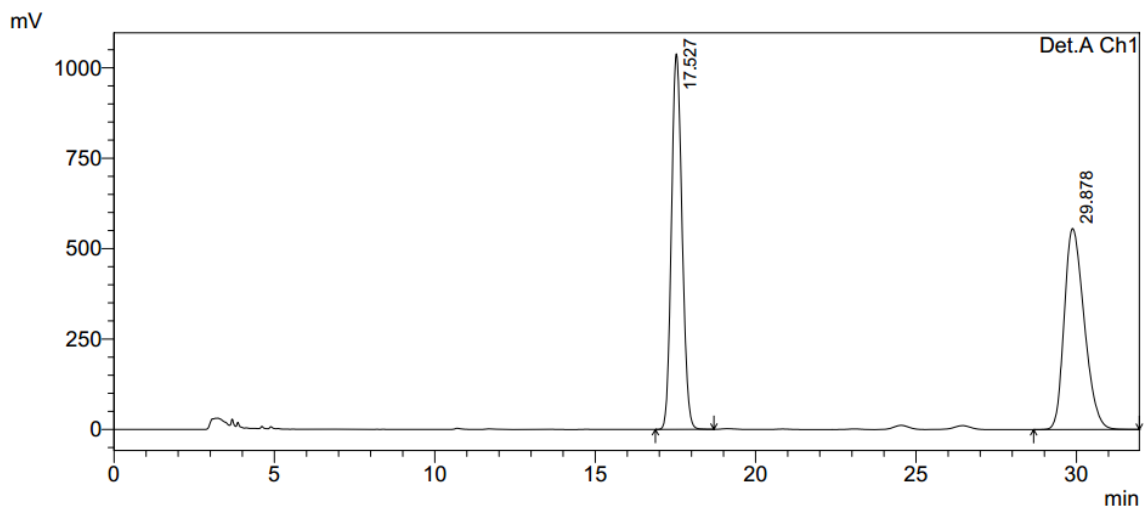
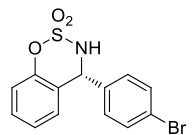


1 Det.A Ch1/220nm

PeakTable

Detector A Ch1 220nm

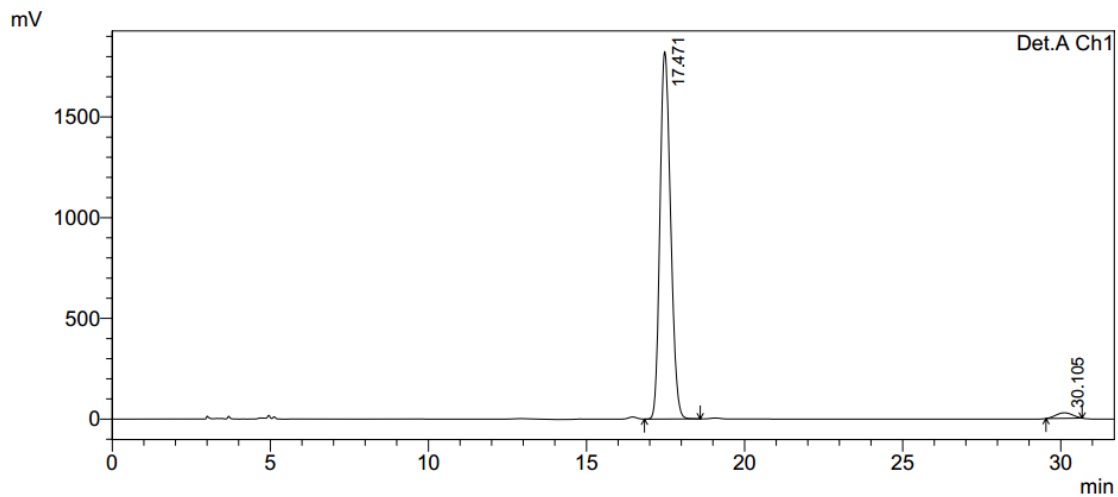
Peak#	Ret. Time	Area	Height	Area %	Height %
1	24.527	251254	8195	2.096	2.376
2	26.428	11737836	336637	97.904	97.624
Total		11989091	344831	100.000	100.000



PeakTable

Detector A Ch1 220nm

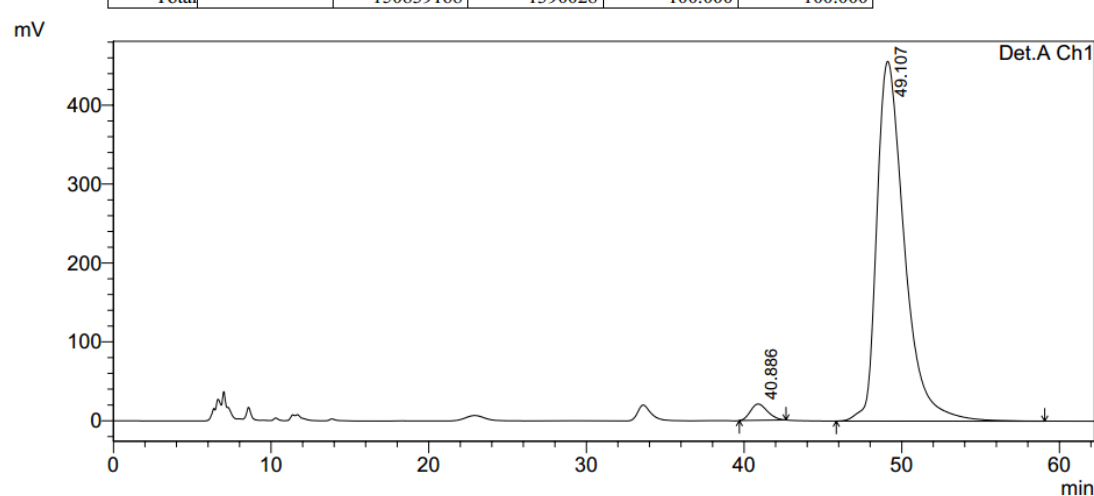
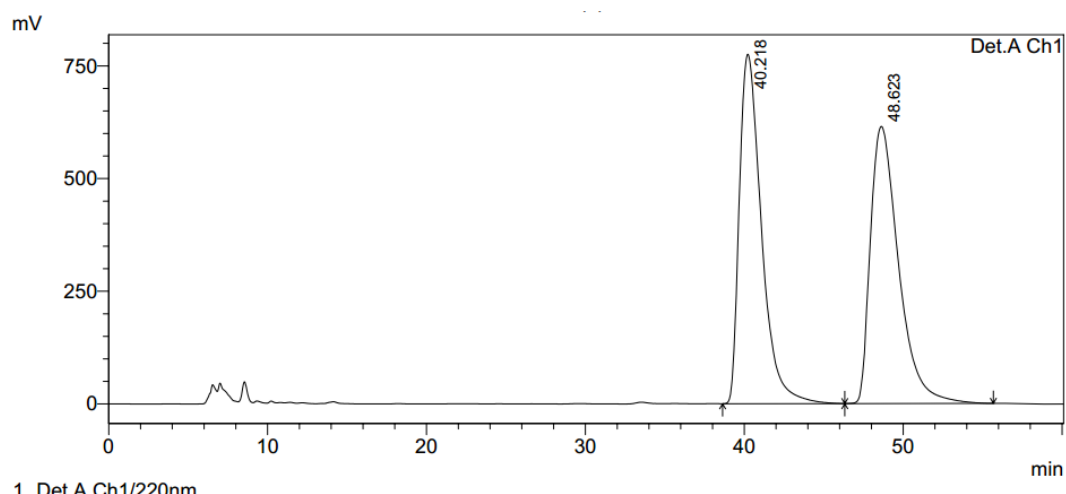
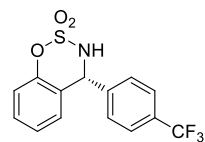
Peak#	Ret. Time	Area	Height	Area %	Height %
1	17.527	23857068	1038749	49.736	65.122
2	29.878	24110523	556339	50.264	34.878
Total		47967592	1595088	100.000	100.000

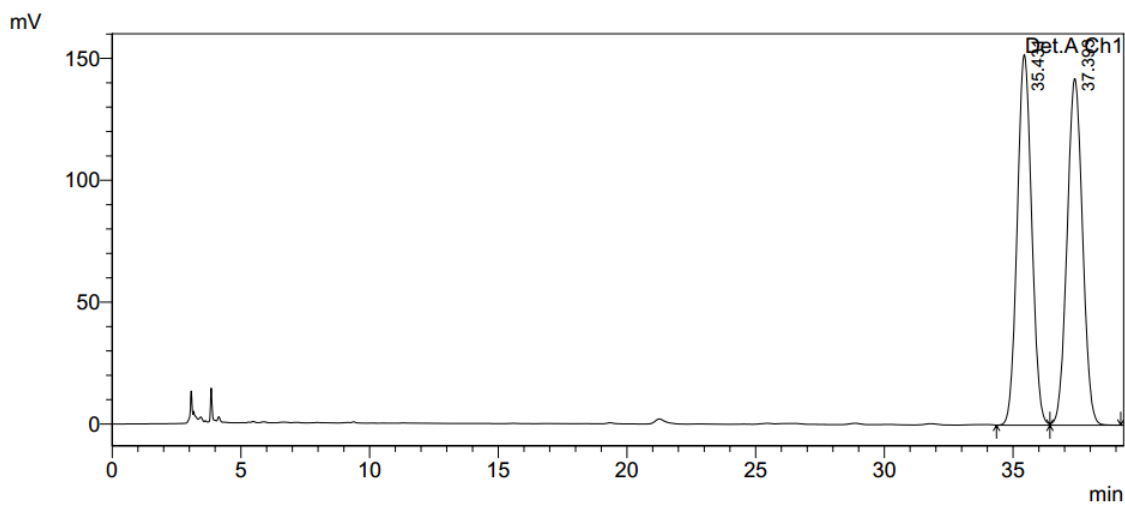
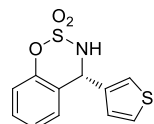


PeakTable

Detector A Ch1 220nm

Peak#	Ret. Time	Area	Height	Area %	Height %
1	17.471	42664704	1824911	97.720	98.516
2	30.105	995295	27488	2.280	1.484
Total		43659999	1852400	100.000	100.000

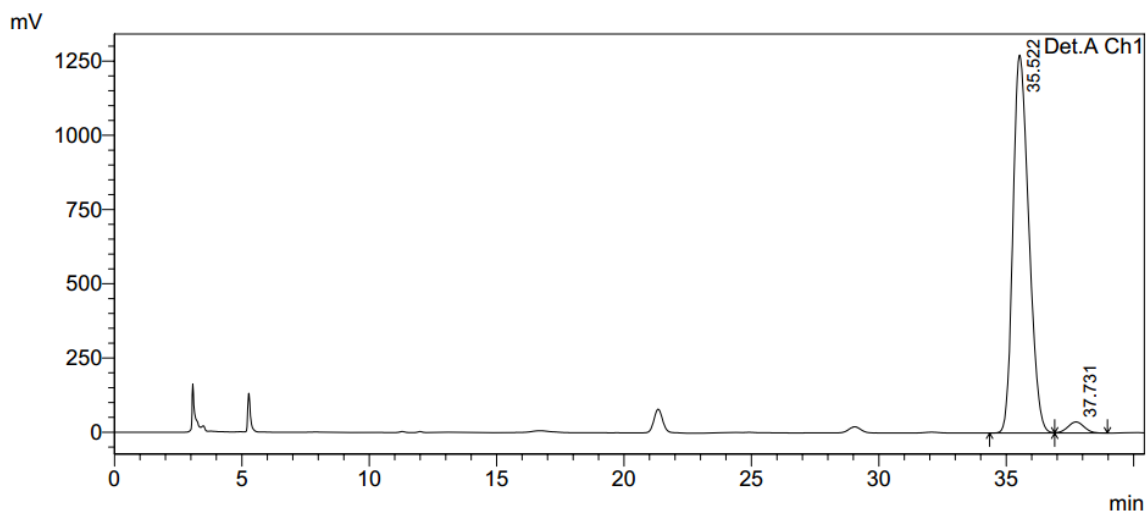




PeakTable

Detector A Ch1 220nm

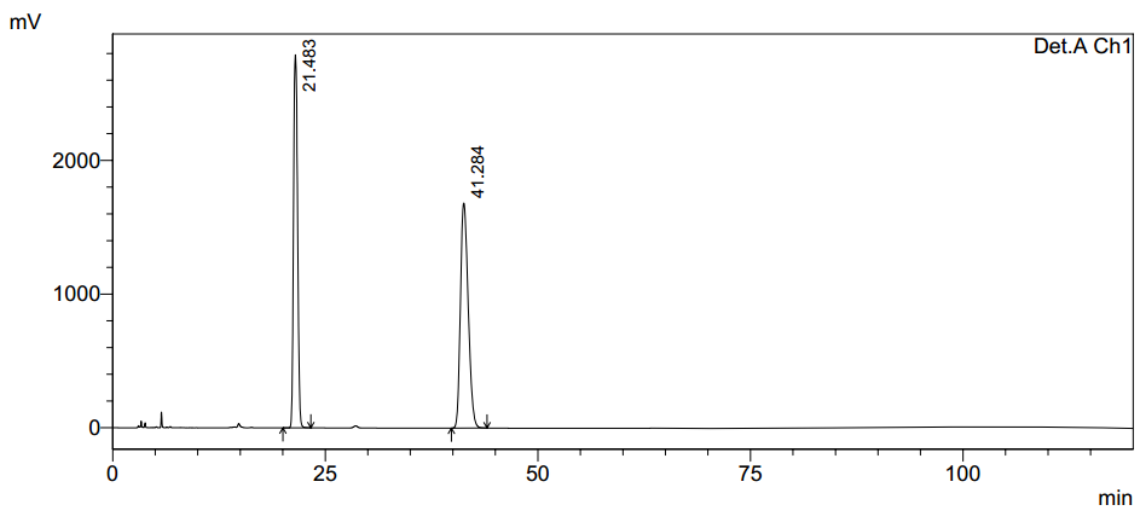
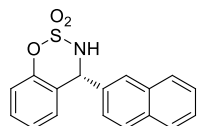
Peak#	Ret. Time	Area	Height	Area %	Height %
1	35.431	5929728	152069	49.964	51.680
2	37.393	5938277	142184	50.036	48.320
Total		11868004	294252	100.000	100.000



PeakTable

Detector A Ch1 220nm

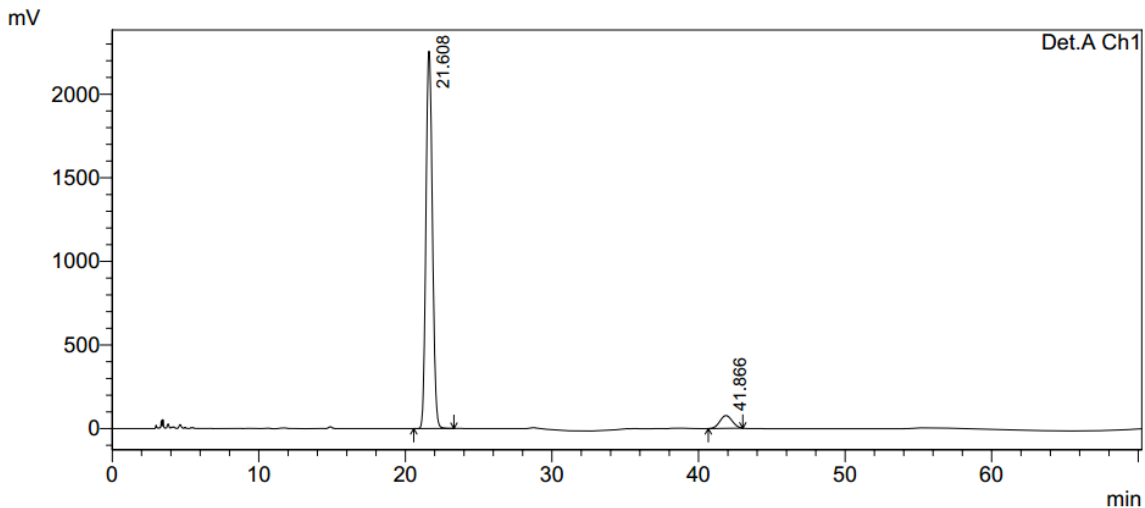
Peak#	Ret. Time	Area	Height	Area %	Height %
1	35.522	54924409	1272810	97.059	97.149
2	37.731	1664416	37347	2.941	2.851
Total		56588825	1310157	100.000	100.000



PeakTable

Detector A Ch1 220nm

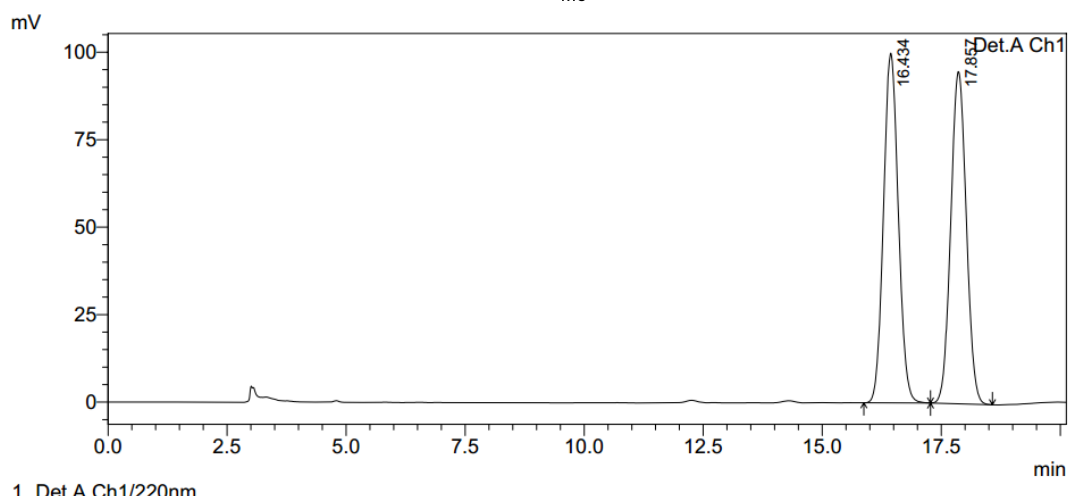
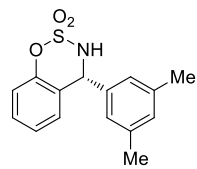
Peak#	Ret. Time	Area	Height	Area %	Height %
1	21.483	92534192	2790697	46.390	62.368
2	41.284	106937580	1683887	53.610	37.632
Total		199471772	4474585	100.000	100.000



PeakTable

Detector A Ch1 220nm

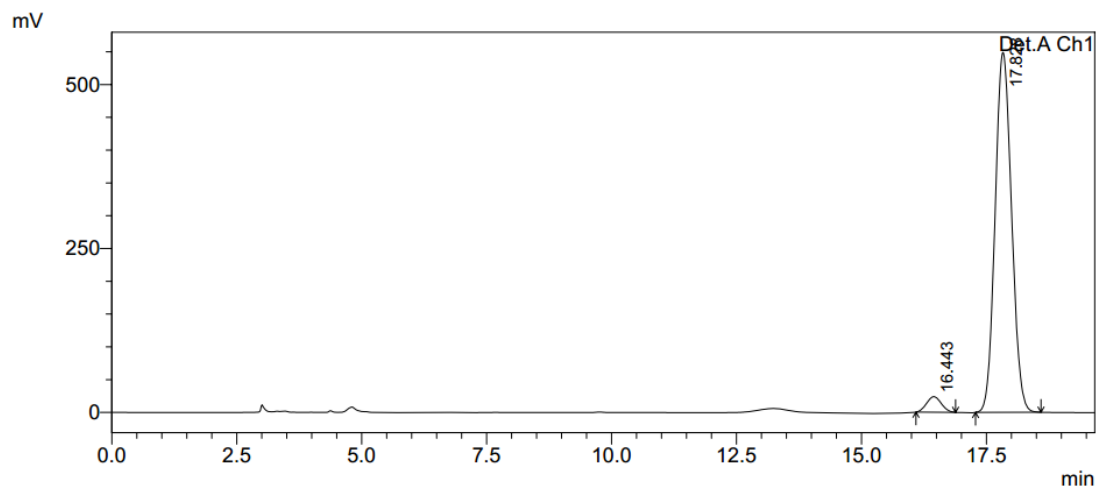
Peak#	Ret. Time	Area	Height	Area %	Height %
1	21.608	69187642	2257889	93.886	96.710
2	41.866	4505653	76809	6.114	3.290
Total		73693294	2334698	100.000	100.000



PeakTable

Detector A Ch1 220nm

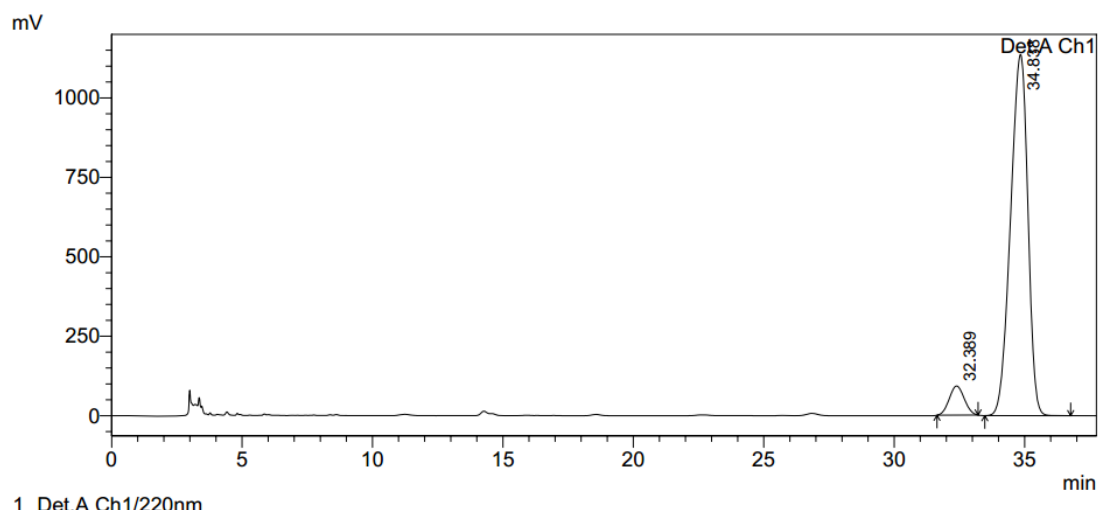
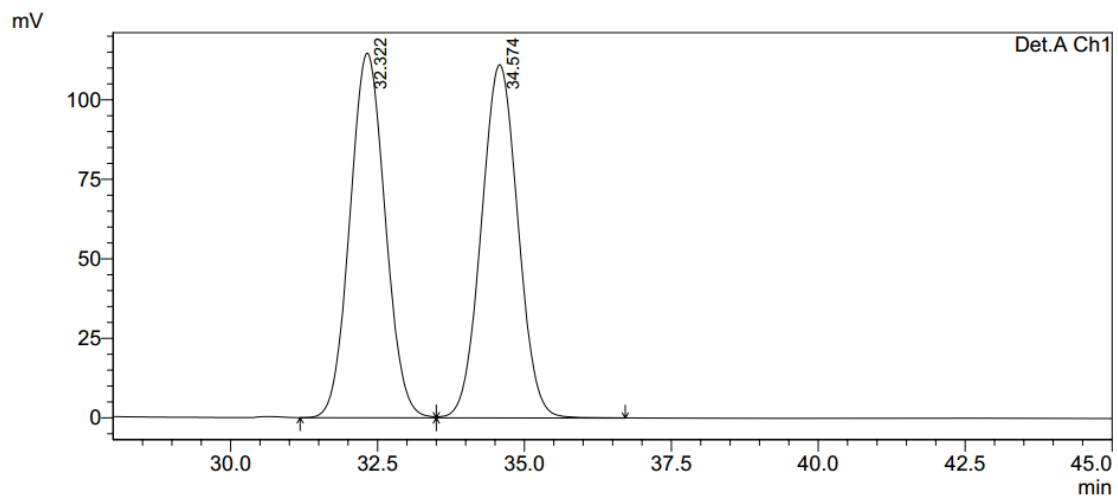
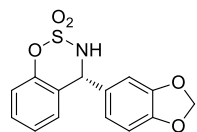
Peak#	Ret. Time	Area	Height	Area %	Height %
1	16.434	2161841	99963	50.157	51.290
2	17.857	2148328	94934	49.843	48.710
Total		4310170	194897	100.000	100.000

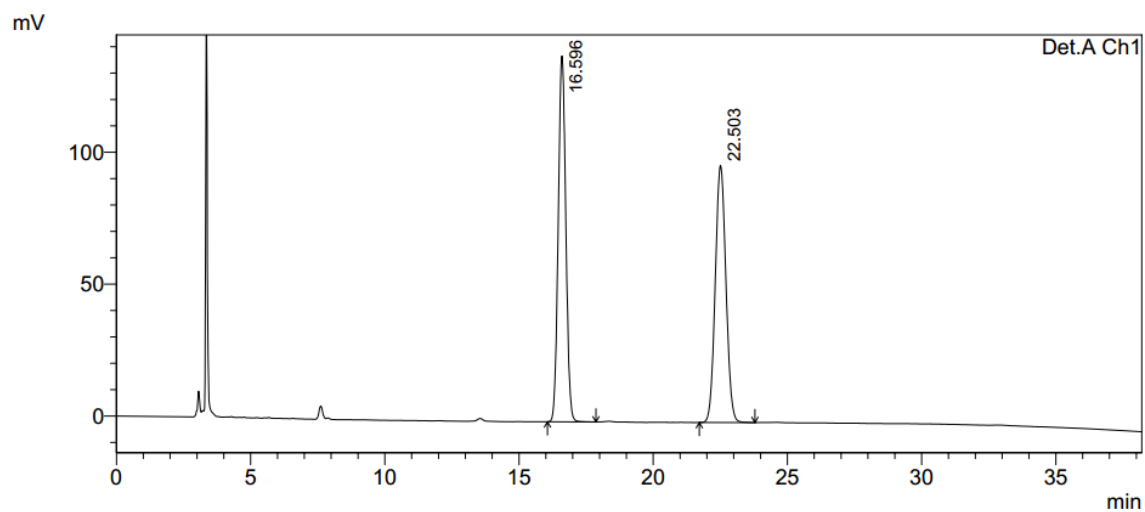
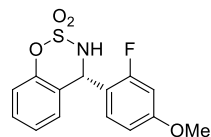


PeakTable

Detector A Ch1 220nm

Peak#	Ret. Time	Area	Height	Area %	Height %
1	16.443	484665	23695	3.724	4.137
2	17.828	12531214	549062	96.276	95.863
Total		13015878	572757	100.000	100.000

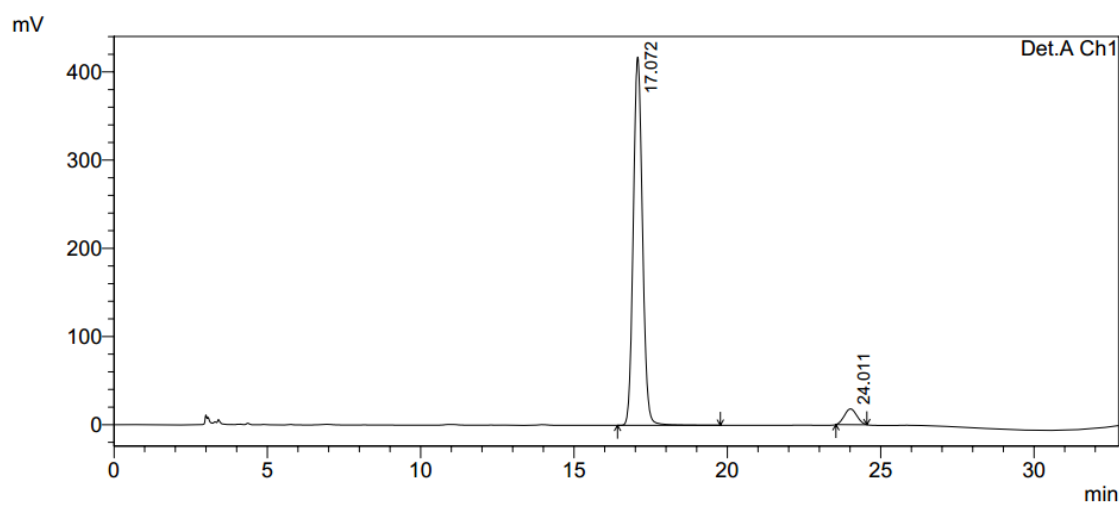




PeakTable

Detector A Ch1 220nm

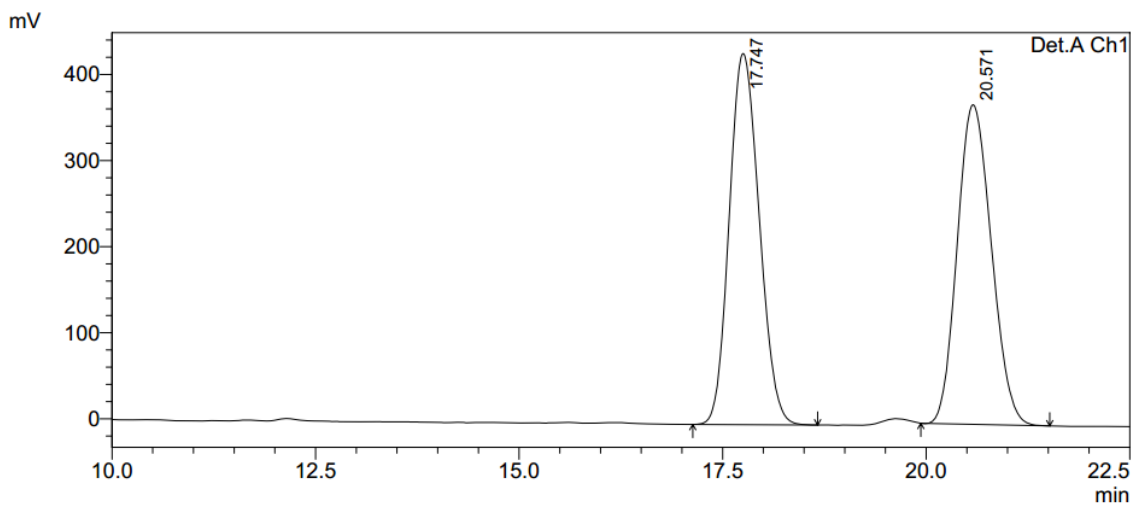
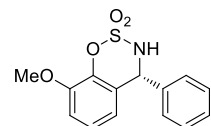
Peak#	Ret. Time	Area	Height	Area %	Height %
1	16.596	2712950	138722	50.284	58.745
2	22.503	2682275	97420	49.716	41.255
Total		5395224	236142	100.000	100.000



PeakTable

Detector A Ch1 220nm

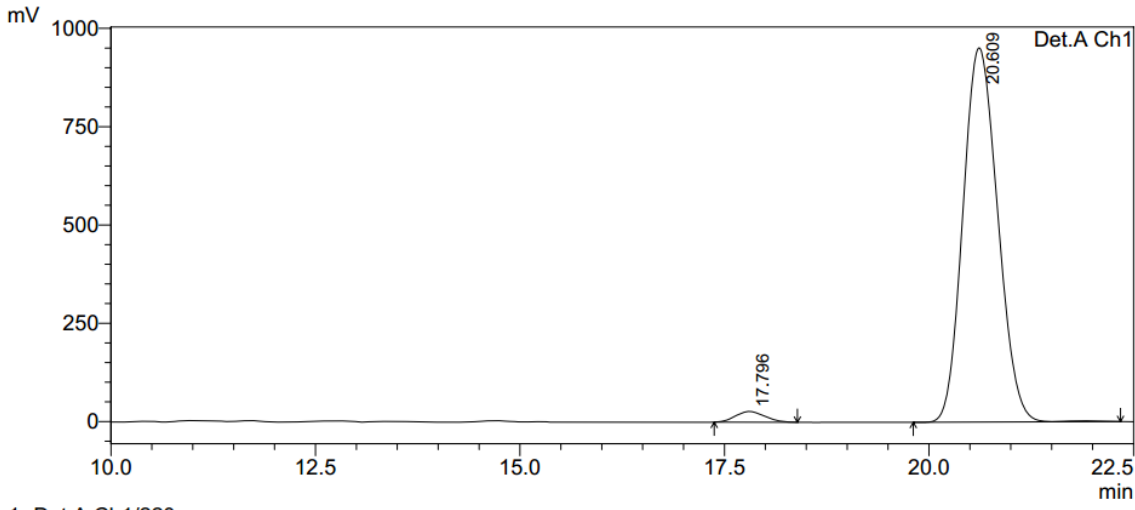
Peak#	Ret. Time	Area	Height	Area %	Height %
1	17.072	8708107	417622	94.583	95.914
2	24.011	498755	17790	5.417	4.086
Total		9206862	435412	100.000	100.000



PeakTable

Detector A Ch1 220nm

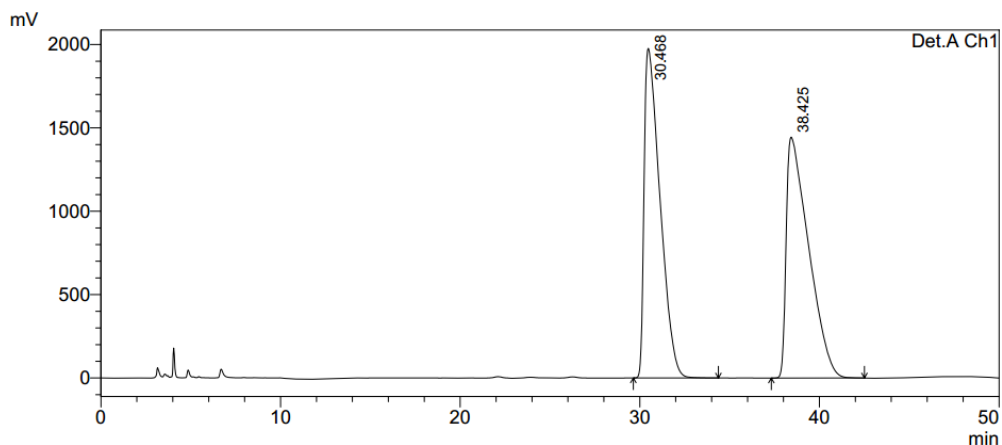
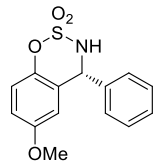
Peak#	Ret. Time	Area	Height	Area %	Height %
1	17.747	11021603	431149	50.451	53.733
2	20.571	10824386	371238	49.549	46.267
Total		21845989	802387	100.000	100.000



PeakTable

Detector A Ch1 220nm

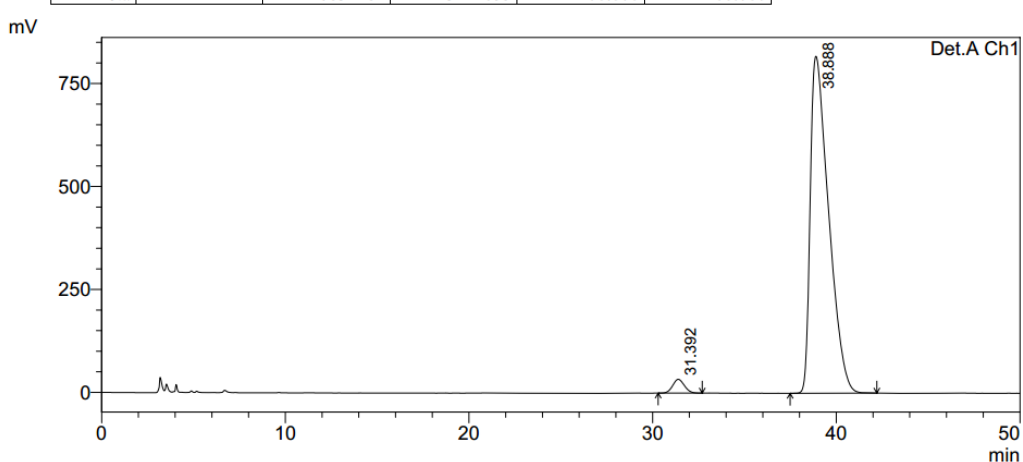
Peak#	Ret. Time	Area	Height	Area %	Height %
1	17.796	675789	27124	2.346	2.771
2	20.609	28124208	951722	97.654	97.229
Total		28799997	978845	100.000	100.000



PeakTable

Detector A Ch1 220nm

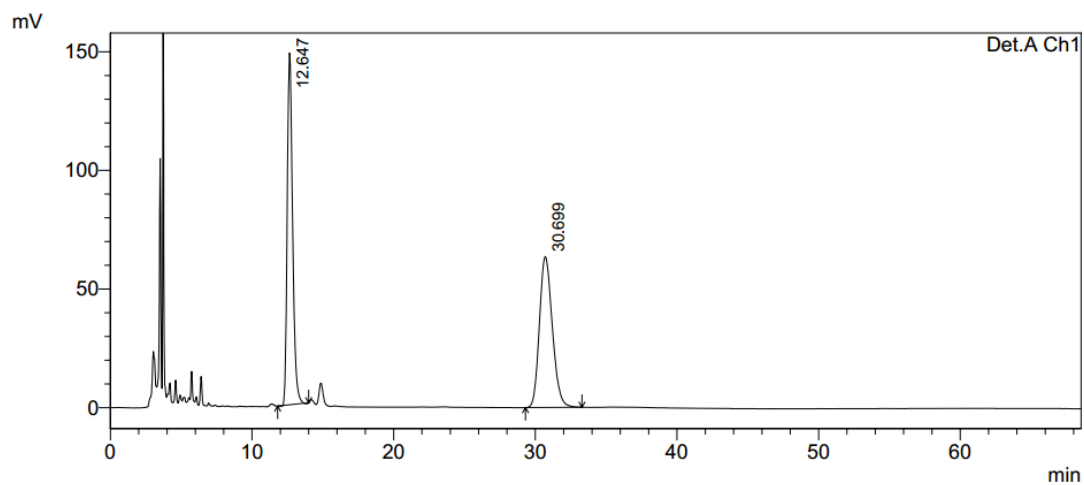
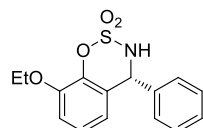
Peak#	Ret. Time	Area	Height	Area %	Height %
1	30.468	121626638	1976417	49.315	57.772
2	38.425	125007626	1444638	50.685	42.228
Total		246634264	3421055	100.000	100.000



PeakTable

Detector A Ch1 220nm

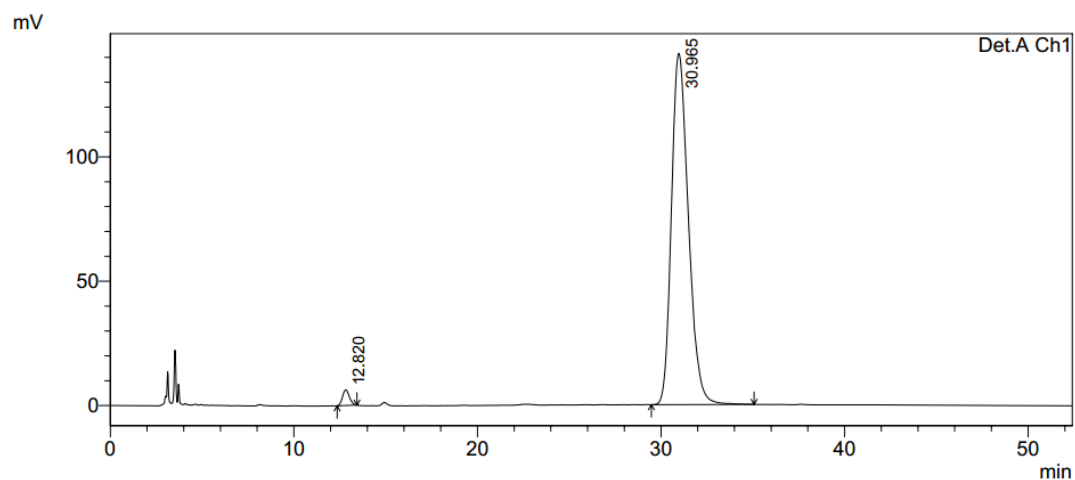
Peak#	Ret. Time	Area	Height	Area %	Height %
1	31.392	1479944	33553	2.536	3.939
2	38.888	56869091	818204	97.464	96.061
Total		58349036	851757	100.000	100.000



PeakTable

Detector A Ch1 220nm

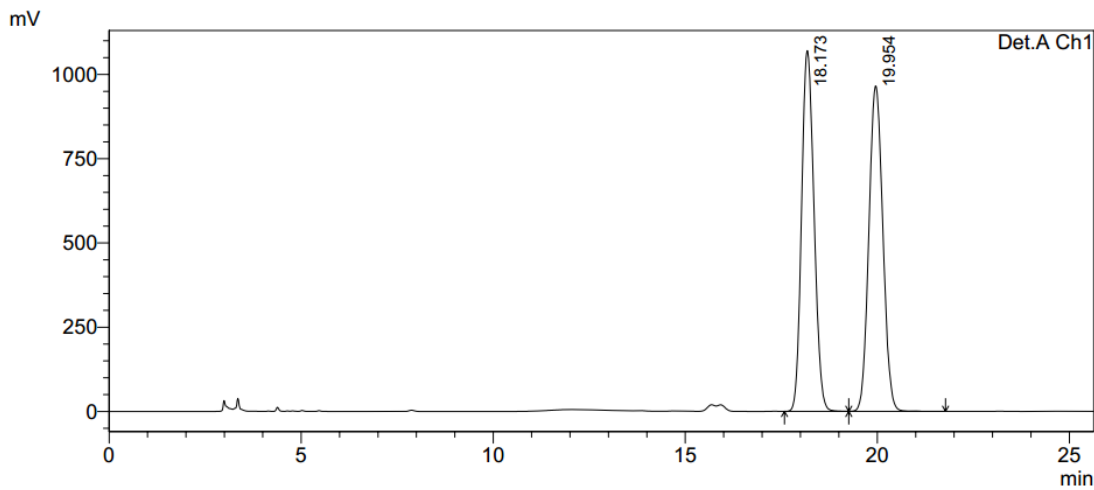
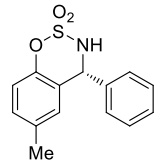
Peak#	Ret. Time	Area	Height	Area %	Height %
1	12.647	3888276	148324	49.197	69.994
2	30.699	4015191	63586	50.803	30.006
Total		7903467	211910	100.000	100.000



PeakTable

Detector A Ch1 220nm

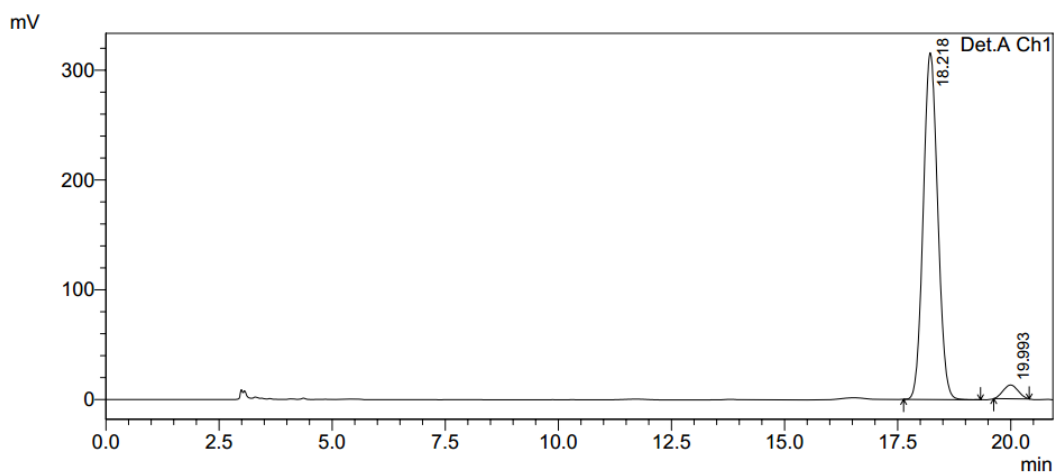
Peak#	Ret. Time	Area	Height	Area %	Height %
1	12.820	163995	6294	1.777	4.266
2	30.965	9062181	141249	98.223	95.734
Total		9226176	147543	100.000	100.000



PeakTable

Detector A Ch1 220nm

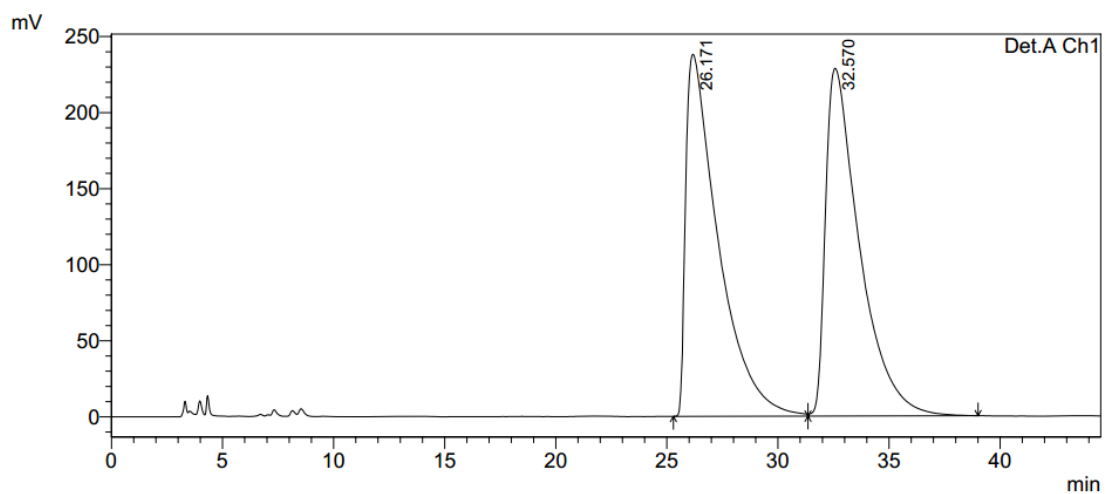
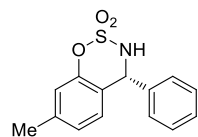
Peak#	Ret. Time	Area	Height	Area %	Height %
1	18.173	24146344	1070577	49.732	52.569
2	19.954	24406329	965939	50.268	47.431
Total		48552673	2036515	100.000	100.000



PeakTable

Detector A Ch1 220nm

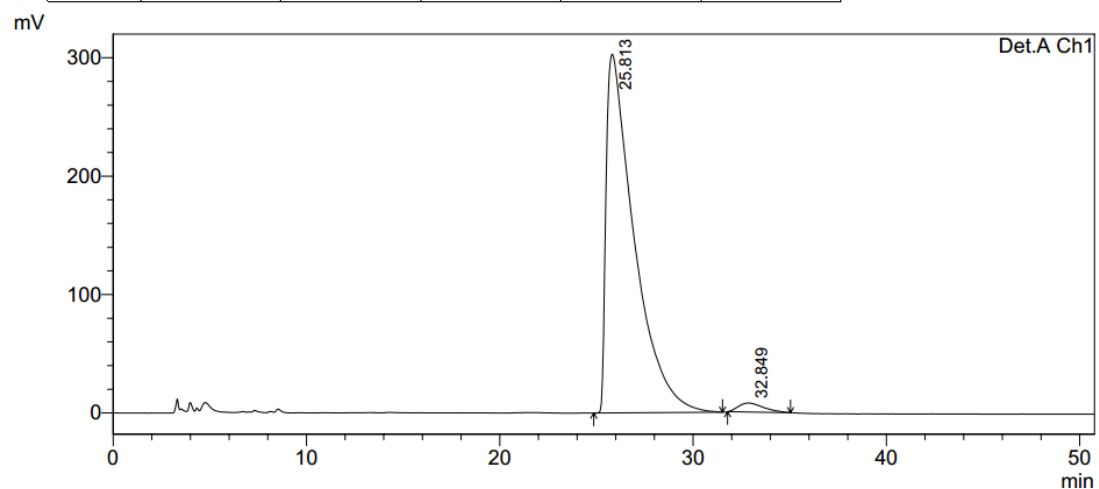
Peak#	Ret. Time	Area	Height	Area %	Height %
1	18.218	7013883	315947	96.027	96.161
2	19.993	290177	12612	3.973	3.839
Total		7304060	328559	100.000	100.000



PeakTable

Detector A Ch1 220nm

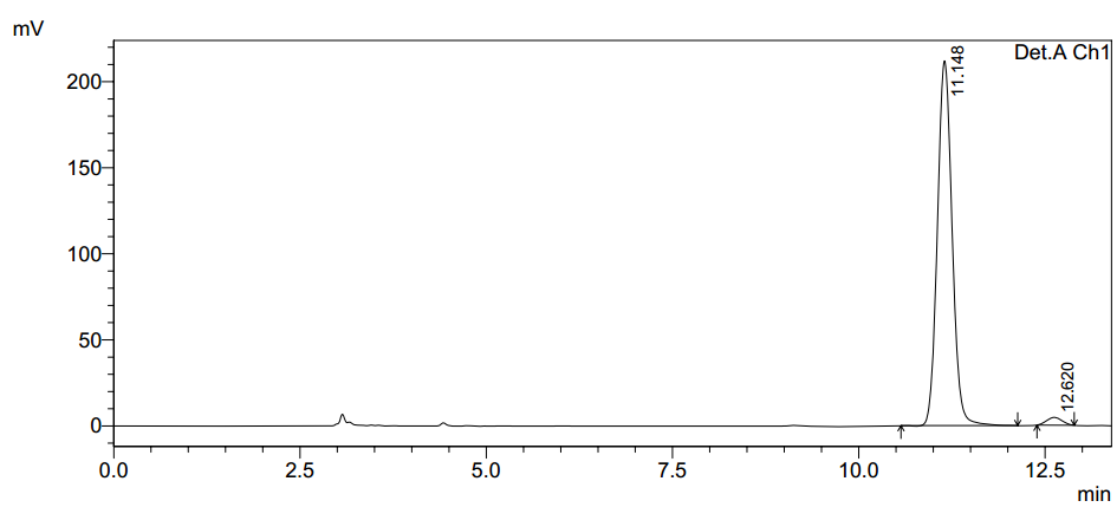
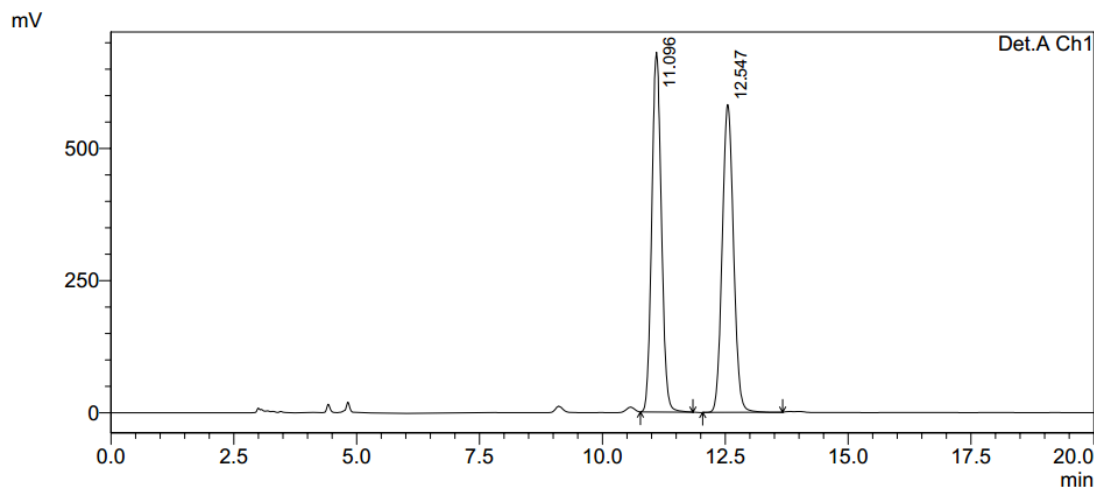
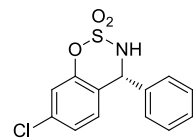
Peak#	Ret. Time	Area	Height	Area %	Height %
1	26.171	24168024	237972	49.841	51.006
2	32.570	24322395	228582	50.159	48.994
Total		48490420	466555	100.000	100.000

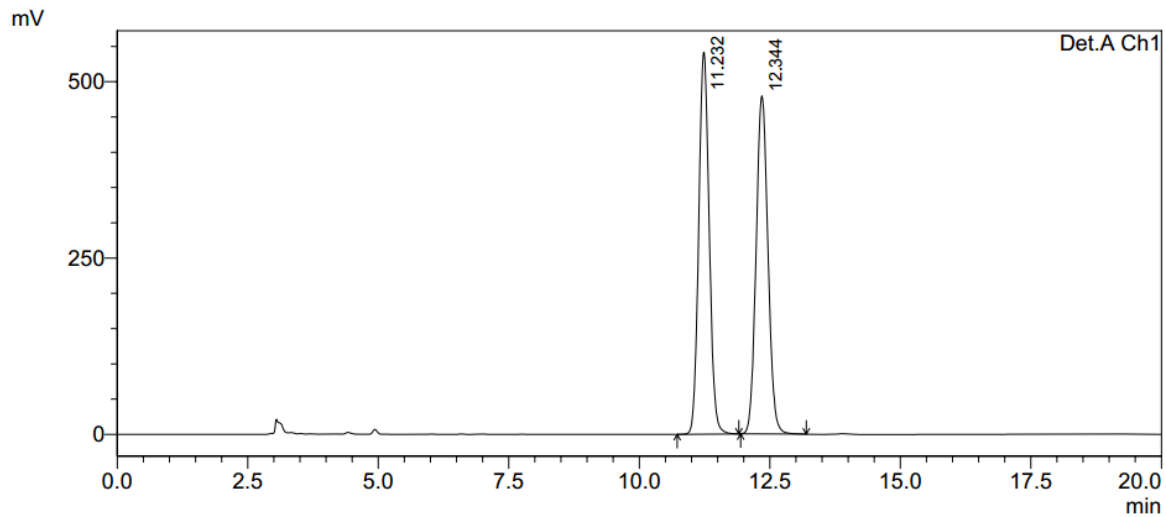
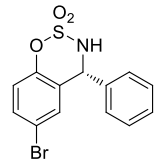


PeakTable

Detector A Ch1 220nm

Peak#	Ret. Time	Area	Height	Area %	Height %
1	25.813	30469571	302972	97.787	97.555
2	32.849	689633	7593	2.213	2.445
Total		31159204	310565	100.000	100.000

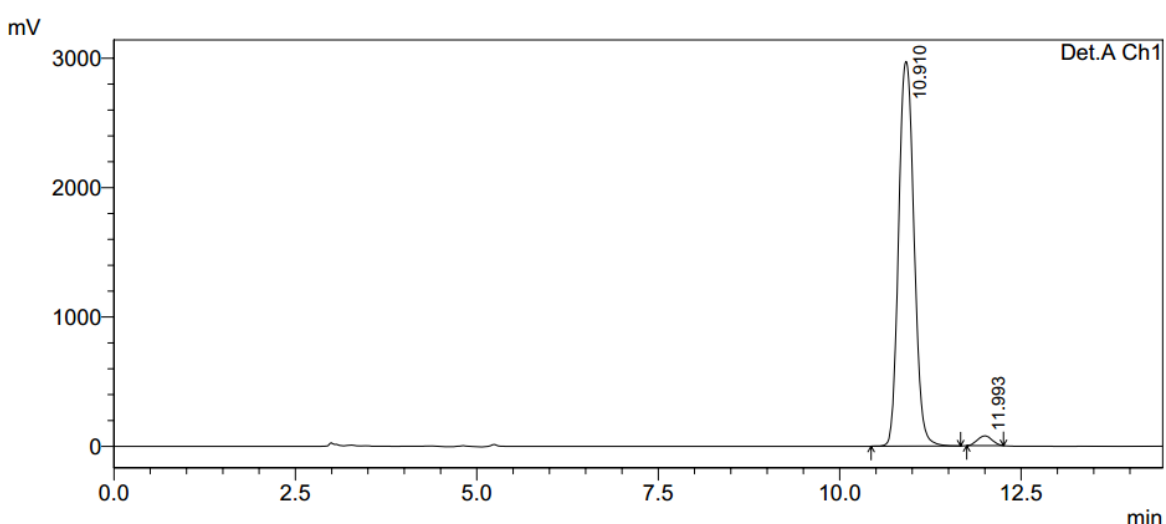




PeakTable

Detector A Ch1 220nm

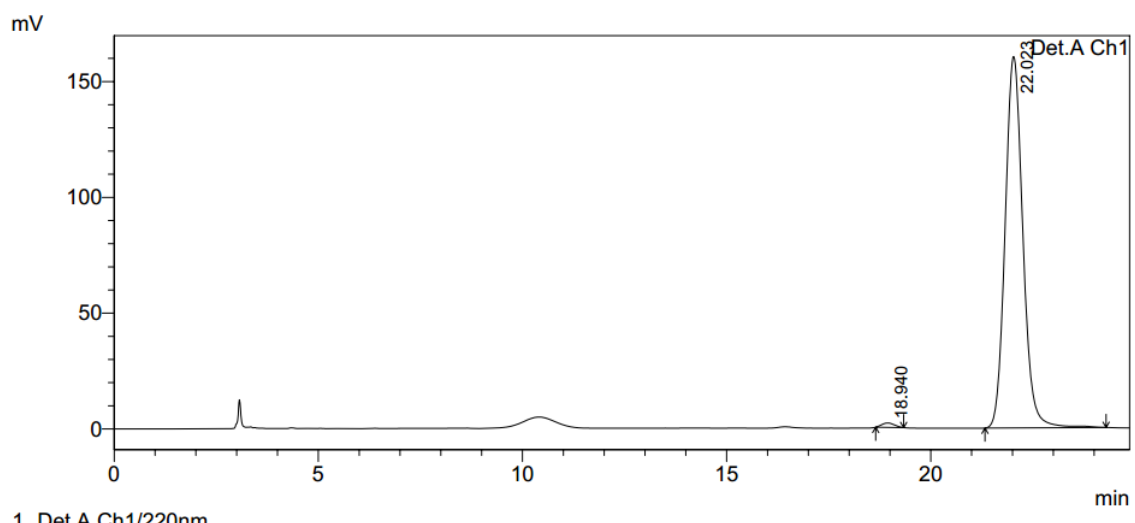
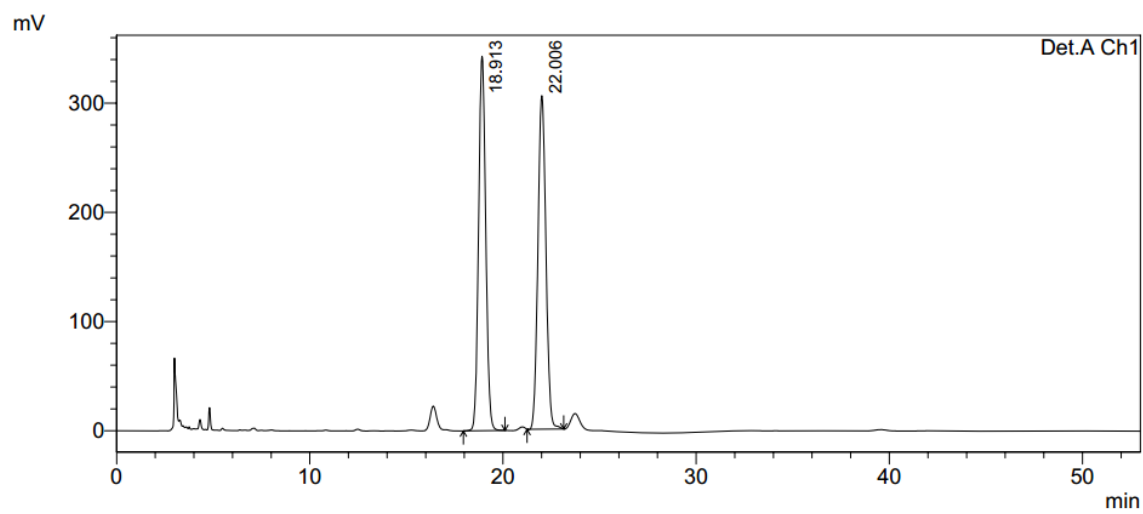
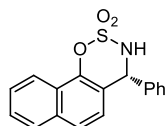
Peak#	Ret. Time	Area	Height	Area %	Height %
1	11.232	7553398	541702	49.994	53.061
2	12.344	7555090	479196	50.006	46.939
Total		15108488	1020898	100.000	100.000

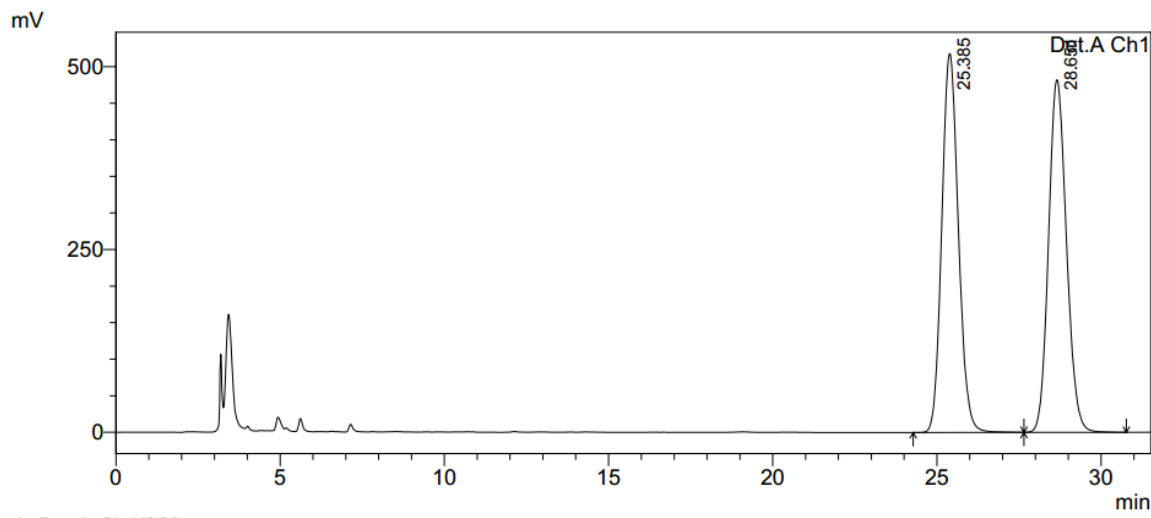
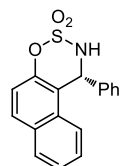


PeakTable

Detector A Ch1 220nm

Peak#	Ret. Time	Area	Height	Area %	Height %
1	10.910	43790572	2974187	97.610	97.489
2	11.993	1072053	76597	2.390	2.511
Total		44862625	3050784	100.000	100.000



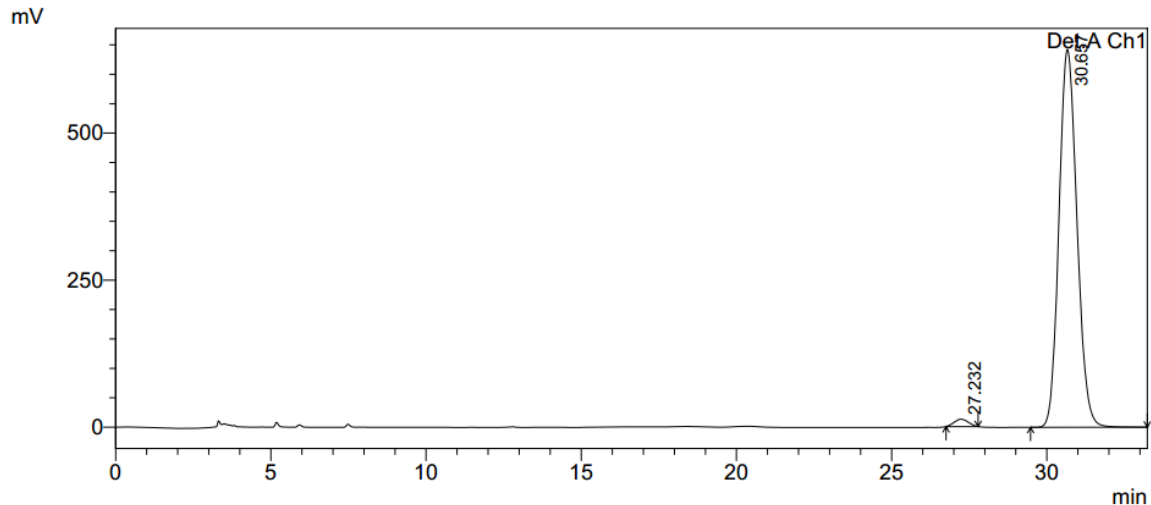


1 Det.A Ch1/220nm

PeakTable

Detector A Ch1 220nm

Peak#	Ret. Time	Area	Height	Area %	Height %
1	25.385	18173216	518454	49.879	51.812
2	28.651	18261294	482198	50.121	48.188
Total		36434511	1000652	100.000	100.000

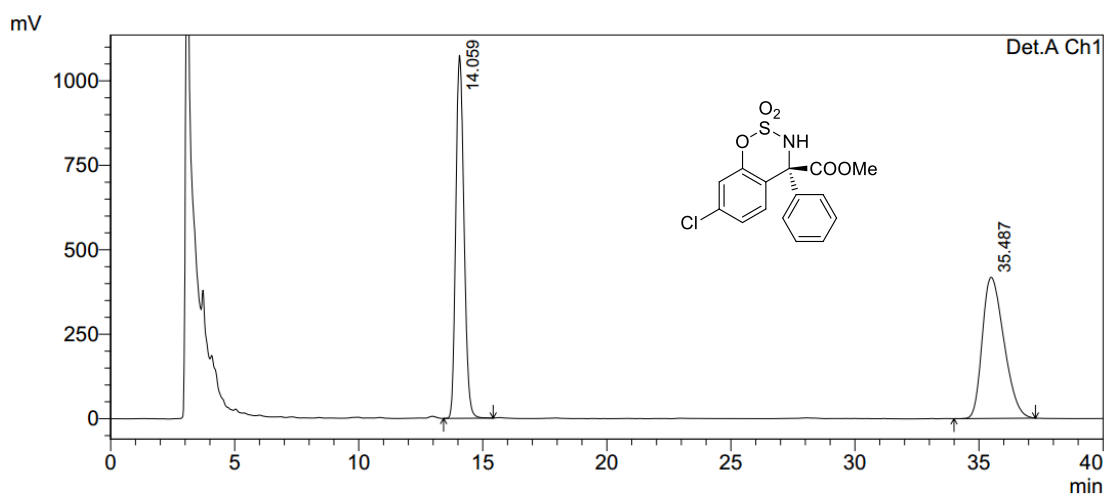


1 Det.A Ch1/220nm

PeakTable

Detector A Ch1 220nm

Peak#	Ret. Time	Area	Height	Area %	Height %
1	27.232	393705	12473	1.501	1.905
2	30.657	25834302	642435	98.499	98.095
Total		26228007	654908	100.000	100.000

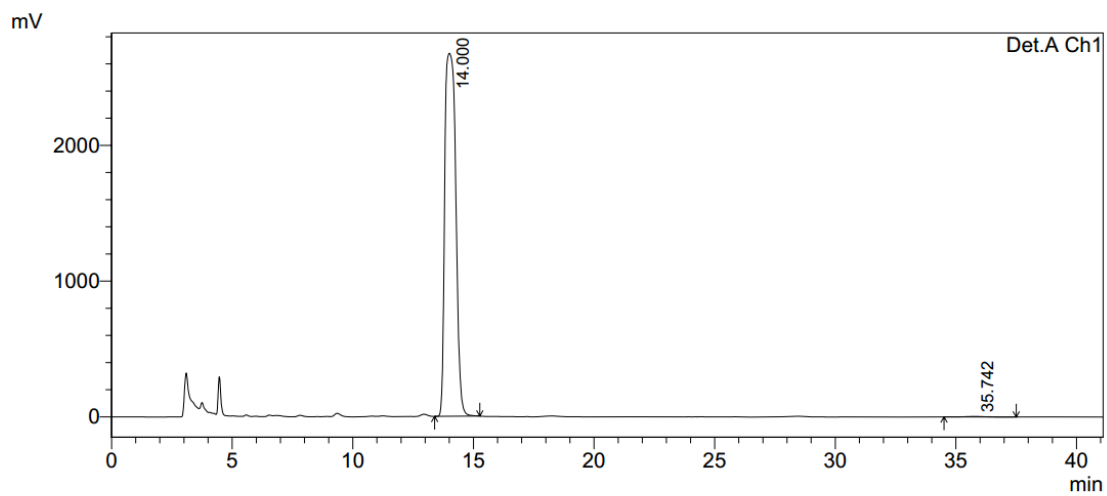


1 Det.A Ch1/210nm

PeakTable

Detector A Ch1 210nm

Peak#	Ret. Time	Area	Height	Area %	Height %
1	14.059	24753943	1074488	49.388	71.994
2	35.487	25367579	417974	50.612	28.006
Total		50121522	1492461	100.000	100.000

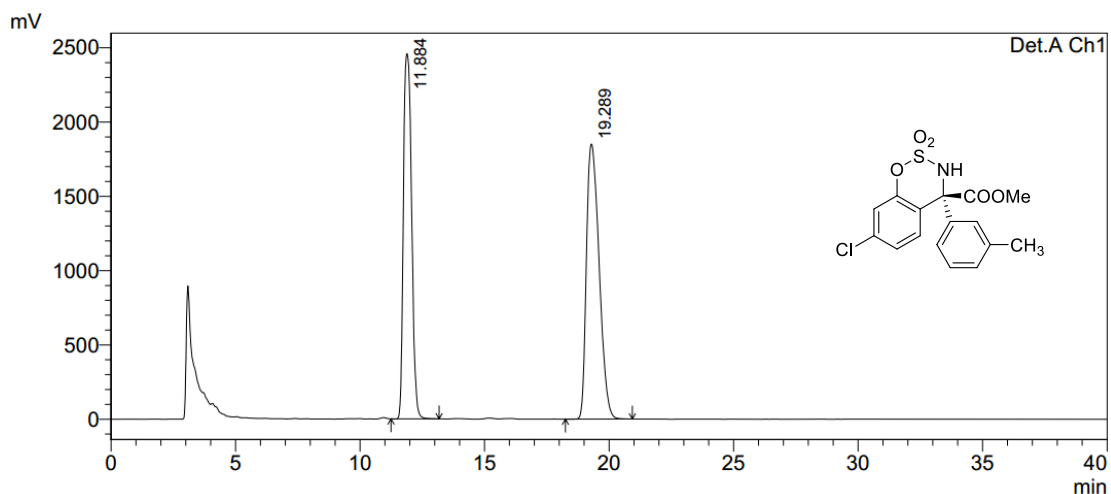


1 Det.A Ch1/210nm

PeakTable

Detector A Ch1 210nm

Peak#	Ret. Time	Area	Height	Area %	Height %
1	14.000	84594704	2674065	99.751	99.858
2	35.742	211264	3803	0.249	0.142
Total		84805968	2677868	100.000	100.000

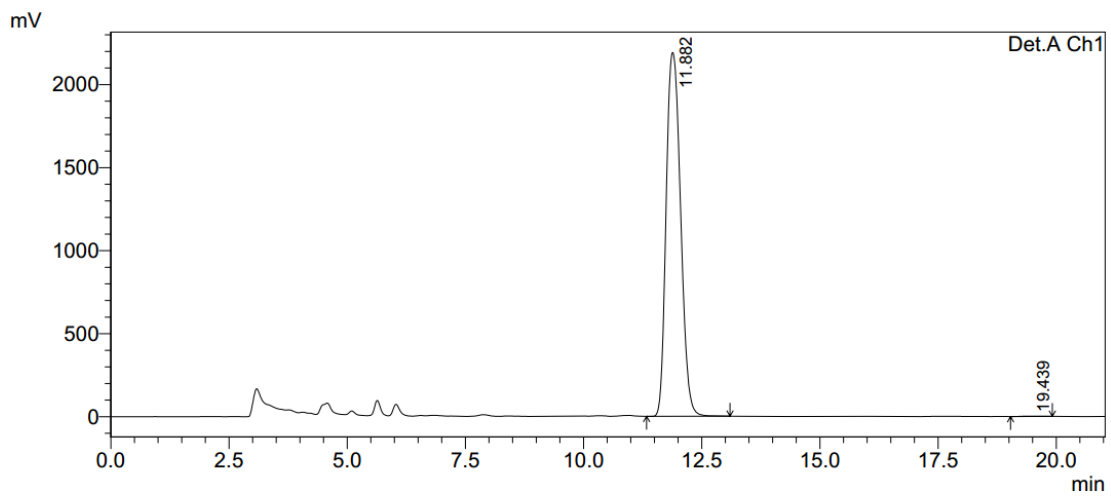


1 Det.A Ch1/210nm

PeakTable

Detector A Ch1 210nm

Peak#	Ret. Time	Area	Height	Area %	Height %
1	11.884	56125104	2458832	46.131	57.050
2	19.289	65538982	1851108	53.869	42.950
Total		121664086	4309940	100.000	100.000

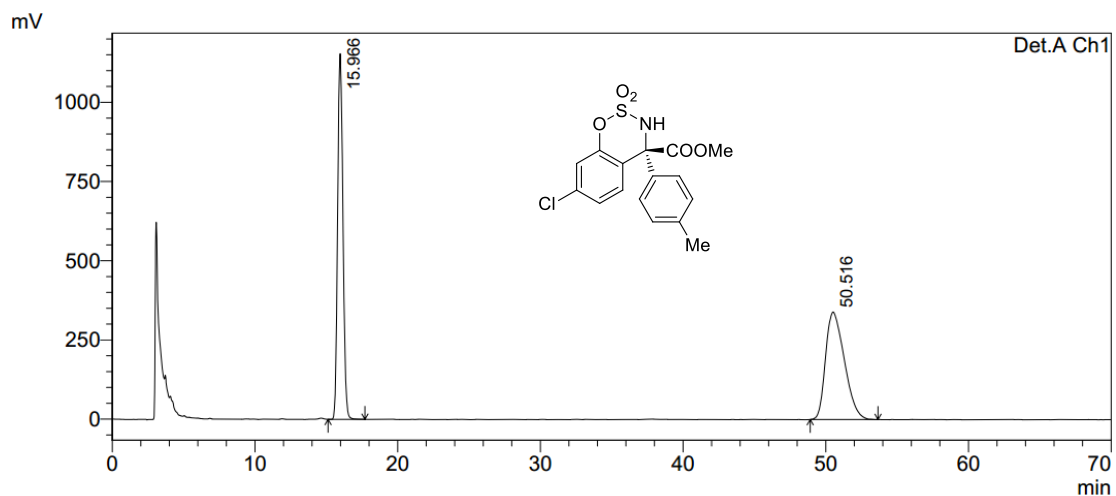


1 Det.A Ch1/210nm

PeakTable

Detector A Ch1 210nm

Peak#	Ret. Time	Area	Height	Area %	Height %
1	11.882	46457118	2191547	99.882	99.894
2	19.439	55039	2321	0.118	0.106
Total		46512157	2193868	100.000	100.000

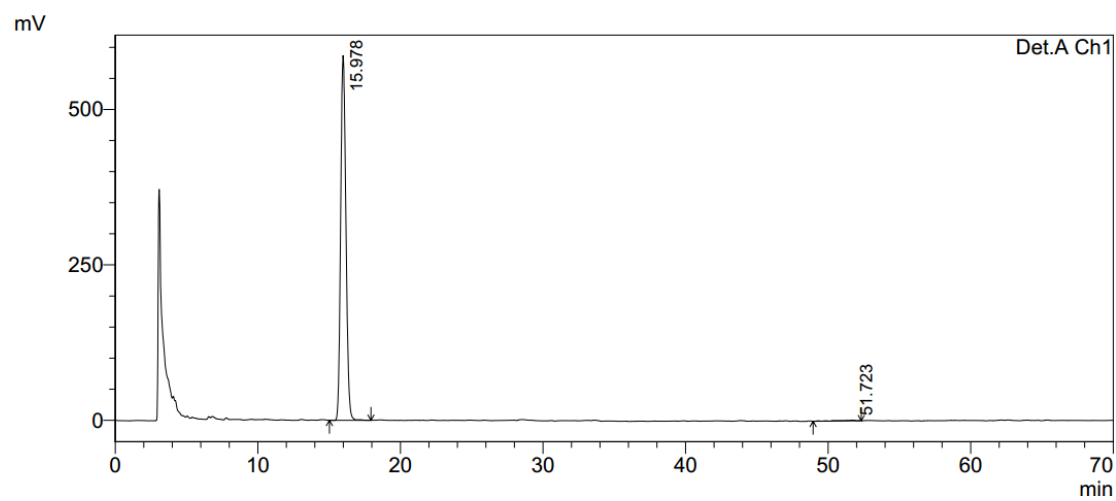


1 Det.A Ch1/210nm

PeakTable

Detector A Ch1 210nm

Peak#	Ret. Time	Area	Height	Area %	Height %
1	15.966	29952297	1154460	49.137	77.284
2	50.516	31003914	339329	50.863	22.716
Total		60956211	1493789	100.000	100.000

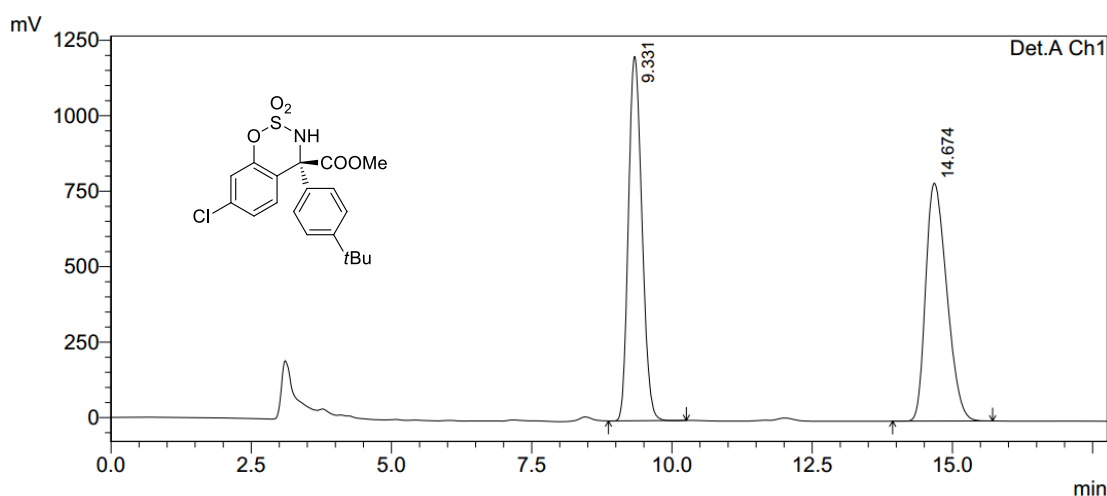


1 Det.A Ch1/210nm

PeakTable

Detector A Ch1 210nm

Peak#	Ret. Time	Area	Height	Area %	Height %
1	15.978	15019714	586719	99.344	99.794
2	51.723	99185	1209	0.656	0.206
Total		15118899	587929	100.000	100.000

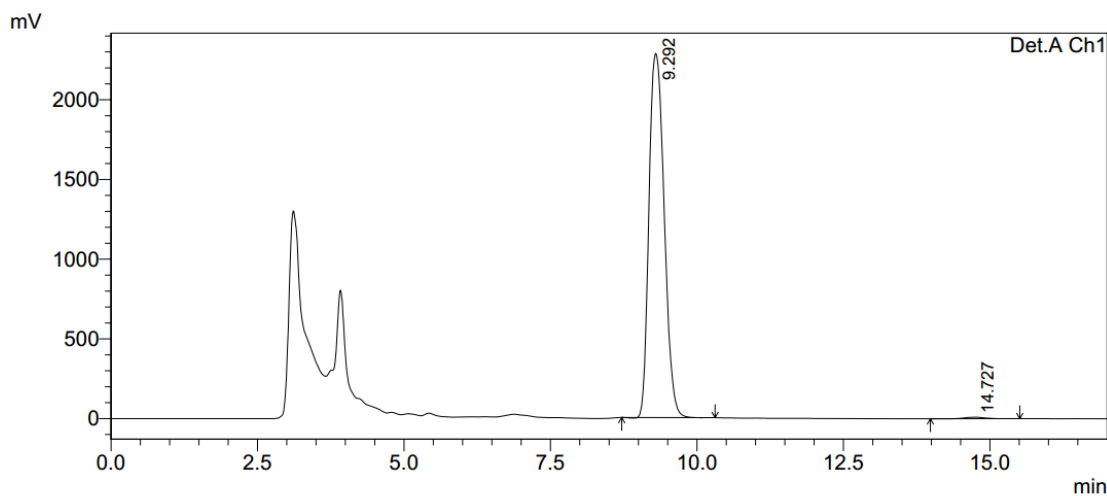


1 Det.A Ch1/210nm

PeakTable

Detector A Ch1 210nm

Peak#	Ret. Time	Area	Height	Area %	Height %
1	9.331	20185466	1207164	49.480	60.492
2	14.674	20609964	788426	50.520	39.508
Total		40795430	1995590	100.000	100.000

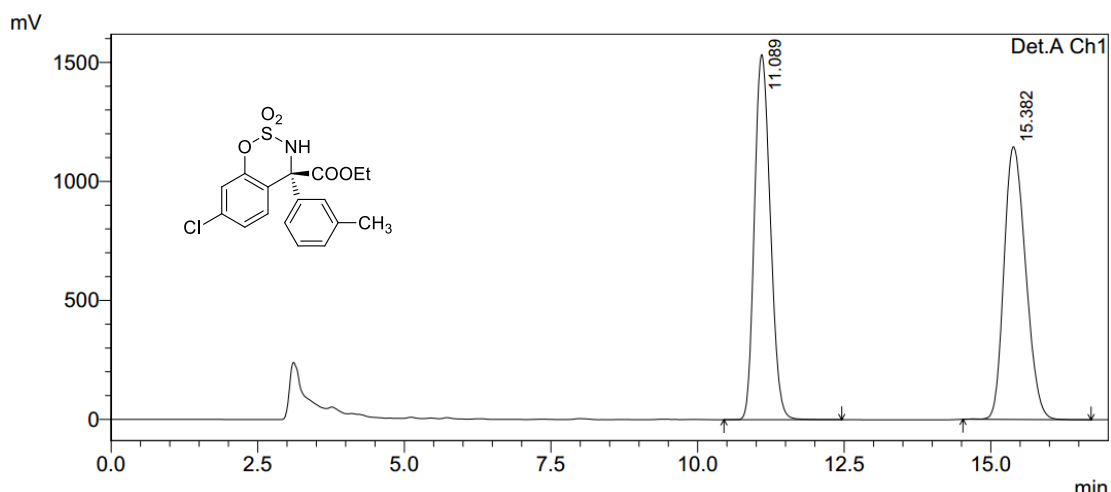


1 Det.A Ch1/210nm

PeakTable

Detector A Ch1 210nm

Peak#	Ret. Time	Area	Height	Area %	Height %
1	9.292	41203887	2283339	99.490	99.594
2	14.727	211016	9310	0.510	0.406
Total		41414903	2292650	100.000	100.000

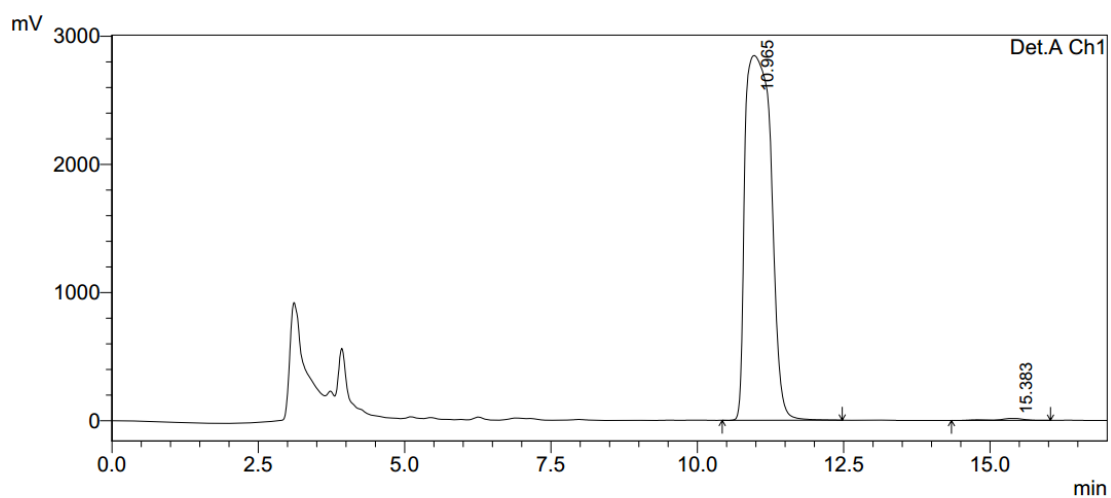


1 Det.A Ch1/210nm

PeakTable

Detector A Ch1 210nm

Peak#	Ret. Time	Area	Height	Area %	Height %
1	11.089	28868287	1533849	49.479	57.235
2	15.382	29475771	1146060	50.521	42.765
Total		58344058	2679909	100.000	100.000

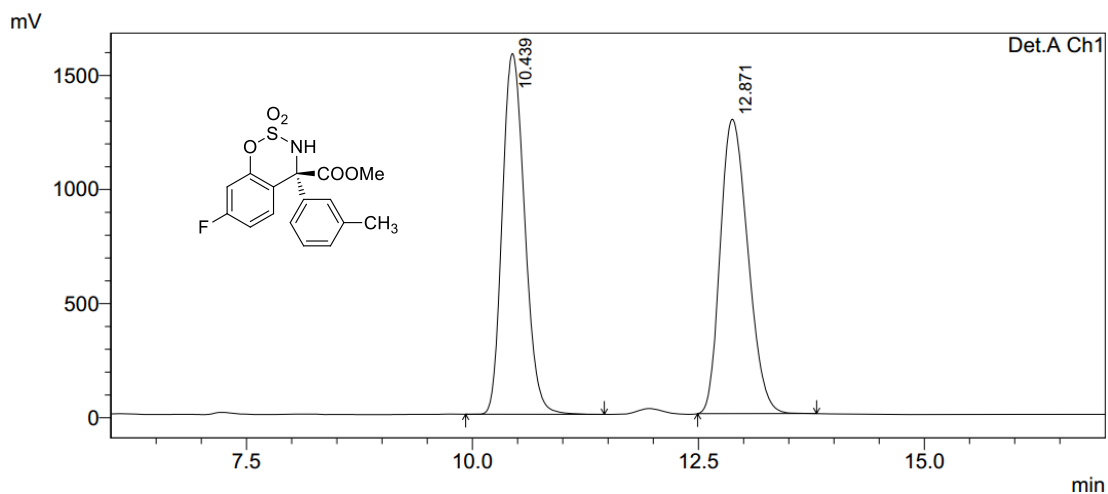


1 Det.A Ch1/210nm

PeakTable

Detector A Ch1 210nm

Peak#	Ret. Time	Area	Height	Area %	Height %
1	10.965	88298334	2846490	99.442	99.442
2	15.383	495827	15984	0.558	0.558
Total		88794162	2862474	100.000	100.000

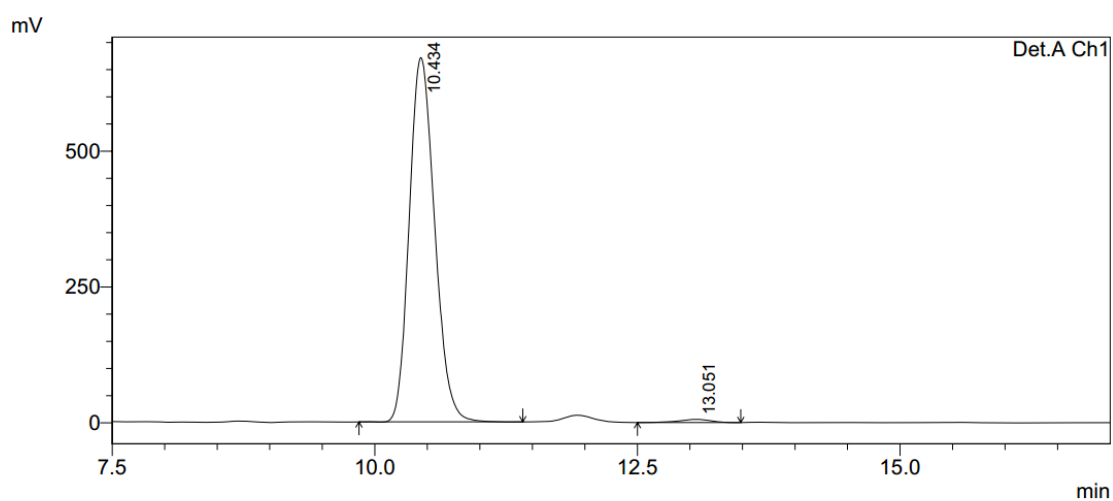


1 Det.A Ch1/210nm

PeakTable

Detector A Ch1 210nm

Peak#	Ret. Time	Area	Height	Area %	Height %
1	10.439	27197640	1581282	49.804	55.060
2	12.871	27411370	1290621	50.196	44.940
Total		54609010	2871903	100.000	100.000



1 Det.A Ch1/210nm

PeakTable

Detector A Ch1 210nm

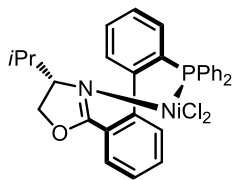
Peak#	Ret. Time	Area	Height	Area %	Height %
1	10.434	11239012	670447	98.934	99.136
2	13.051	121082	5846	1.066	0.864
Total		11360094	676293	100.000	100.000

8. Cartesian Coordinates

(aS)-L1a-NiCl₂

Center	Atomic Number	Atomic Type	Coordinates (Angstroms)			40	6	0	-2.394414	-0.225295	-0.204859
Number	Number	Type	X	Y	Z	41	6	0	-2.632643	-1.005964	-1.338509
1	6	0	-0.687326	-4.389688	-0.692732	42	6	0	-3.325981	-0.225416	0.841660
2	6	0	0.445806	-3.590438	-0.779646	43	6	0	-3.794612	-1.767726	-1.429863
3	6	0	0.612966	-2.524996	0.106490	44	1	0	-1.906692	-1.031316	-2.143675
4	6	0	-0.340301	-2.252386	1.096548	45	6	0	-4.490188	-0.978828	0.741385
5	6	0	-1.452038	-3.093281	1.194608	46	1	0	-3.136084	0.346060	1.745911
6	6	0	-1.631177	-4.144618	0.302909	47	6	0	-4.724435	-1.753076	-0.394018
7	1	0	-0.827572	-5.206316	-1.393181	48	1	0	-3.967230	-2.378231	-2.310626
8	1	0	-2.192722	-2.898527	1.963586	49	1	0	-5.209701	-0.970148	1.554151
9	1	0	-2.513403	-4.771573	0.383540	50	1	0	-5.629398	-2.348644	-0.466964
10	6	0	1.836950	-1.705615	0.004510	51	6	0	-1.183387	2.465125	0.079603
11	7	0	1.913586	-0.517185	-0.471645	52	6	0	-0.104197	3.346192	-0.061610
12	8	0	2.976261	-2.247578	0.427212	53	6	0	-2.464243	2.976261	0.295574
13	6	0	3.302008	-0.033152	-0.307846	54	6	0	-0.301286	4.718726	0.034283
14	6	0	4.038768	-1.340857	0.014771	55	1	0	0.892416	2.957737	-0.254129
15	1	0	3.633897	0.366328	-1.267186	56	6	0	-2.659612	4.353289	0.380186
16	6	0	3.393089	1.072969	0.759210	57	1	0	-3.316246	2.311876	0.388936
17	1	0	4.512300	-1.782325	-0.864602	58	6	0	-1.581379	5.224593	0.255683
18	1	0	4.756687	-1.275636	0.831154	59	1	0	0.541875	5.393899	-0.073349
19	6	0	4.708213	1.836369	0.598260	60	1	0	-3.659717	4.743386	0.541776
20	6	0	3.233590	0.556090	2.189899	61	1	0	-1.738166	6.296621	0.324998
21	1	0	4.787154	2.630290	1.347463	62	28	0	0.653310	0.271959	-1.653570
22	1	0	5.567437	1.167734	0.731613	63	17	0	-0.737027	1.329996	-3.011126
23	1	0	4.787797	2.294927	-0.392901	64	17	0	2.004997	-0.326905	-3.359914
24	1	0	3.091607	1.393386	2.879441	-----					
25	1	0	2.373668	-0.109952	2.296031						
26	1	0	4.126735	0.012708	2.518029						
27	1	0	1.201915	-3.782328	-1.534664						
28	6	0	-0.172632	-1.127155	2.064454						
29	6	0	0.129994	-1.445853	3.389499						
30	6	0	-0.338267	0.226374	1.701637						
31	6	0	0.278385	-0.451264	4.352055						
32	1	0	0.254436	-2.489702	3.661683						
33	6	0	-0.187140	1.215003	2.677318						
34	6	0	0.120215	0.881396	3.993852						
35	1	0	0.514319	-0.720187	5.376794						
36	1	0	-0.319067	2.260049	2.420351						
37	1	0	0.229714	1.666768	4.734910						
38	1	0	2.565320	1.761963	0.548142						
39	15	0	-0.818866	0.679602	-0.016510						

9. X-Ray Crystal Structure Data



(aS)-L1a-NiCl₂

The crystal data of compound **(aS)-L1a-NiCl₂** have been deposited in CCDC with number 1433880. Empirical Formula: C₃₀H₂₈Cl₂NNiOP; Formula Weight: 579.11; Crystal Color, Habit: blue; Crystal Dimensions: 0.42 x 0.40 x 0.32 mm; Crystal System: Orthorhombic; Lattice Parameters: a = 10.1361(3) Å, b = 20.7607(8) Å, c = 14.8742(7) Å, α = 90 °C, β = 90 °C, γ = 90 °C, V = 3130.0(2) Å³; Space group: P2₁2₁2; Z = 4; D_{calc} = 1.229 g/cm³; F₀₀₀ = 1200; Final R indices [I>2sigma(I)]: R1 = 0.0364; wR2 = 0.0860.

L1a was used to coordinate with NiCl₂(DME) to form (aS)-L1a-NiCl₂ and the crystal was obtained from a EtOAc solution at room temperature under N₂.

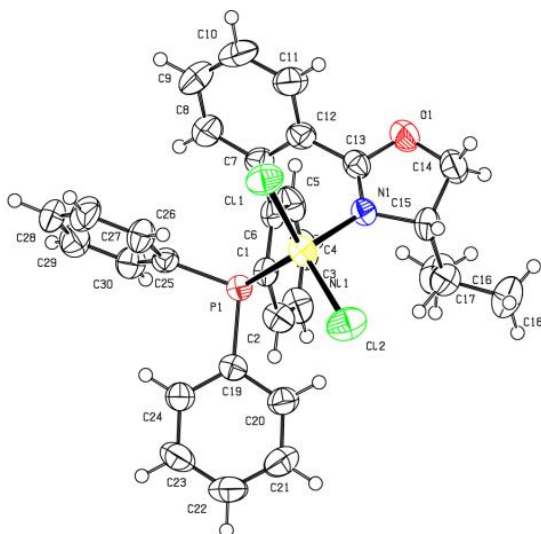


Table S2. Crystal Data and Structure Refinement

Empirical formula	C ₃₀ H ₂₈ Cl ₂ NNiOP
Formula weight	579.11
Temperature/K	293.15
Crystal system	orthorhombic
Space group	P2 ₁ 2 ₁ 2
a/Å	10.1361(3)
b/Å	20.7607(8)
c/Å	14.8742(7)

$\alpha/^\circ$	90.00
$\beta/^\circ$	90.00
$\gamma/^\circ$	90.00
Volume/ \AA^3	3130.0(2)
Z	4
$\rho_{\text{calc}} \text{mg/mm}^3$	1.229
m/mm^{-1}	0.863
F(000)	1200.0
Crystal size/ mm^3	0.42 \times 0.4 \times 0.32
Radiation	MoK α ($\lambda = 0.71073$)
2 Θ range for data collection	5.62 to 50.7 $^\circ$
Index ranges	-12 \leq h \leq 9, -24 \leq k \leq 24, -17 \leq l \leq 16
Reflections collected	20639
Independent reflections	5722 [$R_{\text{int}} = 0.0427$, $R_{\text{sigma}} = 0.0409$]
Data/restraints/parameters	5722/0/327
Goodness-of-fit on F^2	1.026
Final R indexes [$I >= 2\sigma(I)$]	$R_1 = 0.0364$, $wR_2 = 0.0860$
Final R indexes [all data]	$R_1 = 0.0461$, $wR_2 = 0.0916$
Largest diff. peak/hole / e \AA^{-3}	0.37/-0.24
Flack parameter	-0.017(14)

Table S3. Fractional Atomic Coordinates ($\times 10^4$) and Equivalent Isotropic Displacement Parameters ($\text{\AA}^2 \times 10^3$) for the Single Crystal. U_{eq} is defined as 1/3 of the trace of the orthogonalised U_{IJ} tensor.

Atom	x	y	z	U(eq)
Ni1	4968.3(3)	7594.39(17)	7273.5(2)	38.86(12)
P1	3481.9(6)	7557.3(4)	8473.0(5)	33.33(17)
C11	6161.7(8)	8485.5(4)	7207.9(8)	59.6(2)
Cl2	6002.1(8)	6662.0(4)	7158.5(8)	65.2(3)
N1	3742(2)	7641.6(12)	6220.3(15)	37.5(5)
C25	3530(3)	8211.9(14)	9274(2)	36.6(7)
C1	1764(2)	7563.8(14)	8084.6(19)	35.6(6)
C3	-377(3)	7061.1(19)	8004(2)	53.5(9)
C19	3599(3)	6822.6(14)	9135(2)	37.1(7)
C12	2802(3)	8700.4(14)	6561(2)	42.9(7)
C5	-40(3)	8079.3(17)	7335(2)	51.6(8)

C13	3062(3)	8133.9(16)	6004(2)	41.1(7)
C6	1289(3)	8084.5(14)	7592(2)	37.8(7)
C15	3766(3)	7193.0(16)	5449(2)	44.4(8)
C14	3155(3)	7606.3(19)	4701(2)	56.9(9)
C24	3563(3)	6819.1(16)	10068(2)	49.1(8)
O1	2578(2)	8155.9(12)	5169.8(16)	57.2(6)
C29	2509(4)	8869.8(18)	10409(3)	57.8(9)
C20	3687(3)	6239.6(15)	8696(2)	49.2(8)
C8	1909(4)	9232.4(17)	7840(3)	60.8(9)
C2	923(3)	7051.3(17)	8286(2)	46.6(8)
C7	2063(3)	8669.7(14)	7348(2)	42.3(7)
C4	-850(3)	7568.5(19)	7540(2)	54.5(9)
C30	2449(3)	8364.0(16)	9815(2)	49.3(8)
C22	3667(4)	5672.6(19)	10088(3)	64.9(11)
C27	4712(4)	9082.6(16)	9961(3)	62.5(10)
C21	3711(4)	5665.0(17)	9163(3)	60.4(10)
C26	4675(3)	8579.4(16)	9369(2)	49.4(8)
C23	3582(4)	6250.5(19)	10541(3)	64.1(10)
C11	3360(3)	9282.4(17)	6285(3)	58.5(9)
C18	3376(5)	6070(2)	4919(3)	81.5(13)
C28	3643(4)	9230.5(18)	10476(3)	62.8(10)
C9	2487(4)	9803.2(17)	7580(3)	76.9(12)
C17	1589(4)	6643(2)	5782(3)	78.9(13)
C16	3065(4)	6558.7(18)	5648(3)	57.3(9)
C10	3201(4)	9823.9(17)	6791(3)	72.9(12)

Table S4. Anisotropic Displacement Parameters ($\text{\AA}^2 \times 10^3$) for the Single Crystal. The anisotropic displacement factor exponent takes the form: $-2\pi^2[\mathbf{h}^2\mathbf{a}^{*2}\mathbf{U}_{11}+2\mathbf{hka}^{*}\mathbf{b}^{*}\mathbf{U}_{12}+\dots]$.

Atom	\mathbf{U}_{11}	\mathbf{U}_{22}	\mathbf{U}_{33}	\mathbf{U}_{23}	\mathbf{U}_{13}	\mathbf{U}_{12}
Ni1	29.48(17)	47.8(2)	39.3(2)	1.76(19)	-1.07(15)	-0.94(15)
P1	28.2(3)	35.0(4)	36.8(4)	0.2(4)	-2.2(3)	-1.5(3)
Cl1	51.8(4)	49.8(5)	77.1(7)	6.4(5)	0.0(4)	-11.6(3)
Cl2	48.8(4)	56.0(5)	90.6(8)	3.7(5)	9.1(5)	11.5(3)
N1	37.5(12)	42.3(14)	32.8(13)	-0.3(12)	1.6(9)	1.2(11)
C25	37.1(15)	32.9(16)	39.8(18)	1.5(14)	-6.0(13)	3.6(12)
C1	30.1(12)	40.6(16)	36.1(15)	-5.0(14)	0.2(10)	-2.3(12)

C3	40.6(17)	70(2)	50(2)	-2.7(18)	1.7(15)	-16.5(15)
C19	30.8(14)	40.2(17)	40.4(19)	4.2(14)	-0.1(13)	-3.4(12)
C12	40.4(15)	41.9(17)	46(2)	4.2(16)	-7.4(14)	6.4(13)
C5	41.6(16)	74(2)	39.3(18)	-2.1(17)	-7.8(16)	13.3(16)
C13	38.6(15)	48.0(19)	36.8(19)	2.3(16)	-3.3(13)	-6.0(14)
C6	34.2(14)	46.2(17)	33.0(17)	-6.7(14)	-0.4(12)	5.2(12)
C15	39.6(16)	52.2(19)	41.3(19)	-10.3(15)	4.7(13)	0.3(14)
C14	66.5(19)	66(2)	37.7(18)	-2(2)	-4.2(14)	-5.2(18)
C24	56.4(18)	44.1(19)	47(2)	1.9(17)	-10.9(15)	-5.7(15)
O1	69.4(14)	60.0(15)	42.3(14)	1.6(12)	-10.2(12)	9.3(12)
C29	62(2)	58(2)	53(2)	-6(2)	1.0(17)	19.6(18)
C20	56.1(18)	40.0(19)	52(2)	3.4(16)	7.1(16)	-0.3(14)
C8	78(2)	48(2)	57(2)	-4(2)	6.6(19)	7.8(16)
C2	36.3(15)	54.7(19)	49(2)	6.6(17)	-2.3(14)	-7.8(13)
C7	40.9(15)	38.8(16)	47(2)	1.2(16)	-5.6(14)	9.1(12)
C4	27.4(13)	89(3)	47.4(19)	-11(2)	-3.8(12)	-1.4(16)
C30	44.9(18)	52(2)	51(2)	-3.7(18)	3.2(15)	3.5(15)
C22	74(3)	45(2)	76(3)	20(2)	-9(2)	-0.5(18)
C27	70(3)	49(2)	68(3)	-13.4(19)	-4(2)	-18.4(17)
C21	66(2)	40(2)	75(3)	-2.5(19)	8(2)	2.6(17)
C26	42.9(17)	51(2)	54(2)	-11.1(17)	0.1(14)	-6.6(14)
C23	78(2)	66(3)	48(2)	19(2)	-11.7(19)	-9(2)
C11	66(2)	46(2)	63(3)	8.6(19)	3.4(18)	0.8(16)
C18	98(3)	68(3)	78(3)	-27(3)	-3(2)	-3(2)
C28	93(3)	44(2)	51(2)	-14.8(18)	-7(2)	6(2)
C9	107(3)	39(2)	84(3)	-13(2)	-1(3)	11.8(19)
C17	74(3)	75(3)	87(3)	-14(3)	13(2)	-32(2)
C16	65(2)	50(2)	57(2)	-3.8(19)	-4.3(18)	-5.9(16)
C10	95(3)	35(2)	89(3)	11(2)	2(2)	-3.4(17)

Table S5. Bond Lengths for the Single Crystal.

Atom	Atom	Length/Å	Atom	Atom	Length/Å
Ni1	P1	2.3364(8)	C5	C4	1.376(5)
Ni1	Cl1	2.2125(8)	C13	O1	1.335(4)
Ni1	Cl2	2.2078(9)	C6	C7	1.491(4)
Ni1	N1	2.002(2)	C15	C14	1.535(5)

P1	C25	1.809(3)		C15	C16	1.525(5)
P1	C1	1.834(2)		C14	O1	1.460(4)
P1	C19	1.819(3)		C24	C23	1.374(5)
N1	C13	1.274(4)		C29	C30	1.374(5)
N1	C15	1.478(4)		C29	C28	1.375(5)
C25	C30	1.395(4)		C20	C21	1.381(5)
C25	C26	1.396(4)		C8	C7	1.387(5)
C1	C6	1.392(4)		C8	C9	1.377(5)
C1	C2	1.396(4)		C22	C21	1.377(6)
C3	C2	1.383(4)		C22	C23	1.379(6)
C3	C4	1.348(5)		C27	C26	1.368(5)
C19	C24	1.389(4)		C27	C28	1.362(6)
C19	C20	1.379(4)		C11	C10	1.363(5)
C12	C13	1.462(5)		C18	C16	1.519(5)
C12	C7	1.392(5)		C9	C10	1.379(6)
C12	C11	1.396(5)		C17	C16	1.519(5)
C5	C6	1.401(4)				

Table S6. Bond Angles for the Single Crystal.

Atom	Atom	Atom	Angle/ [°]	Atom	Atom	Atom	Angle/ [°]
Cl1	Ni1	P1	114.44(3)	O1	C13	C12	115.6(3)
Cl2	Ni1	P1	109.65(4)	C1	C6	C5	118.1(3)
Cl2	Ni1	Cl1	118.05(3)	C1	C6	C7	125.4(2)
N1	Ni1	P1	101.46(6)	C5	C6	C7	116.5(3)
N1	Ni1	Cl1	105.31(7)	N1	C15	C14	101.7(2)
N1	Ni1	Cl2	106.08(8)	N1	C15	C16	112.7(3)
C25	P1	Ni1	117.46(10)	C16	C15	C14	115.8(3)
C25	P1	C1	103.16(13)	O1	C14	C15	104.6(3)
C25	P1	C19	105.74(13)	C23	C24	C19	121.1(3)
C1	P1	Ni1	111.80(9)	C13	O1	C14	105.6(3)
C19	P1	Ni1	113.53(10)	C30	C29	C28	120.0(3)
C19	P1	C1	103.79(13)	C19	C20	C21	121.4(3)
C13	N1	Ni1	124.9(2)	C9	C8	C7	121.9(4)
C13	N1	C15	108.6(2)	C3	C2	C1	120.4(3)
C15	N1	Ni1	124.47(18)	C12	C7	C6	121.7(3)
C30	C25	P1	121.9(2)	C8	C7	C12	117.7(3)

C30	C25	C26	118.1(3)	C8	C7	C6	119.9(3)
C26	C25	P1	120.0(2)	C3	C4	C5	120.2(3)
C6	C1	P1	120.0(2)	C29	C30	C25	120.6(3)
C6	C1	C2	119.6(2)	C21	C22	C23	120.1(4)
C2	C1	P1	120.4(2)	C28	C27	C26	120.9(3)
C4	C3	C2	120.4(3)	C22	C21	C20	119.5(4)
C24	C19	P1	123.0(2)	C27	C26	C25	120.3(3)
C20	C19	P1	118.9(2)	C24	C23	C22	119.8(4)
C20	C19	C24	118.1(3)	C10	C11	C12	120.2(4)
C7	C12	C13	122.5(3)	C27	C28	C29	120.1(3)
C7	C12	C11	120.3(3)	C8	C9	C10	119.3(4)
C11	C12	C13	117.2(3)	C18	C16	C15	110.0(3)
C4	C5	C6	121.3(3)	C18	C16	C17	112.0(3)
N1	C13	C12	126.8(3)	C17	C16	C15	112.6(3)
N1	C13	O1	117.5(3)	C11	C10	C9	120.4(3)

Table S7. Torsion Angles for the Single Crystal.

A	B	C	D	Angle/°	A	B	C	D	Angle/°
Ni1	P1	C25	C30	157.3(2)	C19	P1	C1	C6	176.3(2)
Ni1	P1	C25	C26	-23.0(3)	C19	P1	C1	C2	-3.2(3)
Ni1	P1	C1	C6	-61.0(2)	C19	C24	C23	C22	1.5(5)
Ni1	P1	C1	C2	119.5(2)	C19	C20	C21	C22	-1.0(5)
Ni1	P1	C19	C24	137.0(2)	C12	C13	O1	C14	169.9(3)
Ni1	P1	C19	C20	-44.9(3)	C12	C11	C10	C9	0.0(6)
Ni1	N1	C13	C12	-14.5(4)	C5	C6	C7	C12	-94.1(3)
Ni1	N1	C13	O1	162.3(2)	C5	C6	C7	C8	76.6(4)
Ni1	N1	C15	C14	-154.7(2)	C13	N1	C15	C14	9.8(3)
Ni1	N1	C15	C16	80.7(3)	C13	N1	C15	C16	-114.8(3)
P1	Ni1	N1	C13	72.4(2)	C13	C12	C7	C6	-11.0(4)
P1	Ni1	N1	C15	-125.6(2)	C13	C12	C7	C8	178.1(3)
P1	C25	C30	C29	-179.1(3)	C13	C12	C11	C10	-177.4(3)
P1	C25	C26	C27	178.8(3)	C6	C1	C2	C3	-0.5(5)
P1	C1	C6	C5	-177.9(2)	C6	C5	C4	C3	0.6(5)
P1	C1	C6	C7	-1.0(4)	C15	N1	C13	C12	-178.9(3)
P1	C1	C2	C3	179.0(3)	C15	N1	C13	O1	-2.1(4)
P1	C19	C24	C23	176.4(3)	C15	C14	O1	C13	12.7(3)

P1	C19	C20	C21	-176.7(3)	C14	C15	C16	C18	75.7(4)
Cl1	Ni1	P1	C25	-4.85(11)	C14	C15	C16	C17	-50.0(4)
Cl1	Ni1	P1	C1	114.11(11)	C24	C19	C20	C21	1.4(5)
Cl1	Ni1	P1	C19	-128.89(11)	C20	C19	C24	C23	-1.7(5)
Cl1	Ni1	N1	C13	-47.2(2)	C8	C9	C10	C11	-1.6(6)
Cl1	Ni1	N1	C15	114.8(2)	C2	C1	C6	C5	1.6(4)
Cl2	Ni1	P1	C25	130.44(11)	C2	C1	C6	C7	178.5(3)
Cl2	Ni1	P1	C1	-110.60(11)	C2	C3	C4	C5	0.6(5)
Cl2	Ni1	P1	C19	6.40(11)	C7	C12	C13	N1	-65.5(4)
Cl2	Ni1	N1	C13	-173.1(2)	C7	C12	C13	O1	117.7(3)
Cl2	Ni1	N1	C15	-11.1(2)	C7	C12	C11	C10	0.9(5)
N1	Ni1	P1	C25	-117.69(13)	C7	C8	C9	C10	2.4(6)
N1	Ni1	P1	C1	1.27(12)	C4	C3	C2	C1	-0.6(5)
N1	Ni1	P1	C19	118.27(13)	C4	C5	C6	C1	-1.6(4)
N1	C13	O1	C14	-7.2(4)	C4	C5	C6	C7	-178.8(3)
N1	C15	C14	O1	-13.4(3)	C30	C25	C26	C27	-1.5(5)
N1	C15	C16	C18	-167.8(3)	C30	C29	C28	C27	-0.7(6)
N1	C15	C16	C17	66.6(4)	C21	C22	C23	C24	-1.1(6)
C25	P1	C1	C6	66.1(2)	C26	C25	C30	C29	1.2(5)
C25	P1	C1	C2	-113.4(3)	C26	C27	C28	C29	0.5(6)
C25	P1	C19	C24	6.8(3)	C23	C22	C21	C20	0.8(6)
C25	P1	C19	C20	-175.1(2)	C11	C12	C13	N1	112.8(4)
C1	P1	C25	C30	33.9(3)	C11	C12	C13	O1	-64.1(4)
C1	P1	C25	C26	-146.4(3)	C11	C12	C7	C6	170.8(3)
C1	P1	C19	C24	-101.4(3)	C11	C12	C7	C8	-0.1(4)
C1	P1	C19	C20	76.7(3)	C28	C29	C30	C25	-0.1(5)
C1	C6	C7	C12	89.0(4)	C28	C27	C26	C25	0.7(6)
C1	C6	C7	C8	-100.3(4)	C9	C8	C7	C12	-1.5(5)
C19	P1	C25	C30	-74.8(3)	C9	C8	C7	C6	-172.6(4)
C19	P1	C25	C26	104.9(3)	C16	C15	C14	O1	109.1(3)

Table S8. Hydrogen Atom Coordinates ($\text{\AA} \times 10^4$) and Isotropic Displacement Parameters ($\text{\AA}^2 \times 10^3$) for the Single Crystal.

Atom	x	y	z	U(eq)
H3	-928	6716	8136	64
H5	-382	8428	7019	62

H15	4687	7101	5294	53
H14A	3824	7746	4278	68
H14B	2483	7367	4378	68
H24	3527	7208	10378	59
H29	1783	8968	10766	69
H20	3732	6233	8071	59
H8	1401	9224	8360	73
H2	1239	6701	8611	56
H4	-1728	7573	7358	65
H30	1681	8121	9772	59
H22	3694	5288	10407	78
H27	5477	9327	10014	75
H21	3757	5276	8855	72
H26	5417	8482	9027	59
H23	3536	6255	11166	77
H11	3843	9301	5754	70
H18A	3054	6225	4351	122
H18B	2956	5668	5059	122
H18C	4313	6008	4884	122
H28	3679	9576	10873	75
H9	2396	10171	7932	92
H17A	1426	7033	6110	118
H17B	1247	6283	6113	118
H17C	1162	6666	5206	118
H16	3428	6391	6213	69
H10	3576	10210	6603	87

Table S9. Solvent Masks Information for the Single Crystal.

Number	X	Y	Z	Volume	Electron Count	Content
1	0.000	0.500	0.153	7	0	
2	-0.023	0.000	0.333	230	27	
3	-0.012	0.500	0.667	231	28	
4	0.000	0.000	0.621	26	3	
5	0.500	0.500	0.379	25	3	
6	0.500	0.000	0.847	7	0	

10. References

1. Synthesis of substrates **1b**, **1c**, **1e**, **1j**, see: (a) Y. Luo, A. J. Carnell and H. W. Lam, *Angew. Chem., Int. Ed.*, 2012, **51**, 6762; Synthesis of substrate **1g**, see: (b) Y. Liu, T.-R. Kang, Q.-Z. Liu, L.-M. Chen, Y.-C. Wang, J. Liu, Y.-M. Xie, J.-L. Yang and L. He, *Org. Lett.*, 2013, **15**, 6090; Synthesis of substrate **1h**, see: (c) Y. Luo, H. B. Hepburn, N. Chotsaeng and H. W. Lam, *Angew. Chem., Int. Ed.*, 2012, **51**, 8309.
2. F. Hu, X. Guan and M. Shi, *Tetrahedron*, 2012, **68**, 4782.
3. M. Quan, G. Yang, F. Xie, I. D. Gridnev and W. Zhang, *Org. Chem. Front.*, 2015, **2**, 398.
4. H. Wang and Xu, M.-H. *Synthesis*, 2013, **45**, 2125.
5. Y. Wang, C. Yu, D. Wang, X. Wang and Y. Zhou, *Org. Lett.*, 2008, **10**, 2071.
6. H. Wang, T. Jiang and M.-H. Xu, *J. Am. Chem. Soc.*, 2013, **135**, 971.
7. Gaussian 09, Revision A.02, M. J. Frisch, G. W. Trucks, H. B. Schlegel, G. E. Scuseria, M. A. Robb, J. R. Cheeseman, G. Scalmani, V. Barone, B. Mennucci, G. A. Petersson, H. Nakatsuji, M. Caricato, X. Li, H. P. Hratchian, A. F. Izmaylov, J. Bloino, G. Zheng, J. L. Sonnenberg, M. Hada, M. Ehara, K. Toyota, R. Fukuda, J. Hasegawa, M. Ishida, T. Nakajima, Y. Honda, O. Kitao, H. Nakai, T. Vreven, J. A. 10 Montgomery, J. E. Peralta, F. Ogliaro, M. Bearpark, J. J. Heyd, E. Brothers, K. N. Kudin, V. N. Staroverov, R. Kobayashi, J. Normand, K. Raghavachari, A. Rendell, J. C. Burant, S. S. Iyengar, J. Tomasi, M. Cossi, N. Rega, J. M. Millam, M. Klene, J. E. Knox, J. B. Cross, V. Bakken, C. Adamo, J. Jaramillo, R. Gomperts, R. E. Stratmann, O. Yazyev, A. J. Austin, R. Cammi, C. Pomelli, J. W. Ochterski, R. L. Martin, K. Morokuma, V. G. Zakrzewski, G. A. Voth, P. Salvador, J. J. Dannenberg, S. Dapprich, A. D. Daniels, O. Farkas, J. B. Foresman, J. V. Ortiz, J. Cioslowski and D. J. Fox, *Gaussian, Inc.*, Wallingford CT, 2009.
8. D. Andrae, U. Haeussermann, M. Dolg, H. Stoll and H. Preuss, *Theor. Chim. Acta.*, 1990, **77**, 123.
9. (a) R. Ditchfield, W. J. Hehre and J. A. J. Pople, *Chem. Phys.*, 1971, **54**, 724; (b) W. J. Hehre, R. Ditchfield and J. A. J. Pople, *Chem. Phys.*, 1972, **56**, 2257; (c) P. C. Hariharan and J. A. Pople, *Theor. Chim. Acta.*, 1973, **28**, 213; (d) P. C. Hariharan and J. A. Pople, *Mol. Phys.*, 1974, **27**, 209; (e) M. S. Gordon, *Chem. Phys. Lett.*, 1980, **76**, 163.
10. (a) F. Tian, D. Yao, Y. Zhang and W. Zhang, *Tetrahedron*, 2009, **65**, 9609; (b) F. Tian, D. Yao, Y. Liu, F. Xie and W. Zhang, *Adv. Synth. Catal.*, 2010, **352**, 1841; (c) Y. Liu, D. Yao, K. Li, F. Tian, F. Xie and W. Zhang, *Tetrahedron*, 2011, **67**, 8445; (d) Y. Liu and W. Zhang, *Angew. Chem., Int. Ed.*, 2013, **52**, 2203; (e) Y. Liu, I. D. Gridnev and W. Zhang, *Angew. Chem., Int. Ed.*, 2014, **53**, 1901.
11. (a) K. W. Quasdorf, A. Antoft-Finch, P. Liu, A. L. Silberstein, A. Komaromi, T. Blackburn, S. D. Ramgren, K. N. Houk, V. Snieckus and N. K. Garg, *J. Am. Chem. Soc.*, 2011, **133**, 6352; (b) T. Sperger, I. A. Sanhueza, I. Kalvet and F. Schoenebeck, *Chem. Rev.*, 2015, **115**, 9532.
12. (a) J. Bouffard and K. Itami, *Org. Lett.*, 2009, **11**, 4410; (b) T. Maekawa, H. Sekizawa and K. Itami, *Angew. Chem., Int. Ed.*, 2011, **50**, 7022; (c) E. Shirakawa, Y. Yasuhara and T. Hayashi, *Chem. Lett.*, 2006, **35**, 768; (d) Y.-C. Hong, P. Gandeepan, S. Mannathan, W.-T. Lee and C.-H. Cheng, *Org. Lett.*, 2014, **16**, 2806.